# Identifying functional roles of neural circuits in two primary auditory cortices

**Inauguraldissertation**

zur

Erlangung der Würde eines Doktors der Philosophie

vorgelegt der

Philosophisch-Naturwissenschaftlichen Fakultät

der Universität Basel

von

Magdalena Sołyga

Basel, Switzerland, 2021,

Originaldokument gespeichert auf dem Dokumentenserver der Universität Basel

http://edoc.unibas.ch

Genehmigt von der Philosophisch-Naturwissenschaftlichen Fakultät

auf Antrag von

Prof. Dr. Tania Rinaldi Barkat,

Prof. Dr. Andreas Lüthi,

Prof. Dr. Max F.K. Happel.

Basel, 22nd June 2021

_____

Prof. Dr. Marcel Mayor

# TABLE OF CONTENTS

# Acknowledgements

First and foremost, I would like to express my sincere gratitude to my supervisor Professor Tania Rinaldi Barkat, for her invaluable support during my Ph.D. study, for showing me that academia is fun, pushing my limits every day, and ensuring me that we can achieve any goal we set for ourselves. Constantly reminding me that if others have stumbled over something, it does not mean that we will do too. I am thankful for her willingness to share the knowledge, experience, and the best role model of mentor, demonstrating a positive attitude toward collaborative learning and growth. I would like to express my sincere gratitude to the Members of my Doctoral Committee: Professor Andreas Lüthi, Professor Daniel Bodmer, Professor Max Happel and Professor Pascal Senn for their insightful comments and suggestions at different stages of the research project.

I am deeply grateful to every Brain & Sound lab member who inspired me in different moments of my Ph.D. Mari and Stiti for welcoming me into the group and introducing me to the world of auditory neuroscience. Gioia, Patricia, and Elisabetta for learning from each other, being invaluable support, and sharing many wonderful moments. Charlotte, for teaching me how to think outside the box. Florian, Suyash, and Sebastian for lengthy discussions and sharing a passion for science. I would also like to thank Ramona Felix, who was invaluable support throughout my Ph.D. times.

I want to express my sincere gratitude to Laura Colombo and Joana Freire for their friendship at every stage of the Ph.D. studies because anything is possible when you have the right people there to support you. I would like to offer my special thanks to all members of the 7$^{th}$ floor in Pharmazentrum for celebrating little successes together and supporting each other even in the most challenging moments.

I want to express my gratitude to my family and friends for their tremendous understanding and encouragement in the past few years. Finally, I would like to offer my special thanks to Marek for always believing in me.

# Abstract

During sound perception, auditory signals have to travel a long way from the cochlea, through the subcortical areas, up to the auditory cortex. How each nucleus on this pathway - especially in the central auditory system - contributes to making sense of the acoustic world is far from understood. In the rodent auditory system, the primary cortex is subdivided into two regions, both receiving direct inputs from the auditory thalamus: the primary auditory cortex (A1) and the anterior auditory field (AAF). To deepen our general knowledge of auditory cortical processing, we studied what sound features are preferentially represented by primary auditory cortices, the spatial organization of these preferences, and their possible perceptual role. Using *in vivo* electrophysiological recordings in the mouse auditory cortex, we found that AAF neurons have significantly stronger responses to tone offset than A1 neurons. These results emphasize the potentially critical role of AAF for temporal processing. By combining electrophysiological recordings in AAF and auditory thalamus with antidromic stimulation, we revealed that cortical offset responses are inherited from the periphery, amplified, and generated *de novo*. Preventing offset responses in animals performing sound termination detection task decreased their ability to detect that the sound stopped, confirming the relevance of cortical auditory offset responses at the behavioral level. Additionally, by studying responses in A1 and AAF evoked by sounds with different spectral complexity, we found that responses in A1, but not in AAF, are influenced by the spectral complexity of the sound, suggesting that A1 is predominantly enrolled in the spectral processing. Our findings open new vistas into understanding the functional roles of A1 and AAF and more general auditory cortex in sound processing and perception. Identifying the specific functions of auditory cortical circuits paves the way for future understanding of the mechanisms behind impairments in spectral or temporal processing arising from both aging and disease.

# Related publications

## Journal papers

- **Sołyga M.**, & Barkat T. R. (2019). Distinct processing of tone offset in two primary auditory cortices. *Scientific reports*, 9(1), 1-12.
- Bhumika S., Nakamura M., Valerio P., **Solyga M.**, Lindén H., & Barkat T. R. (2020) A Late Critical Period for Frequency Modulated Sweeps in the Mouse Auditory System. *Cerebral Cortex, 30*(4), 2586-2599.
- **Sołyga M.**, & Barkat T. R. (under review). Emergence and function of cortical offset responses in sound termination detection.
- **Sołyga M.**, & Barkat T. R. (in preparation). Distinct integration of spectrally complex sounds in mouse primary auditory cortices.

## Conference publications

- **Solyga M.**, Barkat TR., (2017) Towards a better understanding of music processing by studying responses in mouse auditory cortex evoked by complex sounds. 6th International Conference on Auditory Cortex Program Committee, Banff, Canada.
- **Solyga M.**, Barkat TR., (2018) Distinctive roles of primary auditory regions in sound processing. 20th Swiss Society for Neuroscience Meeting, Zurich, Switzerland.
- **Solyga M.**, Barkat TR., (2018) Distinctive roles of primary auditory regions in sound processing. 11th FENS Forum of Neuroscience, Berlin, Germany.
- **Solyga M.**, Barkat TR., (2019) Auditory offset responses: from mechanisms to behavioral relevance. International Inauguration meeting. Hearing Institute-Paris, France.
- **Solyga M.**, Barkat TR., (2020) 12th FENS Forum of Neuroscience, online.
- **Solyga M.**, Barkat TR., (2020) Amplified representation of sound termination in the auditory cortex and its behavioral relevance. Advances and Perspectives in Auditory Neuroscience, online.
- **Solyga M.**, Barkat TR., (2020) Amplified representation of sound termination in the auditory cortex and its behavioral relevance. Neuromatch 3.0, online
- **Solyga M.**, Barkat TR., (2021) The emergence and function of cortical offset responses in sound termination detection. Computational and Systems Neuroscience, Cosyne 2021, online.

# List of abbreviations

| | |
|---|---|
| A1 | Primary auditory field |
| A2 | Secondary auditory field |
| AAF | Anterior auditory field |
| ACx | Auditory cortex |
| BF | Best frequency |
| CN | Cochlear nuclei |
| dB | Decibel |
| DP | Dorsal posterior auditory field |
| FRA | Frequency receptive fields |
| FS | Fast spiking |
| HT | Harmonic tone |
| Hz | Herz |
| IAF | Insular auditory field |
| IC | Inferior colliculus |
| L2/3 | The supragranular layers 2/3 |
| L4 | The thalamorecipient layer 4 |
| LFP | Local field potential |
| MGB | Medial geniculate body |
| MFFT | Missing fundamental frequency tone |
| p2t | Peak-to-trough times |
| PNN | Perineuronal nets |
| PSTH | Peristimulus time histogram |
| PT | Pure tone |
| PV | Parvalbumin |
| RS | Regular spiking |
| SOM | Somatostatin |
| SPL | Sound pressure level |
| SPN | Superior olivary complex |
| t½ | Half decay time |
| Thr | Threshold |
| TRF | Tuning receptive field |
| VIP | Vasoactive intestinal peptide |
| VSDI | Voltage-sensitive dye imaging |

# Chapter 1

# Introduction

Hearing is an astonishing process. As you read the first sentences of this introduction, you have probably not realized what a tremendous job your auditory system is doing. Slow down for a bit to allow yourself to listen to the sounds that are approaching your ears. It may be the coffee machine running in the kitchen, steps of somebody passing by in the corridor, the conversations happening next door, or maybe you are consciously listening to your favorite song. From these examples, you can already realize that your hearing system can readily recognize sounds created both by the objects and the humans, categorize them and assign them meaning. By definition, the sound is a pressure wave, which propagates through the air. Your auditory system has to process an immensely rich and complex combination of many pressure waves in natural settings. But… let's start from the beginning.

## 1.1. Hearing

The hearing process starts in the outer ear, where a sound wave enters the ear canal and travels to the tympanic membrane, producing oscillations (Figure 1). Then, three tiny ossicles (malleus, incus, and stapes), which are a part of the middle ear, transfer the vibrations from the tympanic membrane to the inner ear. Within the inner ear, the structure responsible for hearing is the cochlea. The cochlea is a snail-shaped, bony structure filled with fluid. This fluid, characterized by a unique ionic composition, moves in response to the movement of the middle ear bones.

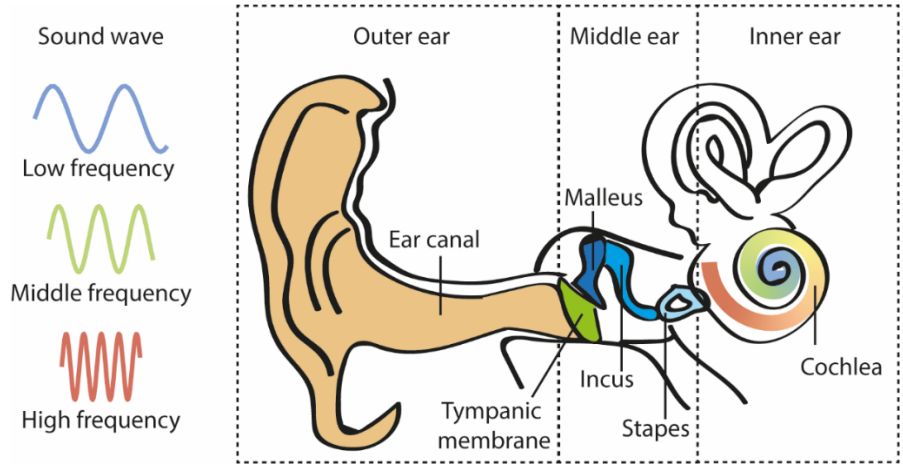


**Figure 1** A diagram of the peripheral auditory system. Different colors in the cochlea indicate the location of hair cells responding to the sound of low (blues), middle (green), or high (red) frequencies.

Along the whole length of the cochlea, on the basilar membrane, four rows of highly specialized sensory hair cells are located. These are the actual receptive cells for hearing. Depending on the frequency components of the acoustic waveform, different parts of the basilar membrane in the cochlea are mechanically stimulated. The high-frequency components stimulate hair cells in the base of the basilar membrane while the low-frequency components at the apex of the basilar membrane. This arrangement of hair cells as a function of their response to tones of different frequencies is called tonotopy. Hair cells transduce the mechanical vibrations produced by the acoustic stimuli into electrical signals by triggering action potentials in afferent auditory nerve fibers. Tonotopically stimulated hair cells provide the first decomposition of the acoustic signal into its frequency components. This tonotopic organization is then maintained throughout the auditory pathway, where neurons responsive to the highest frequencies are located at one end of each brain nucleus and responsive to the lowest frequencies at the other end, with a continuous gradient in between.

### 1.2. The auditory pathway

After the cochlea, auditory signals travel a long way through the cochlear nuclei (CN), superior olivary complex (SPN), inferior colliculus (IC), and medial geniculate body (MGB) up to the auditory cortex (ACx) (Figure 2, left). In this pathway, a core of neurons within each subsequent auditory nuclei maintains the tonotopic organization. This tonotopically-organized pathway is often referred to as lemniscal. The divisions of the auditory nuclei lacking tonotopy are part of the parallel non-lemniscal pathway. In the lemniscal pathway, most neurons in each frequency band project to a homologous frequency band at the next station. This standard hierarchical signal transmission on the lemniscal pathway changes in the auditory cortex (Figure 2, right), where two tonotopically organized auditory regions, namely the primary auditory cortex (A1) and the anterior auditory field (AAF) (Imaizumi et al., 2004) receive tonotopically matching input in parallel.

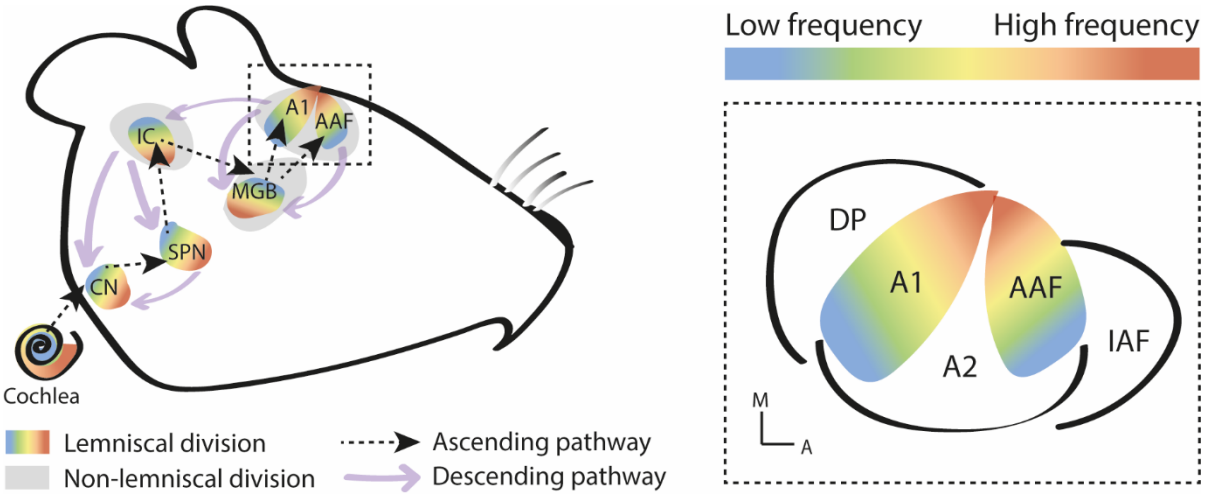


**Figure 2** (Left) Schematic of ascending auditory pathway. CN – cochlear nuclei, SPN – superior olivary complex, IC – inferior colliculus, MGB – medial geniculate body. (Right) Identified auditory cortical areas in the mouse brain. A1 – primary auditory field, AAF – anterior auditory field, A2 – secondary auditory field, DP - dorsal posterior auditory field, IAF - insular auditory field. Adapted from (Guo et al., 2012; Stiebler et al., 1997).

Early studies have distinguished A1 and AAF as two separate auditory fields in mice based on anatomical and functional parameters (Stiebler et al., 1997). Tracing experiments in cats and mice confirmed parallel connections from the thalamus to both A1 and AAF (Lee and Winer, 2011; Takemoto et al., 2014). It was also shown in cats that the vast majority of thalamocortical projections to A1 and AAF originate from largely non-overlapping cell groups of the MGB. A1 receives 80% of projections from the tonotopically organized ventral division of MGB, and AAF 40 and 35% from the ventral division and rostral pole, respectively (Lee et al., 2004; Morel and Imig, 1987). Both A1 and AAF are classified as primary sensory fields as they receive direct input from the ventral division of the auditory thalamus.

In parallel to the ascending auditory pathway, which transmits information from the cochlea to the auditory cortex (bottom-up processing), there is also a descending auditory pathway working in the reverse direction (top-down, Figure 2, left). Bottom-up processing is purely driven by the stimulus and works towards creating a categorical representation of the sound. Top-down processing, originating from multiple levels of the auditory system, refers to the modulation effect of higher onto lower processing centers. ACx was shown to send feedback information both to MGB (cortico-thalamic projections) and directly to IC (cortico-collicular projections) (Andersen et al., 1980; Doucet et al., 2003). This feedback mechanism is thought to be crucial in enhancing the maintenance of goal-relevant sensory information (Caras and Sanes, 2017). In cats, it was shown that A1 and AAF feedback connections terminate within the same subdivision of MGB (Andersen et al., 1980). Nevertheless, it is still unknown whether they have the same function in modulating activity in their preceding nucleus.

Along the ascending processing hierarchy, auditory responsive neurons perform a specific transformation of stimulus representation (Chechik et al., 2006). It is thought that IC is the first integration center where both excitatory and inhibitory inputs from different brainstem regions converge. As a result of this rich integration, neurons in IC can be selective for several sound features, i.e., frequency, amplitude, duration, or direction of frequency modulation. They can create specific responses to complex sounds (Ito et al., 2016). Neurons in MGB and ACx show surprisingly similar responses to those of IC neurons, making it challenging to address the specific function of thalamic and cortical neurons in sound processing (Chechik et al., 2006; King and Nelken, 2009). On the other hand, it was recently shown that subcortical auditory neurons encode well-isolated sound features but not the longer rhythmic patterns, while cortical neurons decode slower changes in stimulus patterns, but not short intervals (Asokan et al., 2021). This suggests that cortical and subcortical neurons have different capacity of encoding sound features in the short and long timescale. ACx is also the first stage where sensory information is integrated within a network responsible for auditory perception, decision-making and learning. In recent years there was a growing realization that processing in ACx is highly context dependent, performs integration of inputs from other sensory systems, motor inputs, but also depends on experience and can be shaped by attention (De Franceschi and Barkat, 2020; Fritz et al., 2003; King

et al., 2018; Schneider, 2020). The specific contribution of the A1 and AAF to this chain of processing is far from understood.

## 1.3. Comparison of A1 and AAF

It is well accepted that the primary auditory region consists of two fields: A1 and AAF. Nevertheless, comprehensive formalization of each region's function is still lacking. Attribution of a specific role to a cortical area can be somehow related to its: (1) laminar and cellular architecture, (2) organization into functional networks with other brain regions, (3) postnatal developmental changes, and (4) neuronal response properties (Genon et al., 2018). The difference between those properties for A1 and AAF are reviewed in the following sections.

### 1.3.1. Laminar architecture

Both A1 and AAF contain six distinct cortical layers with highly specialized inputs, outputs, and interlaminar connections (Figure 3). The different layers are distinguished based on connectional differences and densities of neuronal somas, dendrites, and axons (Rouiller et al., 1991). Primary ACx follows the canonical architecture of the neocortex seen in other sensory modalities. Afferents from the MGB to primary ACx terminate most densely in upper layer 4 (L4) (Winer et al., 2005). Then the information is split into two parallel streams. The first corresponds to an intracortical stream sending a signal to different cells in layer 2/3 (L2/3), which then provides feedforward input to L4 of higher cortical areas (Jabaudon, 2017). The second stream describes signals sent from L4 to L2/3, which in turn project to layer 5 (L5). L5 integrates the input from multiple cortical layers and sends top-down projections to sub-cortical auditory stations and layer 6 (L6) (Williamson and Polley, 2019). L6 neurons propagate information to the MGB but also modulate the signals locally through the local inhibitory network. Layer 1 (L1), containing inhibitory neurons and dendrites of excitatory neurons, is thought to integrate modulatory signals from higher cortical areas (Miller, 2016). Less robust direct projections from MGB to L1 in ACx were also recently described (Takesian et al., 2018). All cortical layers serve as computational units, which must combine local and hierarchical signal processing. Differences in computations performed by cortical layers can reflect their specific function in stimuli processing. Nevertheless, despite clearly non-overlapping inputs coming to A1 and AAF from MGB (Lee et al., 2004), no laminar structure differences were shown to exist between those two primary fields.

### 1.3.2. Tonotopy

Different studies demonstrate that A1 and AAF are both tonotopically organized (Guo et al., 2012; Kelly et al., 1986; Kowalski et al., 1995; Phillips et al., 1988) but differ in the proportion of cortical area tuned to specific frequencies (Bizley et al., 2005; Carrasco and Lomber, 2009b; Imaizumi et al., 2004; Polley et al., 2007). Neurons in A1 tuned to different frequencies are evenly distributed. In contrast, the cortical representation of differentially tuned neurons in AAF, although tonotopic, is irregular with an underrepresentation of cells tuned to mid-range frequencies (Carrasco and Lomber, 2009b). In both

areas, the tonotopic gradients are evident in superficial (L2/3), middle (L4), and deep (L5/6) layers (Guo et al., 2012).

### 1.3.3. Cell types

A1 and AAF are densely innervated both with excitatory and inhibitory neurons. The excitatory cortical network, represented mainly by pyramidal cells, is highly interposed with a diverse population of inhibitory interneurons. Three are three predominant types of inhibitory interneurons in ACx: parvalbumin-positive (PV+), somatostatin-positive (SOM+), and vasoactive intestinal polypeptide-positive interneurons (VIP+). PV+ cells represent the most prominent group. They target cell bodies of pyramidal neurons and are surrounded by perineuronal nets (PNN), an extracellular matrix that protects and stabilizes their connections (Fader et al., 2016; Happel et al., 2014). SOM+ and VIP+ interneurons are present in smaller numbers than PV+ interneurons. SOM+ cells target distal dendrites of excitatory neurons, while VIP+ preferentially target SOM+ and, to a lesser extent, PV+ neurons (Pi et al., 2013). These different target sites of cortical inhibitory interneurons result in their distinct modulation of excitatory neuronal responses. PV+ interneurons provide fast and robust inhibition (Li et al., 2015). Their response patterns are somehow similar to excitatory neurons as they also receive feedforward ascending inputs from L4 but then provide feedforward inhibition to excitatory neurons (Barbour and Callaway, 2008). SOM+ interneurons exert sustained focal inhibition of synaptic inputs to excitatory cells. They do not receive direct ascending inputs; thus, their spiking is significantly delayed compared to the excitatory population (Adesnik et al., 2012). Their late feedback inhibition was suggested to effectively modulate responses to longer duration or spectrally complex sounds (Li et al., 2015). In contrast, the intricate pattern of connectivity of VIP+ interneurons did not allow to establish a clear relationship between their target site and network modulation (Rudy et al., 2011). Until now, only one study tried to assess the differences in interneuron populations between A1 and AAF in mice. This study reported more fast-spiking PV+ cells and perineuronal nets surrounding cell bodies in the AAF than in the A1 (Reinhard et al., 2019). The same study compared the number of SOM+ cells between A1 and AAF and did not find any differences. No study has yet analyzed the level of VIP+ interneurons between two primary regions.

### 1.3.4. Connectivity

A1 and AAF are highly interconnected. In cats, it was shown that A1 provides ~48% of the cortical input to AAF, and AAF supplies ~45% of the cortical input of A1 (Lee and Winer, 2008b). However, modulation of acoustic information between A1 and AAF in the cat's ACx was shown to be dominated by a unidirectional AAF to A1 pathway (Carrasco and Lomber, 2009a). After deactivation of AAF, neurons in A1 decreased their response strength, increased their response thresholds, and showed sharpened tuning fields. In contrast, A1 deactivation did not produce any discernible changes in AAF neuronal responses. These studies led to the speculation that AAF demonstrates an actual primary auditory cortex (response dependent only on thalamic input), whereas A1 reflects features of both

primary and secondary field (response dependent on information from another cortical region). On the contrary, later optogenetic experiments in rats showed that the activation of A1 enhances the sound-evoked responses in AAF, and A1 deactivation results in the opposite effect (Zhang et al., 2017), revealing the existence of A1 to AAF pathway modulation. Thus, the exchange of information between A1 and AAF seems to differ among species and requires more studies to confirm previous findings.

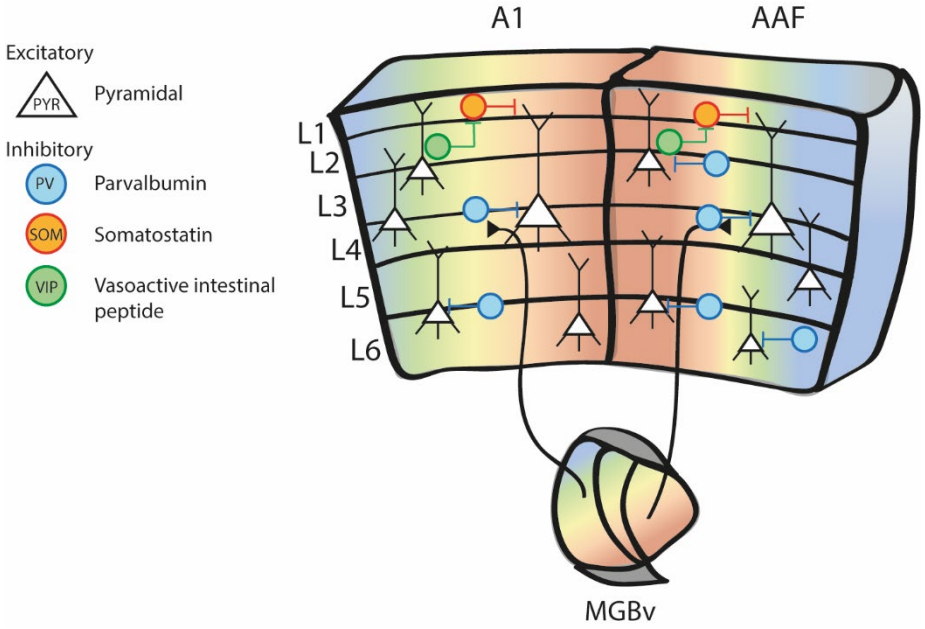


**Figure 3** Architecture, layers, and cell types in A1 and AAF. A1 and AAF receive inputs from non-overlapping MGB populations. MGB inputs to both A1 and AAF terminate mainly in layer 4. The tonotopy in A1 is highly regular. In AAF, cells tuned to middle frequencies are underrepresented. Three main groups of interneurons: parvalbumin, somatostatin, and vasoactive intestinal peptide, are present within both A1 and AAF. The inhibitory network of parvalbumin interneurons is denser within AAF than A1.

### 1.3.5. Projection targets

A1 and AAF project to many common subcortical and cortical targets, but each field also has its target preference. Both regions project to frontal and parietal cortices, striatum, medial geniculate body, and inferior colliculus, where they innervate common or distinct parts of the nuclei (Nakata et al., 2020). It was recently shown that A1 projects more to visual fields, suggesting that it provides auditory information for association with visual information (Nakata et al., 2020). In the same study, AAF was demonstrated to mainly project to the motor and somatosensory cortex, where it possibly provides auditory inputs for association with somatomotor information. These vastly different projection targets ultimately indicate that these fields can have a distinct role in sound processing and beyond.

### 1.3.6. Development

Studying how fields change their properties during postnatal development can reveal crucial functional differences between them. A very recent study compared postnatal development in A1 and AAF to test

if brain maturation mechanisms operate in parallel in those two primary auditory fields or if there are any substantial differences in functional development (Chen et al., 2021). They examined and compared the development of AAF and A1 in mice from postnatal day 11 to 40. They found that mouse A1 and AAF develop in parallel. Both fields exhibit tonotopy from hearing onset, and their temporal response develops slowly during the first postnatal month. This study did not reveal any striking developmental differences between the fields. Whether other response properties apart from tonotopy and response latency mature in parallel in A1 and AAF is still unknown.

### 1.3.7. Plasticity

In addition to differences in response properties, A1 and AAF display different plasticity levels. It was previously shown that noise exposure reduces the density of perineuronal nets in A1 but not in AAF and that A1 and AAF inhibitory cells are differently sensitive to developmental experience (Reinhard et al., 2019). Furthermore, in early-deafened cats, AAF becomes responsive to somatosensory and visual stimuli (Meredith and Lomber, 2011), while A1 does not (Kral et al., 2003), indicating a different level of plasticity. Distinct plasticity reflects functional differences between these auditory cortical areas upon the loss of auditory input.

### 1.3.8. Characteristic of neural responses

Even if A1 and AAF are pretty similar in terms of network architecture, cell composition, and general topography, neurophysiological studies in the auditory cortex revealed that some of the response properties are significantly different between both fields. A1 neurons have narrower tuning, lower response thresholds, and decreased spontaneous activity than AAF neurons, consistently in many species (Bizley et al., 2005; Guo et al., 2012; Imaizumi et al., 2004). It was also previously shown that responses to upward and downward frequency-modulated sweeps lead to distinct responses within A1 but indistinguishable responses within AAF, suggesting that A1 neurons have more robust directional selectivity (Bhumika et al., 2020). On the other hand, AAF neurons show faster temporal modulation than A1 neurons (Schreiner and Urbas, 1988), significantly shorter spectro-temporal receptive field durations and latencies (Linden et al., 2003), better timing precision (Christianson et al., 2011), and fast-pass selectivity for the rate of frequency-modulated sweeps (Trujillo et al., 2011). Despite this knowledge, it is still not clear whether their function in sound processing is distinct.

### 1.3.9. Role in sound processing

The different response characteristics of the auditory evoked responses in A1 and AAF have stimulated the idea that the two primary auditory fields have distinct roles in sound processing (Bizley et al., 2005; Carrasco and Lomber, 2009a; Guo et al., 2012; Linden et al., 2003; Polley et al., 2007). On the other hand, neurons within both fields have frequency tuning fields with similar thresholds and bandwidths, overlapping range of latencies, comparable amplitudes, and similar temporal dynamics of sound-evoked responses. Indeed, there are no known parameters of auditory evoked responses allowing distinguishing

if cells were recorded in A1 or AAF. It is challenging to understand whether minor differences in their neural responses reflect the distinct involvement of these fields in sound processing. Until now, no studies in mice revealed the role of A1 and AAF in sound processing. The reason for this could be manifold. First, more than 90% of studies on the primary auditory cortex were performed in A1, and surprisingly few have examined AAF. Second, most of the studies did not distinguish A1 and AAF and therefore treated those two regions as a one-unimodal field. As the mouse brain becomes the major model for auditory cortex research, it is crucial to understand the role of its two primary regions in sound processing.

## 1.4. Aim of this study

How the auditory cortex contributes to making sense of the acoustic world is far from understood (King et al., 2018). Identifying distinct roles for different auditory cortical regions in sound processing holds the key to understanding how an auditory signal is processed at the cortical level and ultimately leads to its perception. My Ph.D. project aimed to explore the functional role of the two primary auditory cortices in mice, to identify mechanisms contributing to their distinct sound processing and to explore how their neural activity drives a specific behavior.

## 1.5. Thesis outline

*Chapter 2* characterizes offset responses in A1 and AAF based on *in vivo* electrophysiological recordings in anesthetized mice. The analysis is performed on the offset responses evoked by the termination of both pure and harmonic tones. Laminar and local field potential analysis are used complementarily to investigate the subcortical or intracortical origin of offset responses in both primary cortices. Then offset response properties within both fast and regular spiking neurons are characterized in AAF. These results were published in 2019 in Scientific Reports (Solyga and Barkat, 2019).

*Chapter 3* describes the results of a study on the behavioral relevance and mechanisms driving cortical offset responses. First, it provides results of optogenetic deactivation experiments of AAF, where the importance of offset responses in AAF is assessed at the perceptual level. Second, electrophysiological recordings in AAF and MGB are combined with antidromic stimulation in AAF to reveal the proportion of offset responsive cells in AAF and its preceding nucleus and connections between them. Finally, offsets are characterized in both AAF and MGB in response to sounds with varied duration, spectral and temporal complexity to reveal differences in offset processing on the thalamic and cortical levels. These results have been described in a manuscript and are currently under review (Solyga & Barkat B, in review). They are also available as a preprint on BioRxiv (Solyga and Barkat, 2021).

*Chapter 4* provides an analysis of neural responses recorded in A1 and AAF of anesthetized mice evoked by spectrally simple (pure tones) and complex sounds (harmonic tones and missing fundamental frequency tones). The involvement of fast and regular spiking neurons from both primary auditory regions in complex sound processing is evaluated. A laminar analysis is also performed in both A1 and AAF to compare the processing of simple and spectrally complex sounds within the input and supragranular layers. These results have been described in a manuscript and will be submitted for publication (Solyga & Barkat A, in preparation).

*Chapter 5* provides an overview of the results, states their relevance for studies on the primary auditory cortex, proposes a new assignment of A1 and AAF in the stream processing theory framework, and discusses possible future study directions.

*Chapter 6* combines a set of preliminary results obtained during my Ph.D., indicating directions for future experiments. First, the use of the voltage-sensitive dye imaging technique for studies of processing in adjacent cortical regions is discussed. Then results from the electrophysiology recordings performed in IC are presented, and offset processing in this region is compared with MGB and AAF. Finally, AAF responses evoked by multi-jump mouse calls are evaluated.

*Chapter 7* includes final remarks.

# Chapter 2

# Distinct processing of tone offset in two primary auditory cortices

## 2.1. Abstract

In the rodent auditory system, the primary cortex is subdivided into two regions, both receiving direct inputs from the auditory thalamus: the primary auditory cortex (A1) and the anterior auditory field (AAF). Although neurons in the two regions display different response properties, like response latency, firing threshold, or tuning bandwidth, it is still unclear whether they process sound in a distinct way. Using *in vivo* electrophysiological recordings in the mouse auditory cortex, we found that AAF neurons have significantly stronger responses to tone offset than A1 neurons. LFP and laminar analysis suggest that differences in sound responses between these two primary cortices are both of subcortical and intracortical origin. AAF neurons also display faster and more transient responses than A1 neurons. Additionally, offset responses in AAF – unlike in A1, increase with sound duration. These results emphasize the potentially critical role of AAF for temporal processing. Our study reveals a distinct role of two primary auditory cortices in tone processing and highlights the complexity of sound encoding at the cortical level.

## 2.2. Graphical abstract

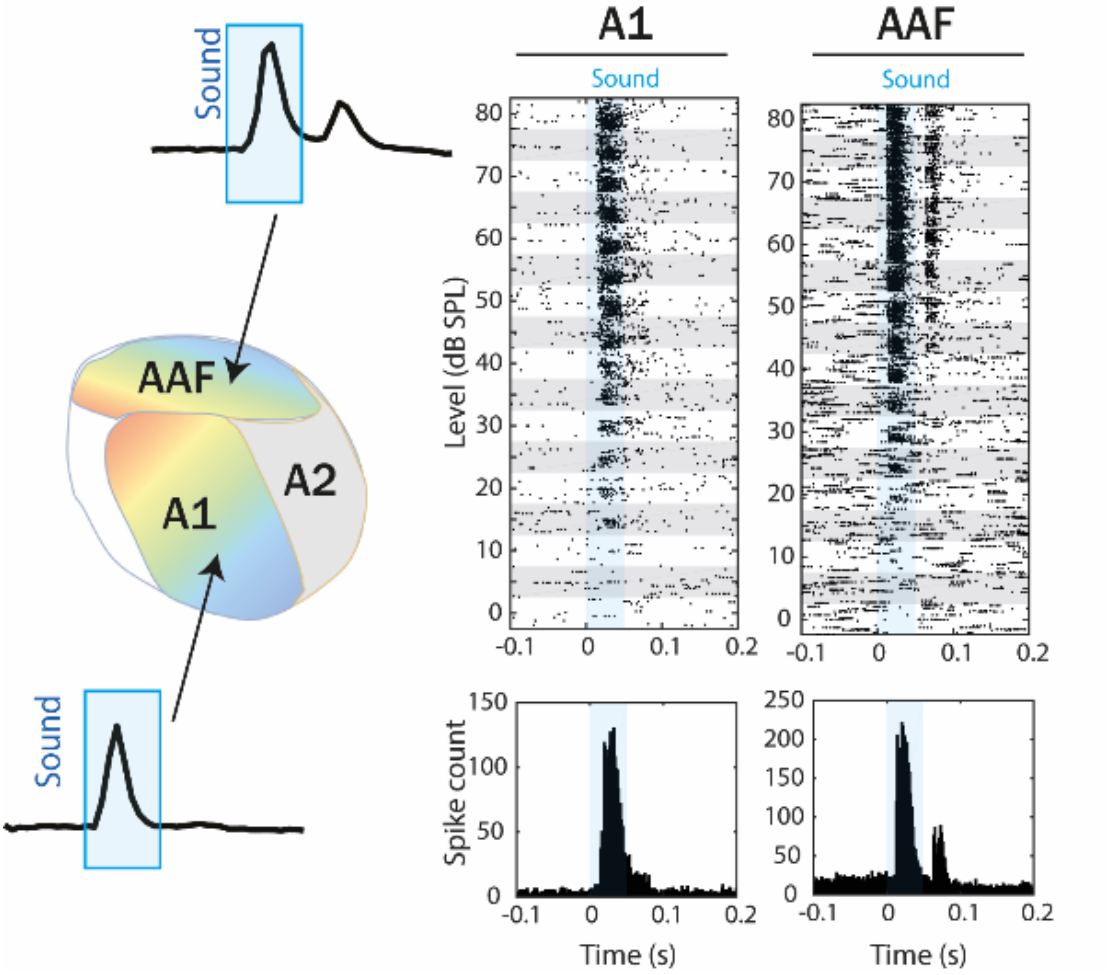


**Highlights:**

- AAF neurons have significantly stronger responses to tone offset than A1 neurons.
- LFP and laminar analysis suggest that differences in sound responses between these two primary cortices are both of subcortical and intracortical origin.
- AAF neurons display faster and more transient responses than A1 neurons.
- Offset responses in AAF – unlike in A1, increase with sound duration.
- These results emphasize the potentially critical role of AAF for temporal processing.

## 2.3. Introduction

For sound perception, auditory signals have to travel a long way from the cochlea through the cochlear nuclei, superior olivary complex, inferior colliculus, and auditory thalamus up to the auditory cortex, where two regions, A1 and AAF, receive them in parallel. An early study already distinguished A1 and AAF as two separate auditory fields in mice based on anatomical and functional parameters (Stiebler et al., 1997). Tracing experiments in cats and mice confirmed parallel connections from the thalamus to both A1 and AAF (Lee and Winer, 2011; Takemoto et al., 2014) and showed that in cats, the vast majority of thalamocortical projections to AI and AAF originate from largely non-overlapping cell groups of the medial geniculate body (MGB) (Lee et al., 2004).

A1 and AAF are both tonotopically organized but differ in the proportion of cortical area tuned to specific frequencies. In cats and ferrets, A1 neurons tuned to different frequencies are evenly distributed but AAF is characterized by an underrepresentation of cells tuned to mid-range frequencies (Bizley et al., 2005; Carrasco and Lomber, 2009a; Imaizumi et al., 2004). Additionally, A1 neurons have narrower tuning, lower response thresholds, and decreased spontaneous activity compared to AAF neurons, consistently in many species (Bizley et al., 2005; Guo et al., 2012; Imaizumi et al., 2004). On the other hand, AAF neurons show faster temporal modulation than A1 neurons (Schreiner and Urbas, 1988), significantly shorter spectro-temporal receptive field durations and latencies (Linden et al., 2003), better timing precision (Christianson et al., 2011), and fast-pass selectivity for the rate of frequency-modulated sweeps (Trujillo et al., 2011). Despite this knowledge, it is still not clear whether their function in sound processing is distinct.

Using *in vivo* electrophysiological recordings in the mouse auditory cortex, we asked whether any tone properties are processed differently in these two primary auditory fields. Our results reveal significantly stronger responses to sound offset in AAF than in A1 neurons. Offset responses were reported previously in auditory cortex (ACx) neurons (Kopp-Scheinpflug et al., 2018; Metherate et al., 2005), but their distinct properties in A1 and AAF were not described. Considering several inter stimuli interval and sound durations, we show that offset is robust in AAF but not in A1 and is positively correlated with sound duration. Local field potentials (LFP) analysis indicates that offset responses are not emergent in the cortex but are of subcortical origin. Comparing response strengths between input (L4) and supragranular (L2/3) layers also suggest that offset responses are equally important in both layers in AAF, unlike in A1, where offsets in the input layers are dominating. Additionally, recordings from AAF neurons revealed that offset responses are poorly tuned and have weak tonotopy. Finally, we demonstrate that offset responses, even if significantly higher in fast-spiking than in regular spiking neurons, are not specifically attributed to one of these two cell types. Our study reveals a crucial function of AAF in processing tone offsets, and thereby the possibility of distinct roles in sound processing for these two primary auditory cortices.

## 2.4. Results

### 2.4.1. Responses to sound onsets and offsets are distinct in A1 and AAF

We first confirmed the primary nature of A1 and AAF by verifying that these two cortical regions receive parallel signals from MGB, combining *in vivo* multi-electrode electrophysiological recordings and retrograde tracing. Both regions were identified based on their functional tonotopy. Pure frequency tones (PTs) varying in frequency from 4 to 48.5 kHz and in level from 0 to 80 dB SPL presented with randomized inter-stimulus-intervals (ISIs) (500 - 1000 ms) were used to determine tuning receptive fields (TRFs). By simultaneous recordings with 4 shank probes (200 µm distance between shanks in a 4x8 electrode configuration), we identified A1 and AAF based on their caudo-rostral and diagonal ventro-dorsal increase in best frequency, respectively. We then injected retrograde tracers in both regions, identifying somas of neurons projecting to A1 or AAF. Confocal imaging of the thalamocortical slices revealed a robust signal in the MGB, confirming that both A1 (Figure 4a) and AAF (Figure 4b) receive signals from the auditory thalamus (Lee and Winer, 2011; Takemoto et al., 2014). Moreover, this reinforced our identification of A1 and AAF through functional tonotopy, in respect to them being both primary cortices (Figure 4c). In subsequent experiments, we therefore based the identification of A1 and AAF on functional tonotopy only.

We then compared sound-evoked response patterns in A1 and AAF. Voltage traces across 32 channels were processed to extract single-unit cluster (SU) activity leading to 202 SU in AAF (7 animals) and 192 in A1 (6 animals). We confirmed that auditory responses have shorter onset latencies in AAF than in A1 neurons (Figure 4d, e) (Bizley et al., 2005; Guo et al., 2012; Imaizumi et al., 2004; Linden et al., 2003). In addition, our data revealed a gradient of response latencies in A1 (neurons tuned to high frequencies respond faster than neurons tuned to low frequencies) and no gradient in AAF (all neurons responded at a similar time independently of their best frequency (BF), defined as the frequency that elicited maximal response across all sound levels; see methods). Even more striking, responses to 50 ms long PTs revealed robust offset responses in AAF neurons, whereas less prominent offset was seen in A1 (Figure 4f-h; Supplementary Figure 2.1: Raster plot of Figure 4f at higher resolution). By grouping A1 and AAF responses according to the neuron's BF, we saw an increase in the average firing rate following the end of the sound, confirming that offset responses in AAF are not frequency specific (Figure 4i, increase in spike count following the end of the blue shadow (tone presentation)).

The analysis of the response decay in A1 and AAF (single exponential decay functions least-squares-fitted to PSTH of each neuron; Supplementary Figure 2.2) allowed us to define other clear criteria to distinguish between A1 and AAF cells. Neurons in A1 showed significantly more sustained responses than AAF neurons (Figure 4i, j). The lack of significance for neurons with BF higher than 32 kHz could be due to a lack of power (n= 8 and 4).

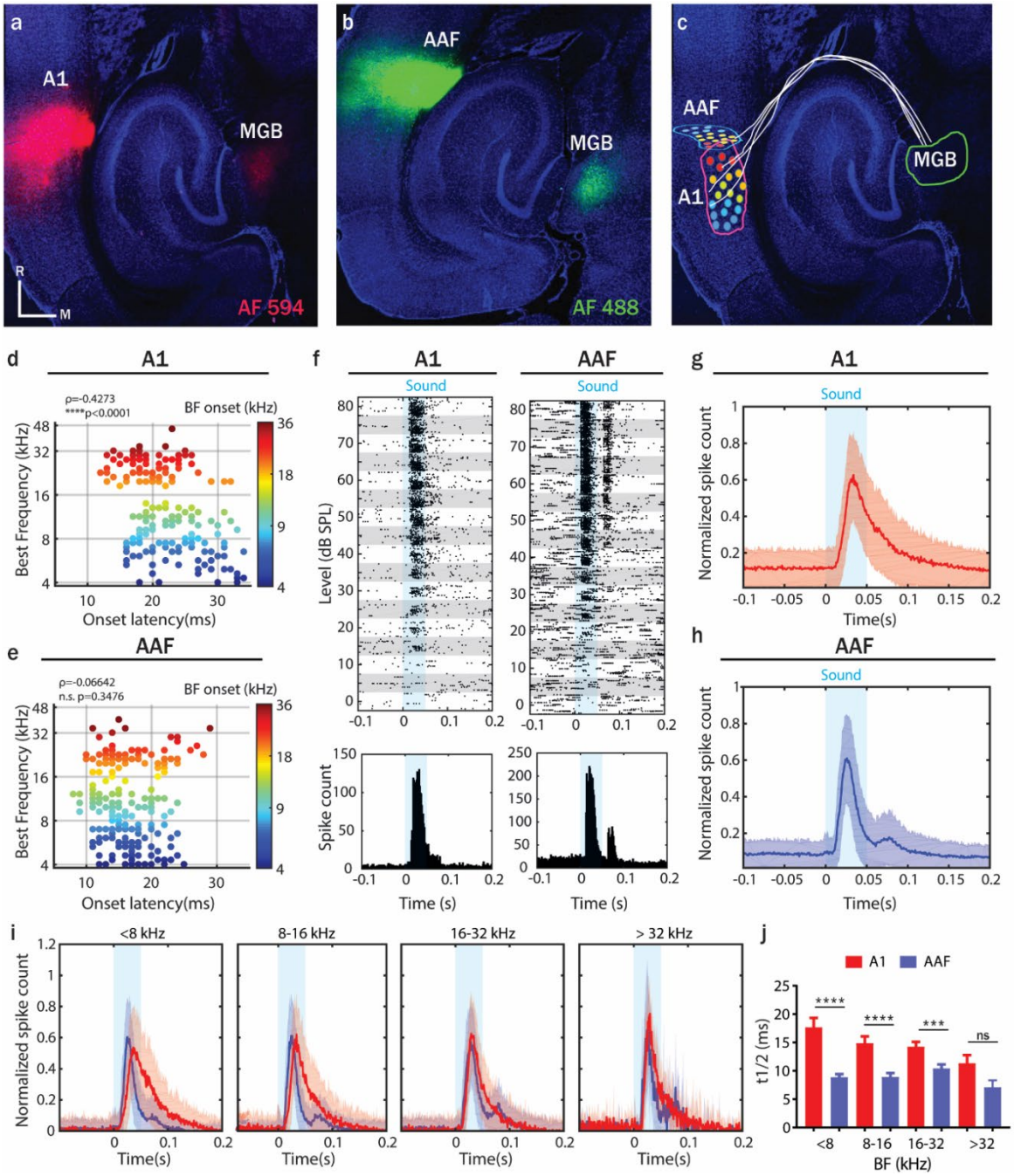


**Figure 4 Responses to sound onsets and offsets are distinct in A1 and AAF.** (**a, b**) Thalamocortical slice with CTB-red injected into A1, CTB-green injected into AAF and retrogradely labeled cells in MGB. (**c**) Thalamocortical slice with a schematic indication of MGB, A1, AAF, their neural connections, and tonotopy. The color code is as in d. (**d, e**) Comparison of response latencies for differently tuned neurons in A1 and AAF. Latencies are color-coded to the neuron's onset BF (correlation between onset latencies and BF: A1, $\rho$=-0.4273, p<0.0001, n=192; AAF, $\rho$=-0.0664, p=0.3476, n=202; Spearman correlation). (**f**) Raster plot and peristimulus time histogram (PSTH) of an example A1 (left) and AAF (right) neuron's response to PTs (frequency varying between 4 - 48.5 kHz, sound level varying between 0 – 80 dB SPL, inter-stimulus-intervals equally distributed between 500 and 1000 ms). The blue shaded bar represents the tone presentation. (**g, h**) Average PSTH of A1 and AAF responses to PTs (same sound stimuli as in f). Panels **g**, **h,** and **i** depict average responses collapsed across frequencies and sound levels. (**i**) Average PSTH of A1 (red) and AAF (blue) responses to PTs grouped according to their onset BF. (**j**) Comparison of half decay time (t½) of responses in A1 and AAF neurons grouped according to their onset BF. Time of half decay (t1/2): A1: 17.67 ms (n=39); 14.9 ms (n=38); 14.26 ms (n=63); 11.35 ms (n=8); AAF: 8.88 ms (n=71); 8.95 ms (n=63); 10.42 ms (n=55); 7.14 ms (n=4) for neurons with BF <8 kHz, 8 16 kHz, 16-32 kHz, >32 kHz respectively). Data represent mean ± SEM. ***p=0.0003, ****p<0.0001, n.s. p=0.1535, Mann-Whitney test.

Response characteristics are to various degrees influenced by anesthesia (Joachimsthaler et al., 2014; Wang et al., 2008). Therefore, we compared recordings in anesthetized and awake mice to establish whether offset responses were not induced by a specific anesthetized state. We tested the same sound protocol as in the previous anesthetized experiment. We extracted 104 and 173 SU from awake recordings in A1 (5 animals) and AAF (6 animals), respectively. Similar to our results in anesthetized preparations, offset responses in awake mice were robust in AAF and weak in A1 (Supplementary Figure 2.3). We also compared the strength of offset responses between anesthetized and awake conditions. Spike rates at the offset were higher in A1 and AAF for awake recordings, but this increase was bigger and more significant in AAF neurons (Supplementary Figure 2.4). This confirms the validity and relevance of our findings for awake and behaving conditions.

### 2.4.2. Offset responses are significantly stronger in AAF

These robust offset responses in AAF may be a crucial indicator of distinct roles of A1 and AAF in sound duration encoding. Thus, we investigated whether offset responses in AAF were correlated to sound duration. We recorded responses to 60 dB SPL PTs (9 kHz) repeated 10 times with varying duration (50 - 500 ms) and ISI (50-2000 ms) (Figure 5a). Based on responses to 500 ms tones played with 2000 ms ISI we found robust offset responses (higher than 2 standard deviations above the spontaneous activity) locked to the sound duration in 86.3 % (164/190) of auditory responsive cells in AAF but in only 40.3 % (77/191) of A1 neurons (Figure 5a, b). In A1, a cluster of cells tuned to high frequencies showed bigger offset responses than neurons with other BFs (Supplementary Figure 2.5). This could be caused by recordings at the edge of A1/AAF, where neurons with high BF are located, or simply represent an offset responsive neuron cluster in A1. We also found that offset responses in AAF increase with sound duration, unlike in A1 (Figure 5c). The strength of offset relative to onset responses was significantly higher in AAF than in A1 for sounds with longer duration (Figure 5c, d). The high offset responses reported for the shortest sounds (50 ms) in A1 neurons result from the overlap between onset and offset responses with these short sounds (Figure 5c, d).

We then estimated the forward suppression that could potentially be caused by offset responses based on the relationship between onset response amplitudes and ISIs. There was no significant difference in forward suppression between A1 and AAF neurons (Figure 5e, f). We additionally analyzed the correlation between offset and onset responses at each ISI (Supplementary Figure 2.6). We found a positive correlation between offset and onset response in both A1 and AAF, demonstrating that the stronger offsets do not influence the following onset response, even when the time between the end of a tone and the start of the next one is short. These results are another indication that onset and offset responses might be driven by non-overlapping sets of synapses (Scholl et al., 2010).

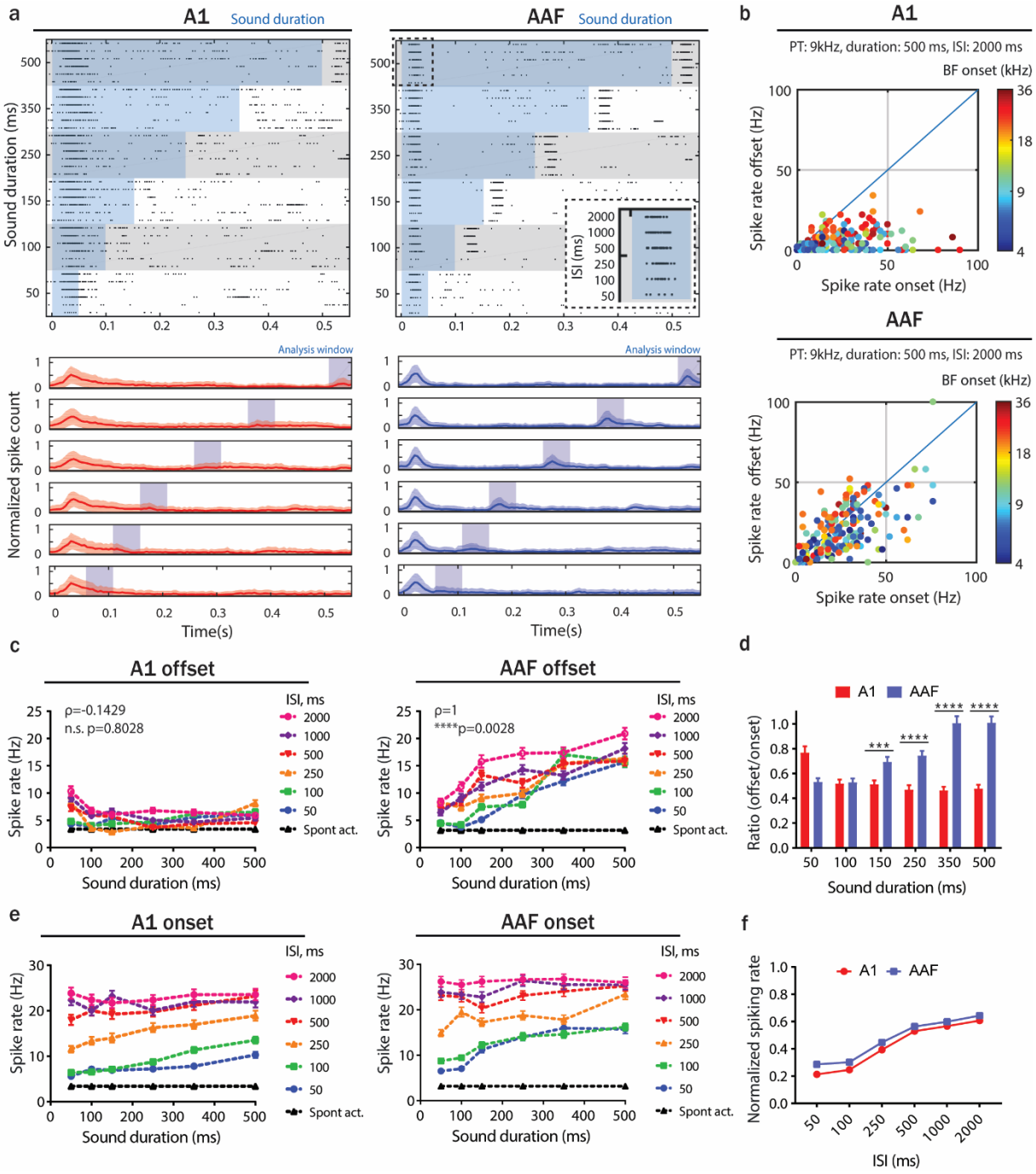


**Figure 5 Offset responses are significantly stronger in AAF than in A1.** (**a**) Raster plot of the example A1 (top-left) and AAF (top-right) neuron's response to 9 kHz PTs played at 60 dB SPL with sound duration varying between 50 and 500 ms and ISI between 50 and 2000 ms and (bottom) PSTH averaged over all neurons population. The blue shaded bars represent the tone. (**b**) Comparison of strength of onset and offset responses in A1 and AAF for 500 ms 9 kHz PTs played with 2000 ms ISIs. Responses are color-coded to onset BF. (**c**) A1 (left) and AAF (right) offset responses to 9 kHz PTs with increasing duration across all ISIs' (correlation between sound duration and response rate: A1, $\rho$=-0.1429, p=0.8028, n=191; AAF, $\rho$=1, **p=0.0028, n=190, Spearman correlation). (**d**) The ratio of offset/onset responses in A1 and AAF for 9 kHz PTs with varying durations (50 – 500 ms) and 2000 ms ISI. Data represent mean ± SEM. ****p<0.0001, ***p=0.0007, Mann-Whitney test. (**e**) Onset responses of A1 (left) and AAF (right) neurons evoked by 9 kHz PTs of different durations (ISIs varied between 50 and 2000 ms). (**f**) Comparison of A1 and AAF onset responses to 9 kHz PTs (500 ms duration) with ISI varied between 50 and 2000 ms. There was no significant difference in forward suppression: p=0.5887, Mann-Whitney test. Spike rates were normalized to the maximum response of each neuron.

### 2.4.3. Robust offset responses in AAF are not unique to pure frequency tone stimulations

In the previous experiments, we used PTs of different frequencies, levels, and durations to investigate the presence of offset responses. To investigate whether offset responses were specific to pure frequency tone stimulation, we performed the same experiment with harmonic tones (HTs) instead of PTs. HTs consisted of four frequency components: $f_0$, $f_1$, $f_2$ and $f_3$, where $f_1=2*f_0$; $f_2=3*f_0$; $f_3=4*f_0$. We recorded responses to 60 dB SPL HTs (9, 18, 27, 36 kHz) with varying duration (50 – 500 ms) and ISIs (50 - 2000 ms) (Figure 6a, b). Based on responses to 500 ms HTs played with 2000 ms ISI we found robust offset responses in 88.4% of auditory responsive cells in AAF and 61.8% in A1. As for PT, we found offset responses increasing with sound duration in AAF but not in A1 (Figure 6c, d). Comparing responses to PT and HT demonstrated that the strength of offset relative to onset responses was significantly higher for HTs than for PTs (Supplementary Figure 2.7). In AAF, HTs did not cause any significant change in offset/onset ratio compared to PTs. Therefore, although the number of A1 cells with significant offset responses to HT was increased compared to PTs, the strength of offset relative to onset responses was again significantly higher in AAF than in A1 for all sound durations longer than 50 ms (Figure 6d). These results lead to the conclusion that predominant offset responses in AAF are not unique to PT stimulations.

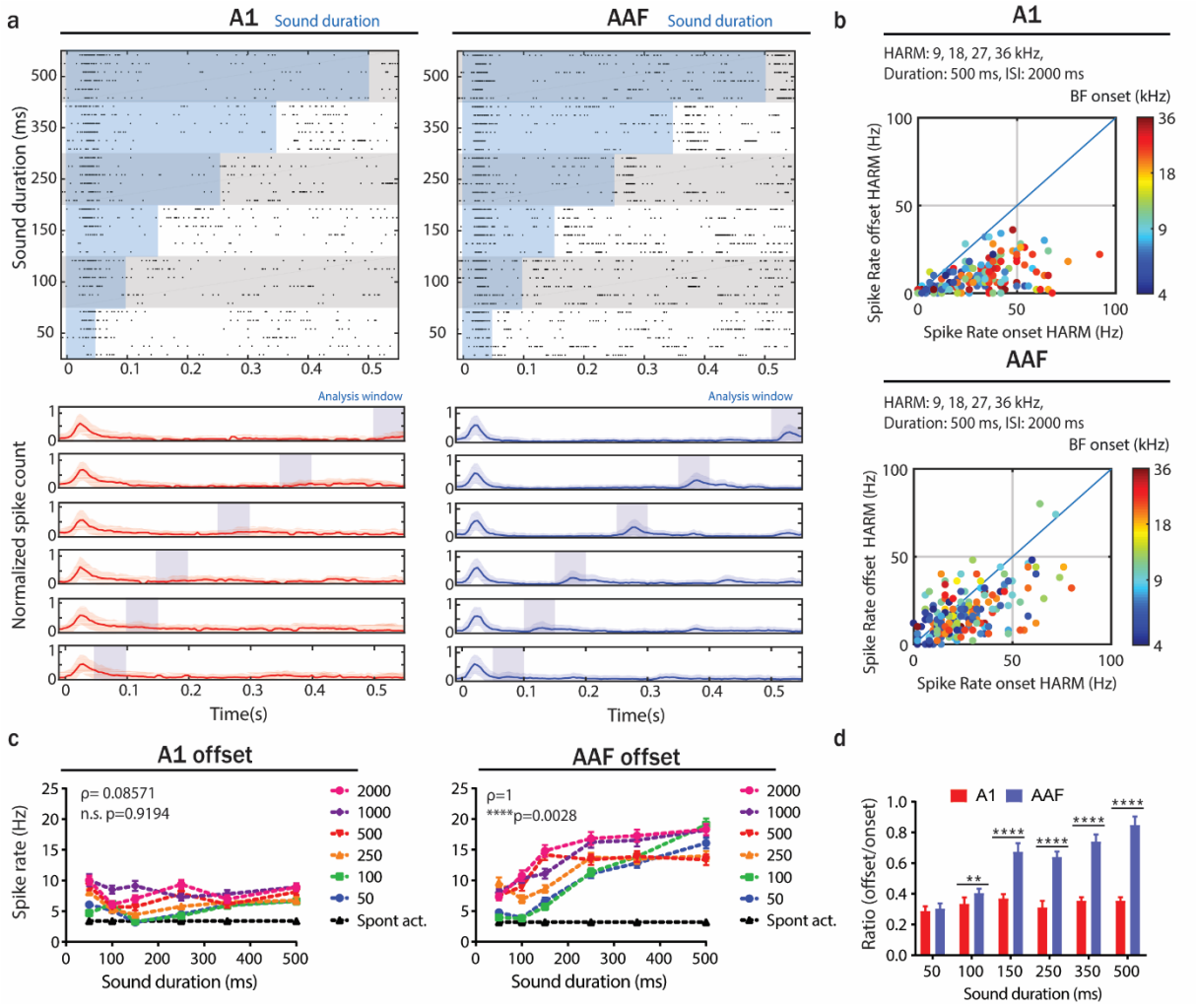


**Figure 6 Offset responses to harmonic tone stimulation are more robust in AAF than in A1.** (**a**) Raster plot of an example A1 (top-left) and AAF (top-right) neuron's response to HTs (9+18+27+36 kHz) played at 60 dB SPL with sound duration varying between 50 and 500 ms and ISI between 50 and 2000 ms and (bottom) PSTH averaged over all neurons. The blue shaded bars represent the tone presentation. The example neurons do not correspond to those presented in Figure 5a. (**b**) Comparison of strength of onset and offset responses in A1 and AAF neurons for 500 ms HTs (9+18+27+36 kHz) played with 2000 ms ISIs. Responses are color-coded to the onset BFs. (**c**) A1 (left) and AAF (right) offset responses to HTs (9+18+27+36 kHz) with increasing duration across all ISIs' (correlation between sound duration and response rate: A1, $\rho$= 0.0857, p=0.9194, n=191; AAF, $\rho$=1, p=0.0028, n=190, Spearman correlation). (**d**) The ratio of offset/onset responses in A1 and AAF for HTs (9+18+27+36 kHz) with varying durations (50 – 500 ms) and 2000 ms ISI. Data represent mean ± SEM. ****p<0.0001, **p=0.0031, Mann-Whitney test.

### 2.4.4. Offset responses do not emerge in the cortex

We next performed local field potential (LFP) analysis of our recordings. Based on the protocols with varied sound duration and intervals, we could see, as for the spike rate analysis (Figure 5), that offset responses in AAF were more robust than in A1 for both PTs (9 kHz; Figure 7a, b) and HTs (9+18+27+36 kHz; Supplementary Figure 2.8). LFP peak amplitude at the sound offset increased together with sound duration (Figure 7b) as previously shown with spike analysis (Figure 5c, right panel). The presence of offset responses within the A1 and AAF LFP signals suggests that offset responses are likely to be inherited from subcortical nuclei rather than only arising in primary auditory regions.

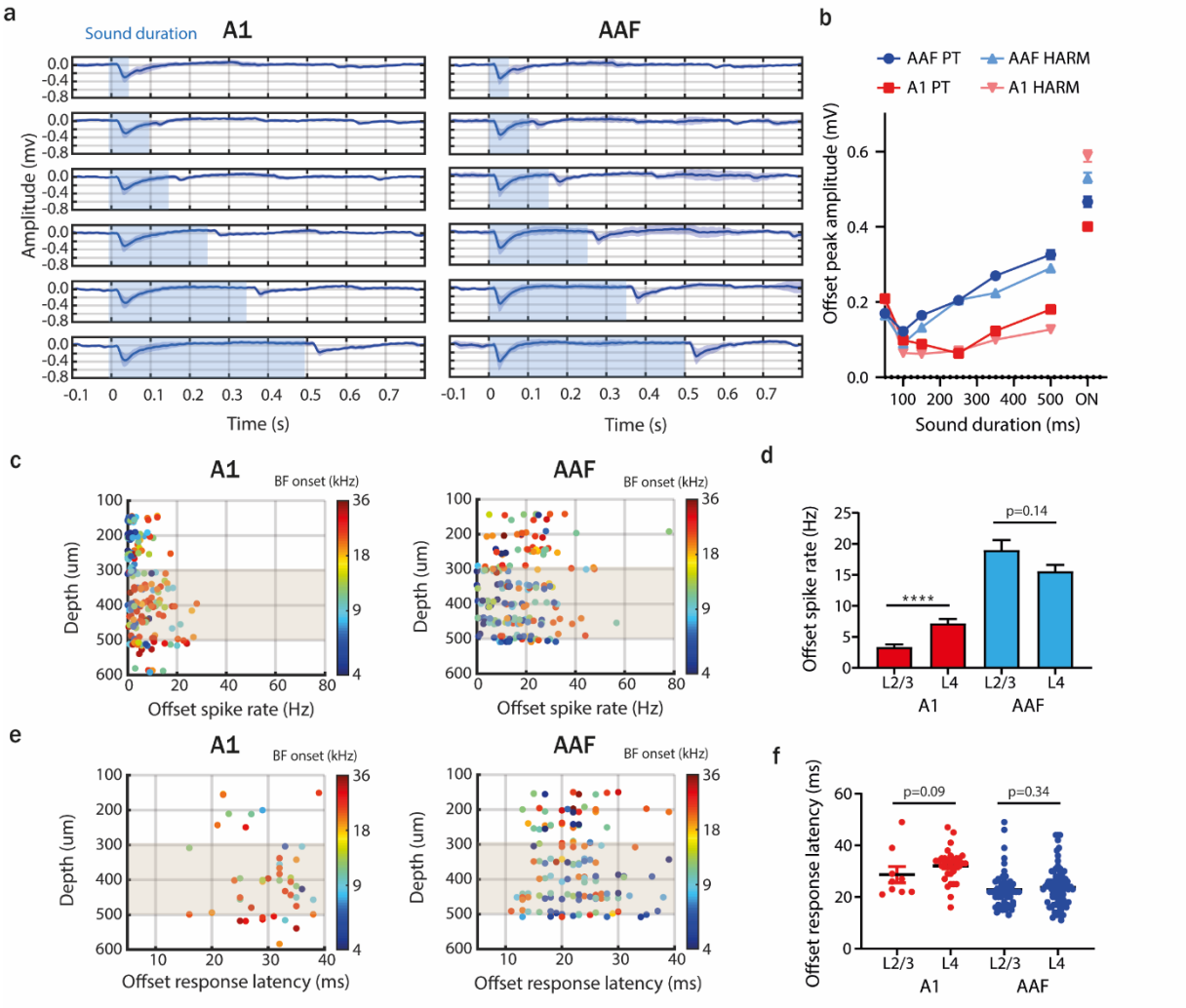


**Figure 7 Offset responses do not emerge in the cortex. (a)** Averaged LFP signal from A1 (6 animals) and AAF (7 animals) neurons in response to 9 kHz PTs played at 60 dB SPL with sound duration varying between 50 and 500 ms and ISI between 50 and 2000 ms. The blue shaded bars represent the tone. **(b)** Comparison of onset and offset peak amplitude of LFP signal in A1 and AAF neurons in response to PTs and HTs with different durations. Data represent mean ± SEM. **(c)** Offset spike rate in A1 (left) and AAF (right) neurons as a function of recording site depth. Responses are color-coded to the neuron's onset BF. The gray shaded bars represent L4. **(d)** Comparison of offset spike rate in L2/3 and L4 of A1 and AAF neurons. Data represent mean ± SEM. (A1: ****p<0.0001, L2/3 n=72; L4 n=88; AAF: p=0.14, L2/3 n=69; L4 n=128, Mann-Whitney test) **(e)** Offset response latency in A1 (left) and AAF (right) neurons as a function of recording site depth. Responses are color-coded to the neuron's onset BF. The gray shaded bars represent L4. **(f)** Comparison of offset spike rate in L2/3 and L4 of A1 and AAF neurons. Data represent means and individual values. (A1: p=0.09, L2/3 n=9; L4 n=31; AAF: p=0.34, L2/3 n=52; L4 n=76, Mann-Whitney test).

Our recordings span the range of 150 µm to 600 µm from the pia surface, corresponding mainly to L2/3 (150-300 µm) and L4 (300-500 µm) (Meng et al., 2017). By analyzing offset responses as a function of recording depth, we show that offset responses are of similar amplitude in all recorded depths in AAF, whereas A1 displays significantly stronger responses in L4 than in L2/3 (Figure 7c, d). This suggests that, in addition to receiving them from subcortical nuclei in the input layer (L4), offset responses are further processed in supragranular layers (L2/3) of AAF but less so in A1. An analysis of latencies indicates that AAF offset responses appear slightly faster, although not significantly, in L4 than in L2/3

(Figure 7e, f). Interestingly the opposite is observed in A1, where offset responses appear slightly faster in L2/3 than in L4 (p=0.09), suggesting that A1 L2/3 offset responses could possibly be of a different origin than the input layer. Altogether, these results indicate that the difference between A1 and AAF offset processing could have two origins. First, AAF receives a stronger offset in the input layer than A1. Second, intracortical processing of offset responses in L2/3 is stronger in AAF than in A1.

### 2.4.5. Offset responses in AAF have weak tonotopy, irregular tuning and are present in both fast and regular spiking neurons

Because of their predominance in AAF, we then characterized offset as a function of onset responses in this primary cortical region. First, we compared onset and offset TRFs for all recorded AAF neurons. We found a few neurons with the clear onset and offset tuning (Figure 8a). Most other cells revealed very broad, irregular, and poorly tuned offset receptive fields (Figure 8b, c). By aligning onset and offset BFs of the recorded neurons according to the electrode shafts, our analysis revealed a robust tonotopy for onset (Figure 8c) but weaker tonotopy for offset responses (Figure 8d). Significant tonotopy for onset was also confirmed for A1 (Supplementary Figure 2.9; $\rho$=0.719, ****p<0.0001, Spearman correlation). 70.7 % of offset responses were tuned to higher frequencies than onset responses, 26.0 % to lower frequencies, and 5.3 % showed the same BF for onset and offset responses (Figure 8e, f; tolerance: 0.1 octaves).

We then asked whether different cell types play distinct roles in the onset and offset responses. We distinguished fast (FS) and regular (RS) spiking neurons based on their spike waveforms and analyzed their responses to 9 kHz PTs played at 60 dB SPL for 500 ms. The peak-to-trough times (p2t) of our sorted units gave a bimodal distribution (Figure 8g; bin size=0.05 ms). FS units were defined as having a p2t smaller than the minimum between the two peaks of the p2t distribution (0.575 ms), in accordance with previous studies (Moore and Wehr, 2013). FS units had significantly shorter onset (Figure 8h, FS: 15.42±1.57, n=12 RS: 20.47±0.51, n=149 cells) and offset (Figure 8i, FS: 17.91±1.25, n=11, RS: 24.09±0.67, n=124 cells) response latencies than RS cells, indicating that FS neurons can play an important role in processing sound onset as well as offset. However, even if significantly stronger in FS than RS cells, offset responses were highly robust in both cell populations (Figure 8j, FS: 33.43±6.33, n=14 cells, RS: 18.33±1.03, n=175 cells), suggesting that offset responses are not specifically attributed to one of these two cell types.

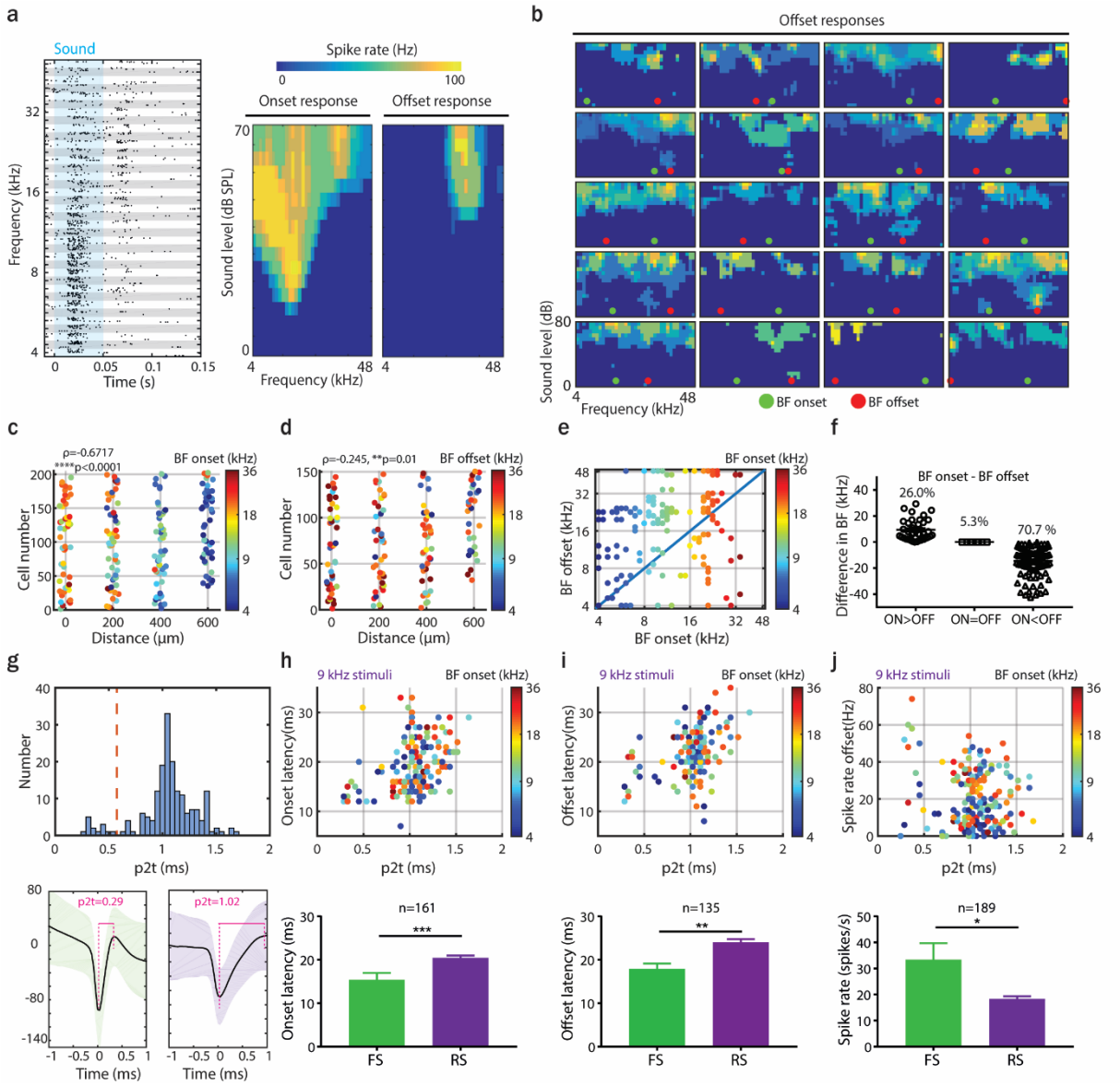


**Figure 8 Offset responses in AAF have weak tonotopy, irregular tuning and are present in both fast and regular spiking neurons.** (**a**) Example of distinct tuning receptive fields (TRF) of onset and offset responses of an AAF neuron. (**b**) Examples of offset TRF of AAF neurons with an indication of onset (green) and offset (red) BF. (**c**, **d**) Comparison of onset and offset BF of AAF neurons, displayed as a relative distance between electrode shafts. Responses are color-coded to onset (c) or offset (d) BF (correlation between BF and relative distance between electrode's shaft: onset, $\rho$=-0.6717, ****p<0.0001, n=202; offset, $\rho$=-0.245, **p=0.01, n=150, Spearman correlation). (**e, f**) Comparison of onset and offset BF for AAF neurons (responses are color-coded to the neuron's onset BF). (**g**) Distribution of peak-to-trough times (p2t) of AAF neurons. The red line defines the middle of the bimodal distribution (p2t=0.575). Example of fast (p2t=0.29; bottom left) and regular (p2t=1.02; bottom right) spiking unit waveforms. (**h**) Comparison of onset latency to onset responses as a function of p2t of spike waveforms to 9 kHz PT (top). Responses are color-coded to onset BF. Corresponding average values for FS and RS neurons (bottom). Data represent mean ± SEM. ***p=0.0003, Mann-Whitney test. (**i**) Comparison of response onset latency of offset responses as a function of p2t of spike waveforms (top). Corresponding average values for FS and RS neurons (bottom). Data represent mean ± SEM. **p=0.0019, Mann-Whitney test. (**j**) Comparison of offset response spike rates as a function of p2t of spike waveforms (top). Corresponding average values for FS and RS neurons (bottom). Data represent mean ± SEM. *p=0.02, Mann-Whitney test.

## 2.5. Discussion

Distinguishing responses to sounds in different auditory cortical regions is crucial to understand how auditory signals are processed at the cortical level. Here we reveal for the first time a higher percentage of neurons responding to sound offset in AAF in comparison to A1. Our observations were drawn from the analysis of neuronal response properties in both anesthetized and awake conditions, with pure or harmonic tones as the auditory stimuli. Our results also reveal that offset responses are equally represented in both input and supragranular layers in AAF, but not in A1, where offsets in the input layers dominate. Finally, we demonstrate that offset responses in AAF, even if significantly higher in FS than in RS neurons, are not explicitly attributed to one of these two cell types. Altogether, our results indicate that both subcortical input and intracortical processing differences contribute to the distinct processing of sound offsets in A1 and AAF.

The high number of offset responses in AAF (more than 85%) has not been previously reported. In general, there has been a significant asymmetry in the relevance of excitatory onset and offset responses in auditory processing. Previous studies reported 25-75% of offset responsive cells (Joachimsthaler et al., 2014; Moshitch et al., 2006; Qin et al., 2007; Qin et al., 2009; Scholl et al., 2010) or even absence of them in A1 (Phillips et al., 2002), but none reported their prevalence in AAF. The fact that the prevalence of offset responses in AAF compared to A1 was not reported before may be manifold. First, most previous studies aimed at investigating offset responses focused on A1, whereas AAF – identified by our study to be crucial for offset, was often neglected. Then, offset responses are highly influenced by duration (Figure 5c), intensity as well as the rise-fall time of the sound (Qin et al., 2007; Scholl et al., 2010; Takahashi et al., 2004), raising the possibility that AAF offset responses could not be seen due to the characteristics of the stimuli used in previous studies. Finally, the use of pentobarbital as an anesthetic might explain the lack of offset responses in some studies. Our anesthetized recordings under ketamine confirm that this anesthetic does not prevent offset response occurrence (Figure 4f, g).

Auditory responses are shaped by stimulus characteristics. For example, our data reflect an increase in the percentage of offset responses evoked in A1 neurons by HTs compared to PTs. This substantial increase was not observed in AAF. HTs elicit bigger auditory responses than PTs in general, and they could therefore contribute to an increased number of offset cells in A1. The lack of increase in AAF could be explained by the fact that the percentage of offset responses to PTs is already high in this brain region. Another possibility could be that A1 and AAF display the different amount of offset responses for distinct stimuli. A broader group of sounds should be tested to fully address this question.

We found offset responses in more than 40 % of A1 and 80 % of AAF neurons. These percentages lead us to expect a bigger involvement of AAF in offset processing, but we cannot exclude the potential functional importance of A1 for the processing of sound termination. In general, it is known that the proportion of offset cells increase in awake animals, especially when animals are engaged in a behavioral task. For example, offset responses were found in 90% of A1 neurons in awake monkeys attending to

tones (Tian et al., 2013). In our study, we measure an increase of offset response strength from anesthetized to awake conditions in A1, but this increase is even higher in AAF (Supplementary Figure 2.4), confirming this field's importance again for offset processing.

Within AAF, onset and offset responses also encode auditory information differently. Their distinct tuning fields (Figure 8a, b), contrasting tonotopy (Figure 8c, d), and lack of offset-onset forward suppression (Figure 5f, Supplementary Figure 2.6) suggest that they could be generated at distinct locations earlier in the auditory pathway (Scholl et al., 2010; Sollini et al., 2018; Suga et al., 1975), and then processed independently.

The predominance of offset responses in AAF and their significantly smaller amount in A1 (Figure 5), the faster and more transient responses in AAF than in A1 (Figure 4e, i, j) as well as the dependence of response strength on tone duration in AAF (Figure 5c, d) reveal intriguing differences between these two primary auditory cortices. What could be the underlying mechanisms leading to such differences? Previous studies indicate that the MGB, the nucleus preceding A1 and AAF in the auditory pathway, contains offset responsive cells (Anderson and Linden, 2016; He, 2001). Our LFP and layer-specific analyses confirm that offset responses do not emerge in the auditory cortex but are received from subcortical nuclei in the input layer (L4) (Figure 7). These responses are, however, significantly stronger in AAF than in A1. In addition, the robust offset responses in L2/3 suggest that AAF (Figure 7c, d) processes offsets further. On the contrary, A1 does not have as strong responses in supragranular layers. These results indicate that the difference in sound offset processing between A1 and AAF are both of subcortical and intracortical origins. Interestingly, A1 L2/3 offset responses appear faster than L4 responses (Figure 7e, f). Could it be that A1 L2/3 offset responses originate from AAF offset responses, as these two regions are highly interconnected (Carrasco and Lomber, 2009a) (Bizley et al., 2015)? Further studies will have to be performed to fully address the mechanisms behind the distinct sound processing in A1 and AAF.

Intracortically, both fast and regular spiking neurons are involved in processing information on sound onset and offset (Figure 8g-j). One could expect FS interneurons to be more involved in offset encoding as they can provide dynamic gain control of neural activity (Keller et al., 2018). Our results indeed reveal higher offset responses in FS than RS cells (Figure 8j). However, as offset responses are robust in both cell types, they cannot be specifically attributed to one of them. Moreover, the involvement of FS neurons is similar for onset and offset responses: they have shorter latencies and stronger firing rates than RS neurons, as also indicated in the awake mouse auditory cortex (Keller et al., 2018). Thus, the stronger offset responses and faster latencies reflect a general principle of the role of this class of inhibitory neurons in cortical processing, where they control and modulate local circuit processing.

With its robust offset responses, transient onset responses, and shorter onset latencies, AAF is likely to have a more prominent role for encoding sound timing (Lomber and Malhotra, 2008) and, by extension, for all time-varying signals so important in vocalization. Functionally, offset responses might be

essential to perceive sound termination, detect gaps in an otherwise continuous sound, or detect changes in amplitude modulated signals (Liang et al., 2002). Previous studies showed that the auditory cortex is required for the detection of short gaps (<75 ms) but not for the detection of long gaps (>100 ms) (Threlkeld et al., 2008). Our data display offset responses predominantly for longer duration signals or shorter signals with longer ISIs (Figure 5c). This reflects a possible particular role of AAF offsets in processing slower transients. The question of the potential role of AAF offset response in gap detection, therefore, remains open. One could speculate that the overlap of onset and offset response we see in A1 for short tones (Figure 4f, Figure 5a) contributes to short gap sensitivity, and that AAF would play a more important role in detecting longer gaps.

Taken together, our findings suggest distinct sound processing in the mouse two primary auditory cortices. The different responses to sound termination in A1 and AAF emphasize sound processing's complexity at the cortical level. Our data also indicate that A1 and AAF should be clearly defined and distinguished during experiments as they represent sound parameters differently. But why does the auditory cortex need two primary regions? One can speculate that auditory stimuli, as compared to other sensory stimuli, have more complex and challenging temporal characteristics. We believe that the distinct roles of A1 and AAF are likely to be used complementary as there is considerable overlap in A1 and AAF response properties. If and how other sound features are differentially encoded in A1 and AAF remains to be elucidated.

## 2.6. Methods

**Surgical procedures.** All experimental procedures were carried out in accordance with Basel University animal care and use guidelines and were approved by the Veterinary Office of the Canton Basel-Stadt, Switzerland. They were performed on adult (7-9 weeks) male or female C57BL/6J mice (Janvier, France).

Mice were anesthetized with an intraperitoneal injection of ketamine/xylazine (80 mg/kg and 16mg/kg, respectively), and subcutaneous injection of bupivacain/lidocain (0.01mg/animal and 0.04mg/animal, respectively) was used for analgesia. Ketamine (45 mg/kg) was supplemented during surgery as needed. For surgery, mice were head-fixed, and their body temperature was kept at 37°C with a heating pad (FHC, ME, USA). Craniotomy (~2x2 $mm^2$) was performed with a scalpel just above the auditory cortex and covered with silicone oil. For awake recordings, the surgery was performed under isoflurane (4% for induction, 1.5 to 2.5% for maintenance), and the brain was additionally covered with a silicone casting compound (Kwik cast, World Precision Instruments, Inc. FL, USA) during the 2h recovery period from the anesthesia.

**Recordings.** The electrophysiological recordings were performed in anesthetized mice (A1: n=6; 4 females: 36, 45, 39, 23 cells; 2 males: 28, 21 cells; AAF: n=7; 3 females: 27, 45, 25 cells; 4 males: 32, 26, 31, 16 cells) except for the data presented in Supplementary Figures 2.3-4 which were acquired in

awake experiments (A1: n=5; 5 females: 16, 26, 23, 22, 17 cells; AAF: n=6; 5 females: 22, 9, 33, 41, 40 cells; 1 male: 28 cells). Mice were head-fixed and placed on a heating pad (or in the cardboard tube for awake recordings) inside a sound box. The body temperature was kept at 37°C. Extracellular recordings were conducted in A1 and AAF, which were identified based on the functional tonotopy (caudal-rostral increase in BF for A1, and ventro-dorsal increase in BF for AAF). Multi-channel extracellular electrodes with 32 channels (A4x8-5mm-50-200-177-A32, Neuronexus, MI, USA) were inserted orthogonally to the brain surface with a motorized stereotaxic micromanipulator (DMA-1511, Narishige, Japan) at a constant depth (tip of the electrode at 575 ± 25 µm from pia). Responses from extracellular recordings were digitized with a 32-channel recording system (RZ5 Bioamp processor, Tucker Davis Technologies, FL, USA) at 24414 Hz. The single unit cluster was identified from raw voltage traces using kilosort (CortexLab, UCL, London, England) followed by manual corrections based on the inter-spike-interval histogram and the consistency of the spike waveform (phy, CortexLab, UCL, London, England) and further analyzed in MATLAB (Mathworks, MA, USA). Neural activity was considered as auditory responsive when it exceeded twice the standard deviation of the spontaneous activity. Local Field Potential signal was obtained by applying low pass-filtering with a cut-off of 100 Hz on the raw voltage traces.

**Auditory stimulation.** Sounds were generated with a digital signal processor (RZ6, Tucker Davis Technologies, FL, USA) at 200 kHz sampling rate and played through a calibrated MF1 speaker (Tucker Davis Technologies. FL, USA) positioned at 10 cm from the mouse's left ear. Stimuli were calibrated with a wide-band ultrasonic acoustic sensor (Model 378C01, PCB Piezotronics, NY, USA).

*Tuning receptive fields*: To determine best frequency and tuning receptive fields, we used PTs (50 ms duration, randomized ISI distributed equally between 500 and 1000 ms, 2 repetitions, 4 ms cosine on, and 0.01 ms cosine off-ramps) varying in frequency from 4 to 48.5 kHz in 0.1-octave increments and level from 0 to 80 dB SPL in 5 dB increments. Tuning receptive fields, best frequency, and spiking rates were calculated in fixed time windows: A1 onset: 10-60 ms, A1 offset: 60-110 ms, AAF onset: 8-58 ms, AAF offset: 58-108 ms. TRFs were smoothed with a median filter (4x4 sampling window) and thresholded to 0.2 of peak amplitude. d', a parameter used to assess the tuning quality of the TRF, was calculated as the difference in mean spike count within the tuning field and mean spike count outside the boundary of tuning field divided by their arithmetic average standard deviation (modified method from (Guo et al., 2012)). For all Figures, we used units with onset response tuning quality higher than 1 (d'>1). For Figure 8d-e, we also assessed offset response tuning quality and analyzed cells with d'>0.5. Best onset and offset frequency were defined as the frequency that elicited maximal response across all sound levels. Onset and offset latency was determined as the first time point in which the smooth PSTH (kernel=hann(9)) collapsed across all tested stimuli exceeded with 2 standard deviations the spontaneous activity (binning size: 1ms). In Figure 4, onset response latency was calculated based on the protocol used to determine tuning receptive fields (PTs, 50 ms duration, randomized ISI distributed equally

between 500 to 1000 ms, 2 repetitions, 4 ms cosine on and 0.01 ms cosine off-ramps; varying in frequency from 4 to 48.5 kHz in 0.1-octave increments and level from 0 to 80 dB SPL in 5 dB increments). In Figure 8, onset and offset response latencies were calculated based on the responses to 9 kHz PTs of 500 ms presented with ISIs of 250, 500, 1000, or 2000 ms at 60 dB SPL, 10 repetitions, 4 ms cosine on and 0.01 ms cosine off-ramps. The number of cells presented in Figure 8h-j differs because for some cells, onset or offset response latency could not be assessed if the smoothed neuron's onset or offset response was lower than twice the spontaneous activity standard deviation. Single exponential decay functions were least-squares-fitted to PSTH of each neuron's onset response. The exponential fit was accepted if the explained variation (n2)

$$ExplainedVariation = 1 - \frac{\sum(\text{ObservedResp} - \text{predictedResp})^2}{\sum \text{ObservedResp} - \text{mean}(\text{ObservedResp}))^2}$$

was bigger than 0.7.

*Tone duration responses:* To study responses to tones with different durations, we used 10 repetitions of PTs (9 kHz) or HTs (9+18+27+36 kHz) with 4 ms cosine on and 0.01 ms cosine off-ramps, which were varied in duration (50, 100, 150, 250, 350, 500 ms), ISI (the gap between 2 stimuli of 50, 100, 250, 500, 1000, 2000 ms) and played at 60 dB SPL. For this protocol, $f_0$ was fixed to 9 kHz because of (1) irregular and poorly tuned offset receptive fields found in AAF, which did not allow to designate offset BF with high accuracy, and therefore any analysis of responses as a function of offset BF would be imprecise, (2) the fact that 9 kHz PTs evoked significant offset responses in almost all tested AAF but not A1 neurons irrespectively of their tuning (Supplementary Figure 2.5), (3) the wish to test harmonic stimuli with $f_0$ to $f_3$ within the range of our stimulation parameters.

**Retrograde Tracers.** Retrograde tracing was performed as previously described (Hackett et al., 2011). Briefly, mice were anesthetized with ketamine/xylazine (80 mg/kg). Following the initial microelectrode mapping, retrograde tracers, cholera toxin beta subunit (CTB) conjugated to either 594 (red, Invitrogen cat# 34777) or Alexa 488 (green, Invitrogen cat# 34775) were injected into A1 or AAF, (N=2 for each region). After injections, the surgical area was closed, and the animal was allowed to recover for approximately 96 hours before transcardial perfusion. Animals were first perfused with 0.9% saline and then with a cold (4°C) solution of 4% paraformaldehyde prepared in 0.1 M phosphate buffer (pH 7.4). Following perfusion, the brains were removed and placed in 30% sucrose for 1 to 3 days. Blocks containing the auditory cortex were cut with a vibratome in a modified horizontal plane that included A1 and MGB. Slices (80µm) were visualized with a confocal laser-scanning microscope (Zeiss LSM700) with a Plan-apochromat 10x/0.8 NA objective.

**Statistical Analysis**. Statistical tests were performed with GraphPad Prism software version 7.03 (GraphPad Software, USA). The standard error of the mean was calculated to quantify the amount of variation between responses from different populations. A Nonparametric, unpaired Mann-Whitney test

was used to calculate whether there were any significant differences between medians of recordings in A1 and AAF. Wilcoxon paired test or paired t-test were used to compare differences between paired values obtained in different treatments which have (paired t-test) or not have (Wilcoxon test) Gaussian distribution. Spearman correlation tests were used to test for significant associations between pairs of variables measured with rankings.

## 2.7. Supplementary data

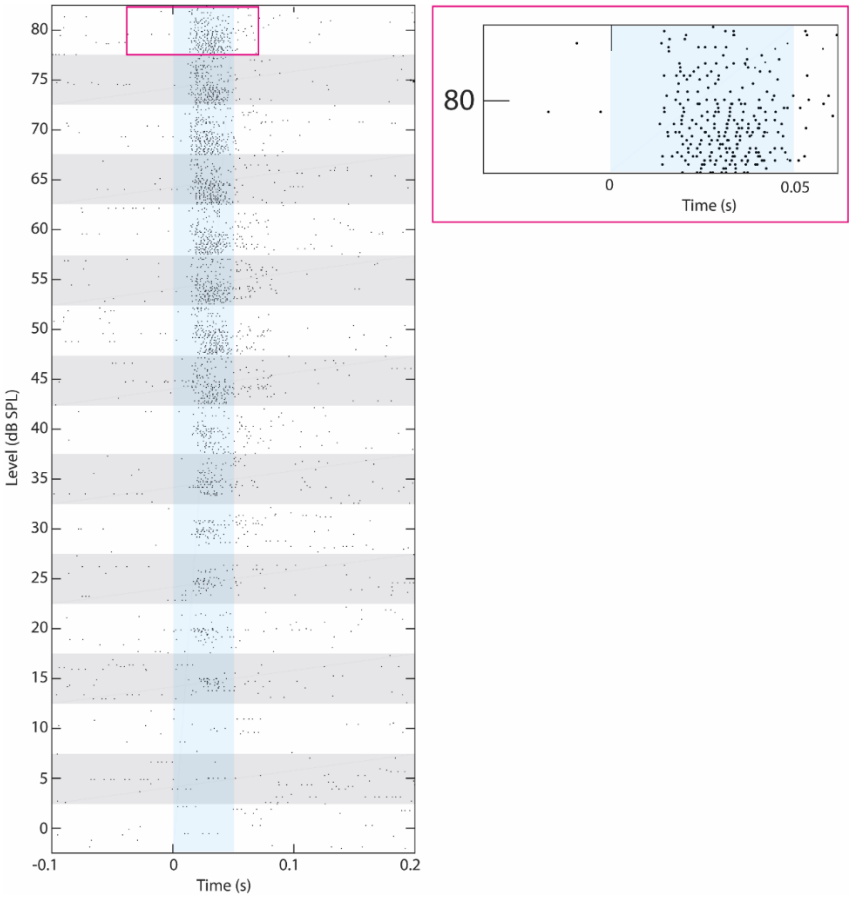


**Supplementary Figure 2.1 Raster plot of Fig. 5f (left) at higher resolution**. Each line of the raster plot represents spikes evoked by two repetitions of a tone at one frequency and one sound level. 37 frequencies (varying between 4 - 48.5 kHz in 0.1-octave increments) were tested for each sound level. The blue shaded bar represents the tone presentation.

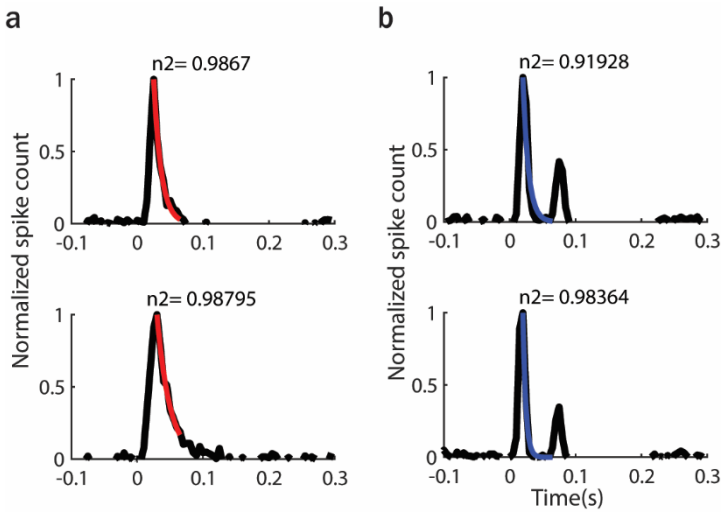


**Supplementary Figure 2.2 Exponential decay model used to assess the sustainability of neuron's response.** (**a, b**) Example fit of exponential decay model to PSTH of 2 A1 (**a**) and 2 AAF (**b**) neurons' responses (n2: the amount of variance explained).

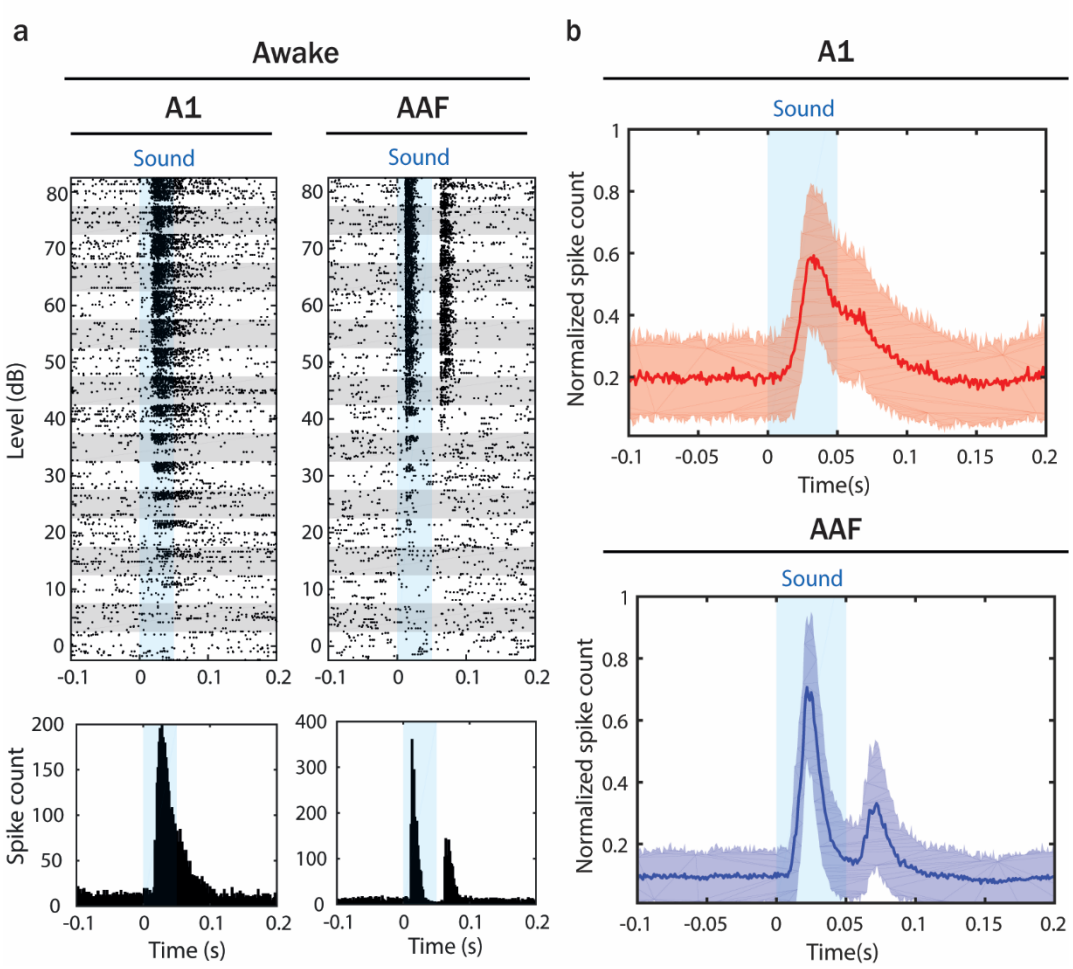


**Supplementary Figure 2.3 Prominent offset responses in AAF are not induced by anesthesia.** (**a**) Raster plot and peristimulus time histogram (PSTH) of an example A1 (left) and AAF (right) neuron's response to PTs (tone duration: 50 ms, frequency varying between 4 - 48.5 kHz in 0.1-octave increments, sound level varying between 0-80 dB SPL in 5 dB increments, inter-stimulus-intervals randomized between 500 – 2000 ms) recorded in awake animals. The blue bar represents the tone. (**b**) Averaged PSTH of A1 (top, n=104) and AAF (bottom, n=173) neuron's response to PTs (same sound stimuli as in a) collapsed across frequencies and sound levels.

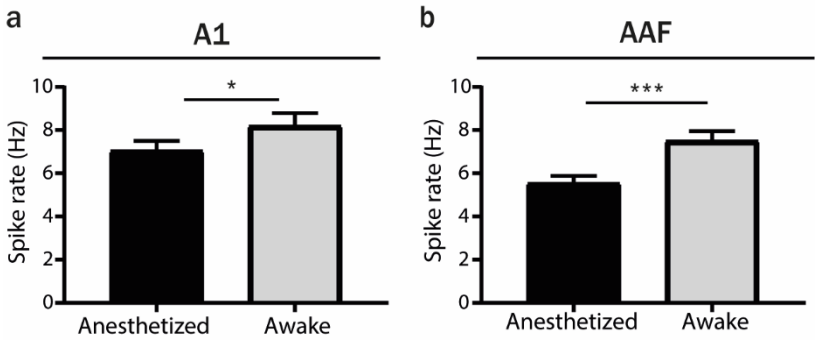


**Supplementary Figure 2.4 Offset responses increase in awake states as compared to anesthesia.** (**a, b**) Comparison of average offset spike rate in A1 (a) and AAF (b) neurons in anesthetized and awake conditions evoked by 50 ms pure tones with frequency varying between 4 - 48.5 kHz in 0.1-octave increments, sound level varying between 0 80 dB SPL in 5 dB increments, inter-stimulus-intervals randomized between 500 – 2000 ms. Data represent mean ± SEM. A1: *p=0.038, anesthetized n=191, awake n=104, AAF ***p=0.0008, anesthetized n=190, awake n=173 , Mann-Whitney test. Higher spike rates at the offset in A1 result from sustained onset responses, which overlap with the offset response analysis window.

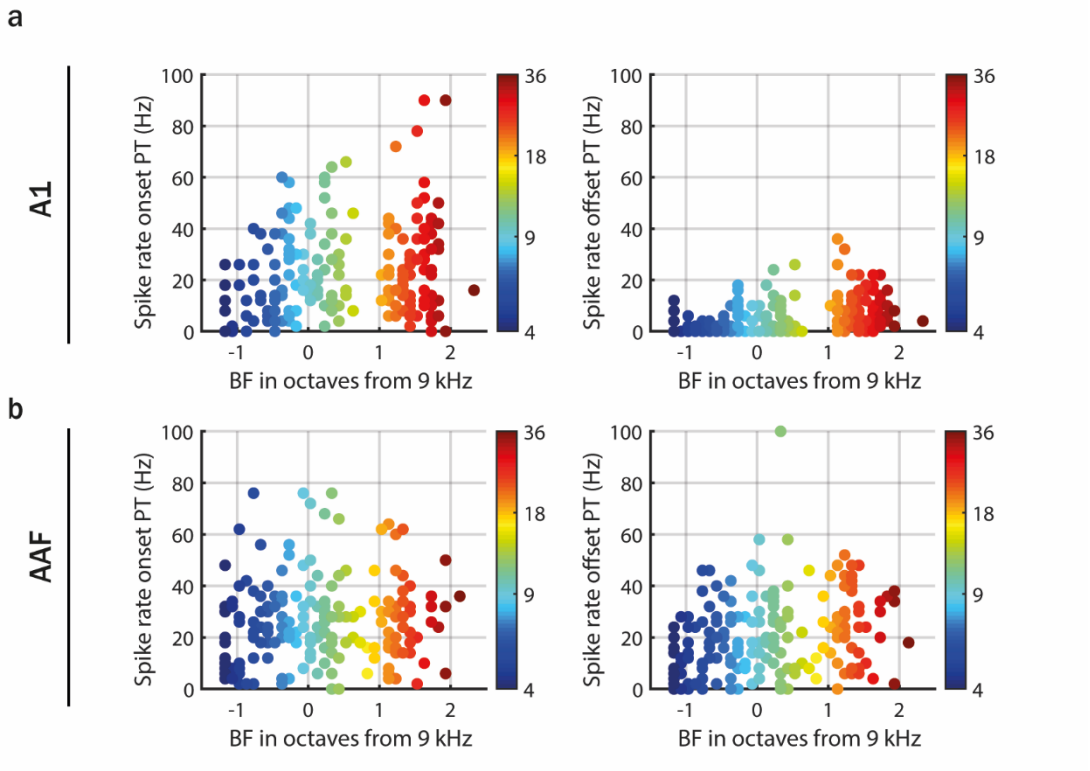


**Supplementary Figure 2.5 Onset and offset responses evoked by 9 kHz PT in A1 and AAF neurons tuned to different frequencies.** (**a, b**) Onset (left) and offset (right) responses in (**a**) A1 (n=191) and (**b**) AAF (n=190) as a function of distance of BF from 9 kHz (stimuli used in experiments). Responses are color-coded to the neuron's onset BF.

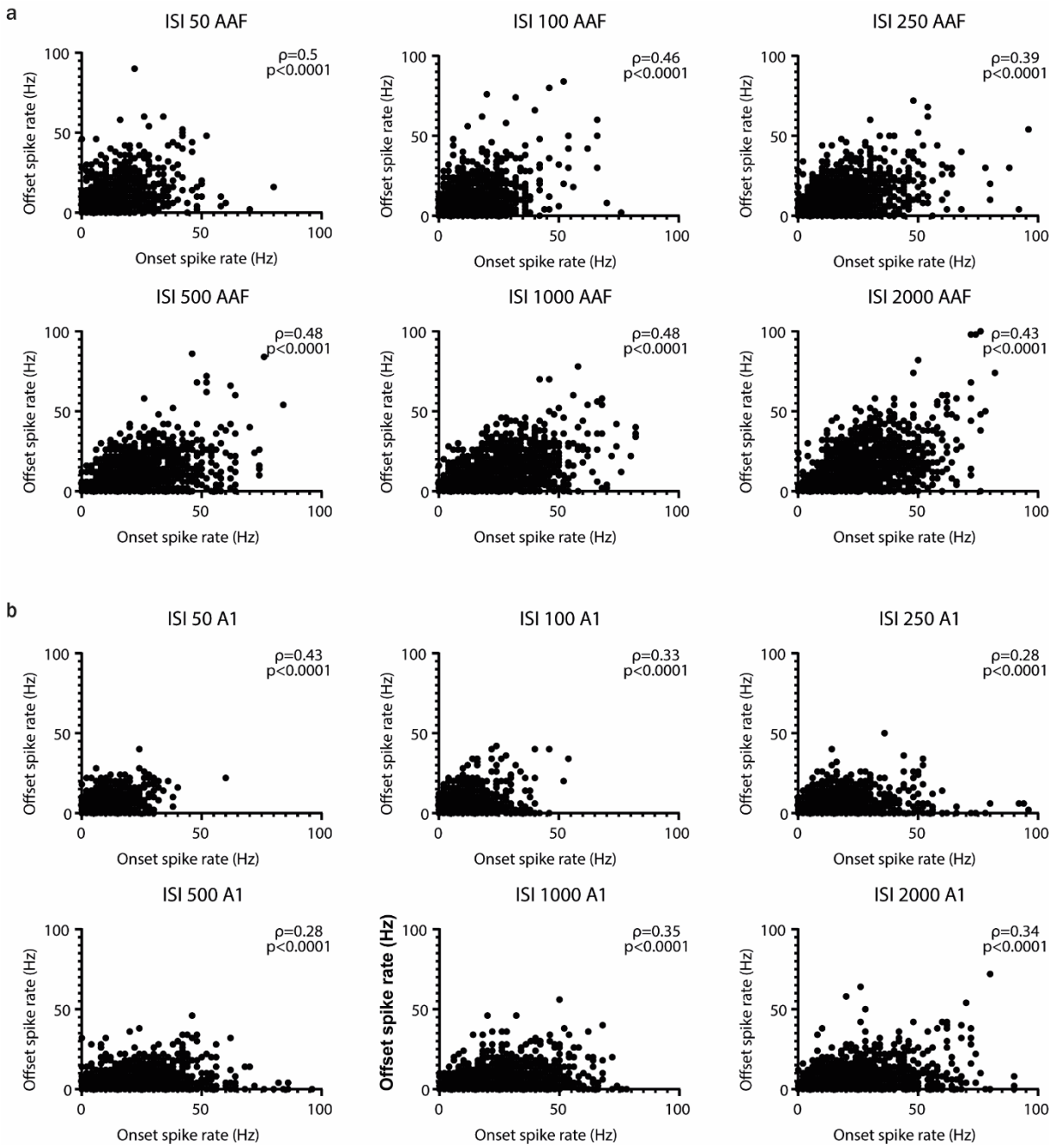


**Supplementary Figure 2.6 Offsets in AAF do not suppress the following onset response.** (**a, b**) Correlation between offset and onset responses at each ISI in (**a**) AAF and (**b**) A1 neurons. AAF: n=190, A1: n=191, Spearman correlation.

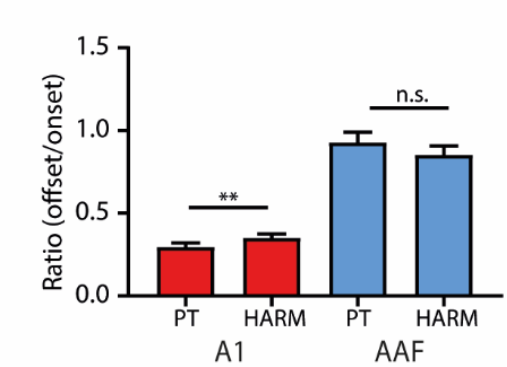


**Supplementary Figure 2.7 Offset responses in A1 are bigger for harmonic than for pure tones.** Firing rates of offset relative to onset responses evoked by PTs and HTs in A1 and AAF neurons. Data represent mean ± SEM. A1: **p=0.0035, n=184, AAF: p=0.14, n=187, Wilcoxon Test.

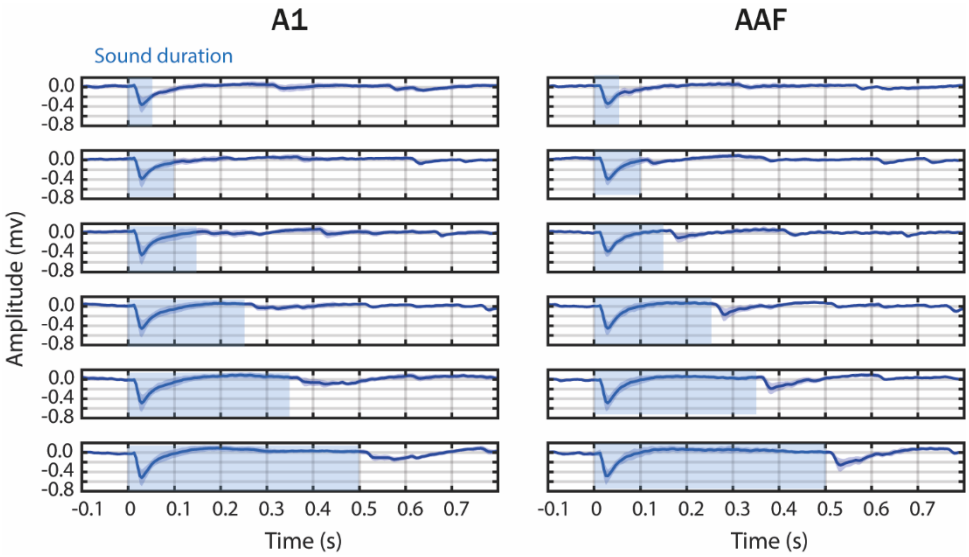


**Supplementary Figure 2.8** Averaged LFP signal from L4 A1 (6 animals) and AAF (7 animals) neurons in response to HTs (9+18+27+36 kHz) played at 60 dB SPL with sound duration varying between 50 and 500 ms and ISI between 50 and 2000 ms. The blue shaded bars represent the tone.

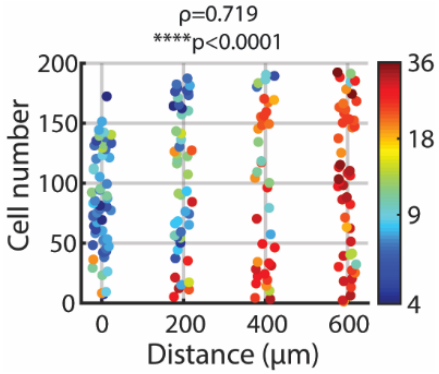


**Supplementary Figure 2.9 Confirmation of tonotopy in A1.** Comparison of onset BF of A1 neurons displayed as a relative distance between electrode shafts. Responses are color-coded to onset BF (correlation between BF and relative distance between electrode's shaft: $\rho$=0.719, ****p<0.0001, n=191, Spearman correlation).

—

# Chapter 3

# Emergence and function of cortical offset responses in sound termination detection

## 3.1. Abstract

Offset responses in auditory processing appear after a sound terminates. They arise in neuronal circuits within the peripheral auditory system, but their role in the central auditory system remains unknown. Here we ask what the behavioral relevance of cortical offset responses is and what circuit mechanisms drive them. At the perceptual level, our results reveal that experimentally minimizing auditory cortical offset responses decreases the mouse performance to detect sound termination, assigning a behavioral role to offset responses. By combining *in vivo* electrophysiology in the auditory cortex and thalamus of awake mice, we also demonstrate that cortical offset responses are inherited from the periphery, amplified, and generated *de novo*. Finally, we show that offset responses code more than silence, including relevant changes in sound trajectories. Together, our results reveal the importance of cortical offset responses in encoding sound termination and detecting changes within temporally discontinuous sounds crucial for speech and vocalization.

### 3.2. Graphical abstract

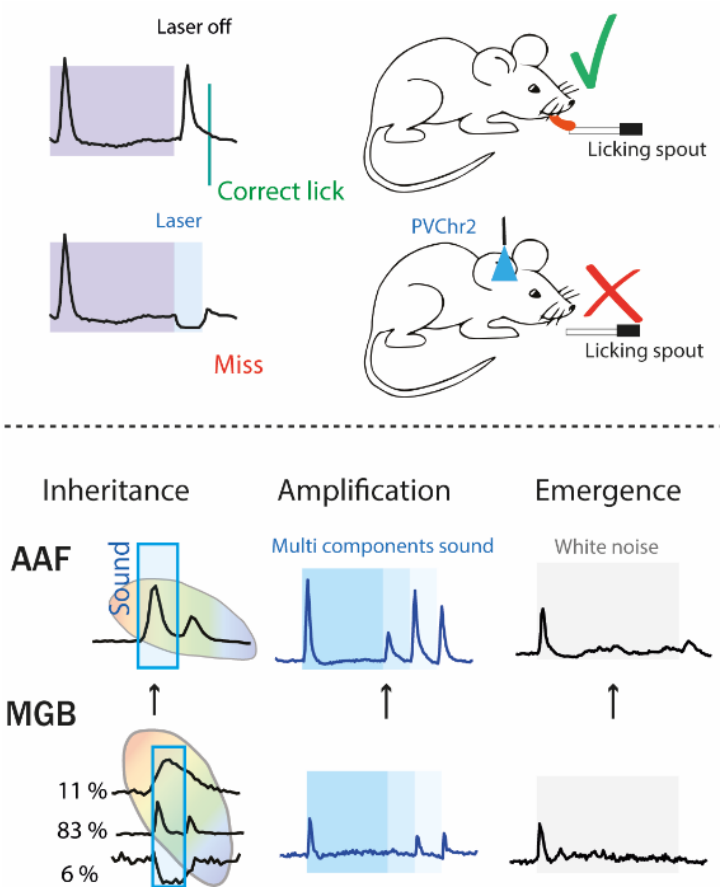


**Highlights:**

- Experimentally minimizing auditory cortical offset responses decreases the mouse performance to detect sound termination.
- Cortical offset responses are not only inherited from the periphery but also amplified and generated *de novo*.
- Offset responses code more than silence, including relevant changes in sound trajectories.
- These results reveal the importance of cortical offset responses in encoding sound termination and detecting changes within temporally discontinuous sounds crucial for speech and vocalization.

## 3.3. Introduction

Offset responsive neurons are present through the whole auditory pathway starting from the cochlear nucleus (CN) (Ding et al., 1999; Suga, 1964; Young and Brownell, 1976) to the superior paraolivary nucleus (SPN) (Dehmel et al., 2002; Kulesza et al., 2003), the inferior colliculus (IC) (Akimov et al., 2017; Kasai et al., 2012), the medial geniculate body (MGB) (Anderson and Linden, 2016; He, 2001, 2002; Yu et al., 2004) and the auditory cortex (ACx) (Qin et al., 2007; Recanzone, 2000; Scholl et al., 2010; Takahashi et al., 2004). Multiple mechanisms were proposed to produce offset responses (Bondanelli et al., 2019; Kopp-Scheinpflug et al., 2018; Xu et al., 2014). Generally, it is thought that signals from the cochlea can generate offset responses in both the CN (Suga, 1964) and the SPN (Kopp-Scheinpflug et al., 2011), but strong offset responses were mainly described in the SPN. This structure is considered to be specialized for offset response generation based on the strong inhibitory signal it receives during the sound and on the precise firing when sound ends. The SPN then sends strong inhibitory inputs to the IC (Kulesza and Berrebi, 2000; Saldana et al., 2009), which might further convey the signal to the MGB. Offset responses in the MGB and the ACx are generally thought to be driven by excitatory/inhibitory inputs from IC rather than by other neural mechanisms (Kopp-Scheinpflug et al., 2018). *De novo* generation or amplification of offset responses in these areas have not been demonstrated yet (Bondanelli et al., 2019; He, 2003; Kasai et al., 2012; Yu et al., 2004).

The perceptual significance of offset responses has been difficult to assess. They have been postulated to play a role in sound duration selectivity (He, 2002; Qin et al., 2009), in gap detection (Syka et al., 2002; Threlkeld et al., 2008; Weible et al., 2014a; Weible et al., 2014b) or in perceiving communication calls (Eggermont, 2015; Felix et al., 2018; Kopp-Scheinpflug et al., 2018). For example, Qin et al. showed that onset-only neurons in the primary ACx of cats could not discriminate duration and suggested that sustained and offset responses underlie discrimination of sound duration (Qin et al., 2009). In another study, Weible et al. demonstrated that the cortical post-gap neural activity in mice is related to detecting brief gaps in noise (Weible et al., 2014b). Still, the relative contributions of sound offset and onset responses are unclear (Kopp-Scheinpflug et al., 2018). No evidence has yet demonstrated whether the increased neuronal activity of sound offset responses accounts for these perceptual skills.

Compared to onset responses, offset responses in the central auditory pathway are typically less prevalent (Phillips et al., 2002; Pollak and Bodenhamer, 1981; Solyga and Barkat, 2019). They are generally weaker and slower than onset responses (Qin et al., 2007). At the cortical level, offset responses have been shown to cluster within the anterior auditory field (AAF) - a primary region of the ACx - where they have been observed in twice as many cells as in the primary auditory cortex (A1) (Solyga and Barkat, 2019). Offset responses are also highly influenced by different sound parameters. For example, the amplitude, duration, frequency, fall time, and spectral complexity of the sound have all been reported to influence auditory offset responses (He, 2002; Scholl et al., 2010; Solyga and Barkat,

2019; Takahashi et al., 2004). However, no study has yet systematically addressed these influences. The involvement of the different nuclei of the central auditory system and their cellular and circuit mechanisms are thus poorly understood.

We combined behavioral experiments with optogenetics, electrophysiological recordings, and antidromic stimulation to better understand the role cortical offset responses play in sound perception and the properties that distinguish them from the subcortical ones. Our results reveal that the AAF is highly specialized for processing information on sound termination and that minimizing its offset responses decreases the mouse performance to detect when a sound ends. By studying the influence of different sound parameters on AAF and MGB offset responses, we demonstrate that cortical offsets are inherited, amplified, and sometimes even generated *de novo*. First, we found that the AAF, unlike the MGB, shows a significant increase in offset response amplitudes with sound duration. Then, we report that white noise bursts - unlike pure tones - only evoke offset responses in the AAF but not in the MGB. Finally, we show that offset responses are present in the AAF whenever a frequency component is removed from multi-frequency stimuli and may have a further role than solely coding silence.

Taken together, our findings suggest a particular involvement of AAF offset responses in sound termination processing and point to the importance of this cortical subfield for advanced processing such as tracking sound duration or detecting changes in frequency and level within temporally discontinuous sounds.

## 3.4. Results

### 3.4.1. Cortical offset responses improve sound termination detection

The perceptual significance of cortical offset responses has been difficult to assess. Indeed, confounds about perceiving a sound and its termination are intricately linked. Changing the neuronal activity of sound offset responses without changing any other parameters of the sound response has not been tested. To assess the behavioral relevance of auditory offset responses, we developed a sound termination detection task in which mice expressing Channelrhodopsin-2 (ChR2) in parvalbumin-positive (PV+) cells learned to detect the end of 9 kHz frequency pure tones (Figure 9a). Animals were placed in a cardboard tube with a speaker 10 cm away from their left ear. A piezo sensor attached to a licking spout was used to measure sound termination detection during the task. To accelerate the learning process, mild air puffs were given when mice licked to sound onset. The duration of the tones was varied randomly (1, 1.5, or 2 s) to avoid a putative expected behavioral response at a fixed delay after sound onset. Mice were initially trained with a tone played at 80 dB SPL. A reaction time window was set to 3 s during initial training sessions and progressively shortened to 1 s in the final training sessions. An increase in correct offset detection (hit rate) and decreased reaction time over the training sessions reflected successful learning (Figure 9b). Trials with licks at the tone onset were discarded from the analysis (Supplementary Figure 3.1).

After this training phase, animals underwent a craniotomy, and the AAF was mapped. On the following day, they were tested with tones played at 60 dB SPL. In half of the trials, laser light was delivered above the AAF for 200 ms starting at sound termination (Figure 9c) in order to activate PV+ cells (Figure 9d) and to significantly reduce offset responses in non PV+ cells (Figure 9e). Comparing the animals' performance during laser on and laser off trials showed that preventing AAF offset responses significantly decreased the performance to detect sound termination (Figure 9f-h). This experiment demonstrates that offset responses in the AAF are behaviourally relevant.

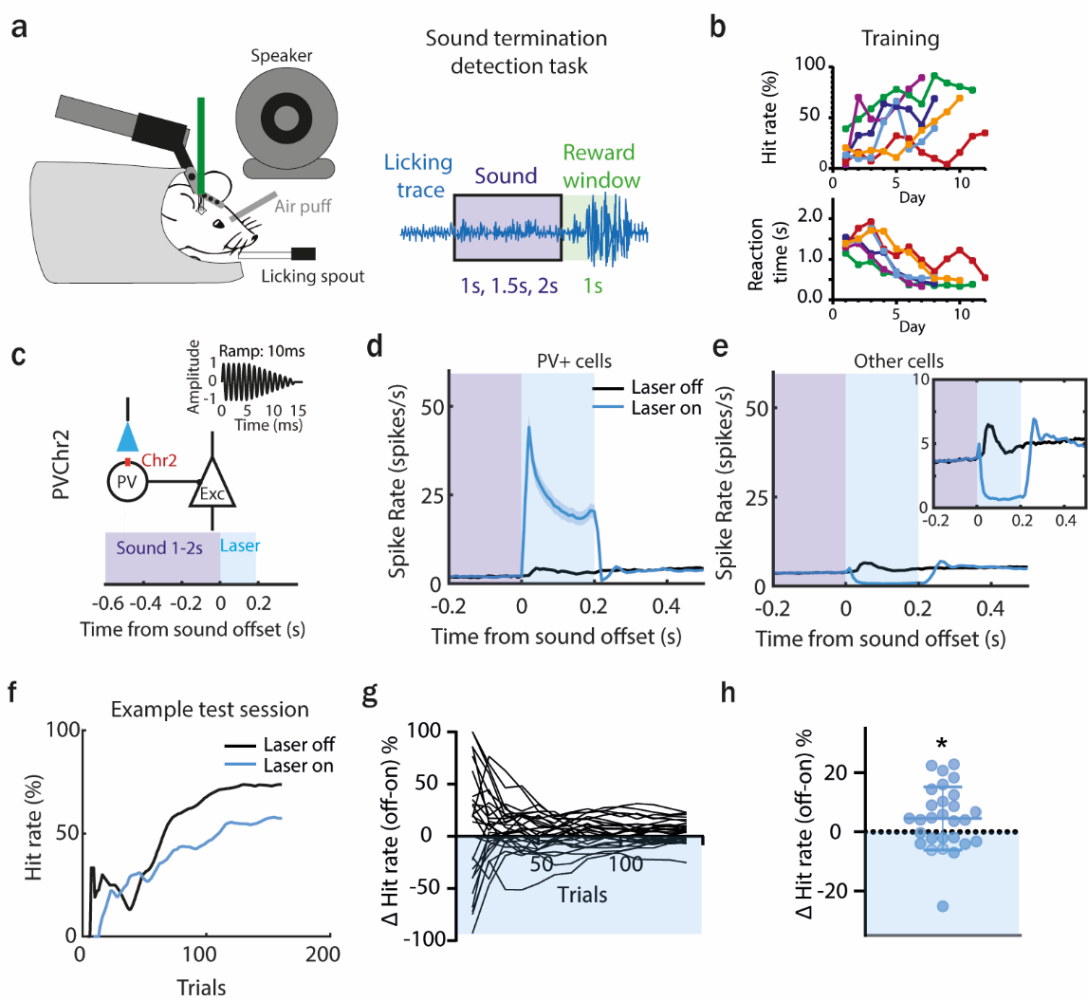


**Figure 9 Preventing AAF offset responses decreases the ability of a mouse to detect sound termination.** (**a**) Illustration of head-fixed behavioral setup. Piezo sensor attached to licking spout measured behavioral response to detection of sound termination (left). Schematic of the behavioral paradigm of offset detection task. The animal had to detect a sound offset of 9 kHz PT played with three different durations: 1s, 1.5s, 2s within a reward window of 1s. (**b**) Indications of successful learning. Increasing hit rate of offset detection over training days (top, n=6 animals). Decreasing reaction time for offset detection over training days (bottom, n=6 animals). (**c**) Schematic of laser manipulation. Laser light was used for 200 ms following sound termination in animals expressing Chr2 in PV cells. Inset: zoom in. (**d**) Activity of PV+ cells (mean± SEM) following sound termination in laser on (blue) and laser off (black) trials, n=336 cells, 28 sessions, 6 animals. (**e**) The activity of other cells (mean± SEM) following sound termination in laser on (blue) and laser off (black) trials, n=2249 cells, 28 sessions, 6 animals. (**f**) Hit rates within an example session during offset detection task. Blue and black lines represent the hit rate for laser on and laser off trials, respectively. (**g**) The difference in hit rate between laser off and laser on trials during individual sessions (n=28 sessions, 6 animals) (**h**) Overall difference in correct hit rate for laser off and laser on trials at the end of the training (mean± SEM), p=0.0264, n=28 sessions, 6 animals, One sample Wilcoxon test. See also Supplementary Figure 3.1.

### 3.4.2. Bigger offset responses correlate with better detection of sound termination

Previous studies illustrated how offset responses in the ACx of rats and cats strongly depend on the fall time of a sound (Qin et al., 2007; Takahashi et al., 2004). We used a faster fall-ramp to evoke higher amplitude offset responses and asked whether the amplitude of offset responses and the animal's ability to detect sound termination are correlated. We used a similar experimental paradigm as in Figure 9, where the animal had to detect the end of the 9 kHz tone played at 60 dB SPL with, this time, a fall-ramp of 10 or 0.01 ms. As expected from previous studies, fast fall–ramps (0.01 ms) lead to significantly higher offset responses than longer ones (10.0 ms), as tested during awake passive recordings (Figure 10a, Supplementary Figure 3.2) or when animals were performing a behavioral task (Figure 10b). We confirmed that the sounds with a 0.01 ms fall-ramp are not causing an additional artificial onset response (Supplementary Figure 3.3). The analysis of hit rates showed that mice could correctly detect when sounds ended for tones with both short and long ramps, and no significant difference in detection rate between the two ramps was observed when looking at the end of test sessions (Figure 10c-e). However, at the beginning of the test sessions, mice were significantly better at detecting sound offset when the ramp was fast. This suggests that sounds terminated with a fast fall-ramp, and therefore triggering a bigger offset response, were significantly easier to detect at the beginning of the sessions when the task was still new and possibly more challenging than after exposure to more trials. This result is in line with previous findings showing cortical involvement in difficult but not easy tasks (Ceballo et al., 2019; Christensen et al., 2019; Dalmay et al., 2019; Kawai et al., 2015). There was no significant difference in the reaction times for both tested ramps (Supplementary Figure 3.4).

To confirm that bigger offset responses help mice detecting sound termination, we performed another behavioral experiment with optogenetics, this time manipulating offset responses evoked by fast ramp (Figure 10f). As previously shown (Figure 9d, e), the laser significantly activated PV+ cells, resulting in the suppression of high amplitude offset responses in non-PV+ cells (Figure 10g). Minimizing high amplitude offset responses in the AAF significantly decreased the performance to detect sound termination (Figure 10h, i). To control that the light itself, without ChR2, was not causing any changes in behavioral performance, we repeated the same experiments in wild-type animals (Figure 10j). The laser alone had no effect, neither at the neural (Figure 10k) nor the behavior level (Figure 10l, m). Together, these experiments confirm that changing offset responses in the AAF influences behavioral performance. They demonstrate that the animal uses the neuronal activity following sound termination in the AAF to detect sound termination.

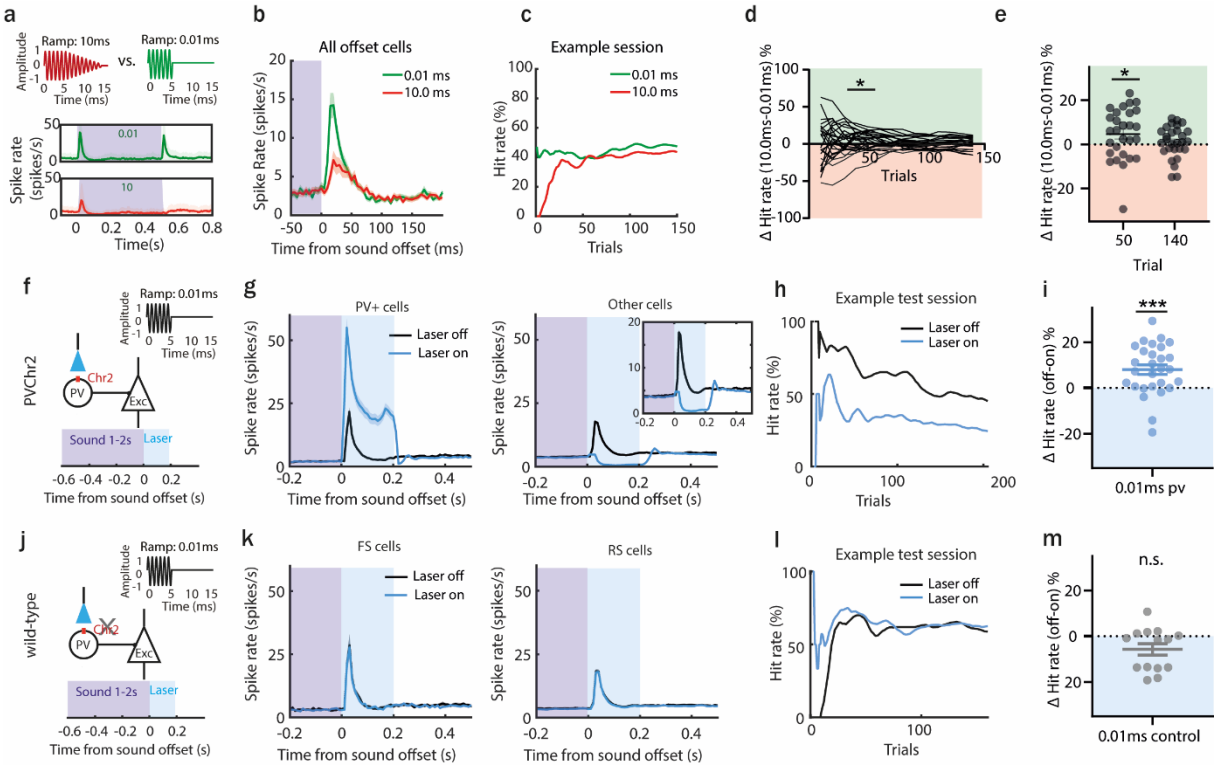


**Figure 10 Bigger offset responses correlate with better detection of sound termination.** (**a**) Schematic of sounds used in the behavior task (0.01 ms or 10 ms fall-ramp) and PSTH (mean± SEM) of responses evoked in acute AAF recordings. (**b**) PSTH (mean± SEM) averaged over AAF neurons (n=169, 2 animals) during sound termination detection task (green line: 0.01 ms offset ramp; red line: 10.0 ms offset ramp). (**c**) Hit rates of example session during offset detection task. Green and red lines represent the hit rate for short (0.01 ms) and long (10 ms) offset ramps. (**d**) The difference in hit rate for sounds with short and long offset ramps through the behavior session. The Green and red shaded areas indicate that offset detection was better for short or long ramps, respectively. (**e**) Comparison of correct hit rate for 0.01 ms and 10.0 ms ramp at $Trial_{50}$ (p=0.0247, n=28 sessions, 10 animals, Wilcoxon test) and $Trial_{140}$ (p=0.3052, n=28 sessions, 10 animals, Wilcoxon test). (**f**) Schematic of experimental design: the sound of 9 kHz with 0.01 ms fall ramp was used, and laser was applied for 200 ms following sound termination in animals expressing Chr2 in PV cells. (**g**) The activity of PV+ cells (mean± SEM) following sound termination in laser on (blue) and laser off (black) trials (left), n=336 cells, 28 sessions, 6 animals. The activity of other cells (mean± SEM) following sound termination in laser on (blue) and laser off (black) trials (right), n=2249 cells, 28 sessions, 6 animals. (**h**) Hit rates within an example session during offset detection task. Blue and black lines represent the hit rate for laser on and laser off trials, respectively. (**i**) Difference in correct hit rate for laser off and laser on trials at the end of the training (mean± SEM), p=0.0006, n=28 sessions, n=6 animals, One sample Wilcoxon test. (**j**) Schematic of control experiment: the sound of 9 kHz with 0.01 ms fall ramp was used, and laser was applied for 200 ms following sound termination in wild-type animals. (**k**) Population activity (mean± SEM) following sound termination in laser on (blue) and laser off (black) trials in fast (left), n=104 cells, 14 sessions, 3 animals, and regular spiking neurons (right), n=951 cells, 14 sessions, 3 animals. (**l**) Hit rates within an example session during offset detection task. Blue and black lines represent the hit rate for laser on and laser off trials, respectively. (**m**) Difference in correct hit rate for control animals in laser off and laser on trials at the end of the training (mean± SEM), p=0.0906, n=14 sessions, 3 animals, One sample Wilcoxon test. See also Supplementary Figure 3.2-3.4.

### 3.4.3. The activity of AAF neurons in a sound termination detection task can be predictive of the animal's performance

As the suppression of auditory offset responses in the AAF affects performance, we asked if AAF activity during a single trial could be predictive of the animal's behavior. We used a logistic regression model to predict the mouse's action from the single-trial population activity (cross-validated, L2 penalty,

see methods). We examined the classifier accuracy for the model trained and tested on the *spontaneous*, *onset*, *sustained*, *offset,* and *late* response (Figure 11a) from an equal number of hit and miss trials from all experiments with fast ramp. We compared the classifier accuracy trained on different response types and found that offset and late responses allowed for significantly better action decoding than spontaneous or onset responses (Figure 11c). These results suggest that AAF offset responses can be informative on the animal's decision. They emphasize the behavioral relevance of AAF offset responses again.

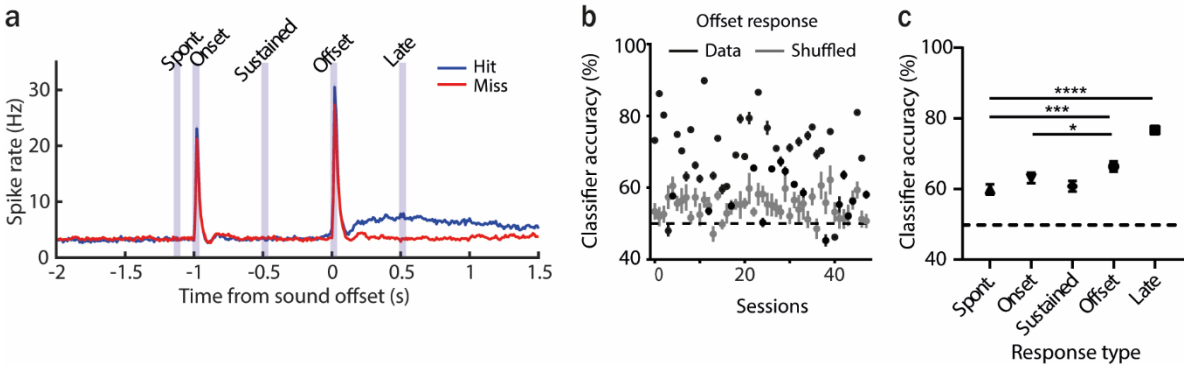


**Figure 11 The activity of AAF neurons can be predictive of animal performance.** (**a**) Averaged PSTH (mean± SEM) of AAF neuron's response to 1 s long PT (9 kHz) played at 60 dB SPL during hit (blue) and miss (red) trials, n=5076 cells, 59 sessions, 12 animals. (**b**) Classification accuracy based on offset responses (mean ± SEM) for real and shuffled data. (**c**) Comparison of classifier accuracy of decoders trained and tested on spontaneous activity, onset, sustained, offset, and the late response of AAF neurons (mean± SEM): spont. vs offset: p=0.0005; offset vs onset: p=0.0489; spont. vs late: p<0.0001, n=48 sessions, 12 animals, Wilcoxon test.

### 3.4.4. The AAF is highly specialized for processing information on sound termination

Knowing those offset responses in the AAF are behaviourally relevant and influence sound termination perception, we next asked what mechanisms are driving these cortical offset responses and what properties distinguish them from subcortical ones. We performed awake electrophysiological recordings in the AAF and the MGB and analyzed the response profile dynamics of cells within both regions. We recorded multi-unit activity evoked by 50 ms pure tones (PT) with varying frequency (4 to 48.5 kHz) and sound level (0 to 80 dB SPL) presented with randomized inter-stimulus-intervals (ISI) (500–1000 ms).

K-means clustering of spike-sorted unit (SU) activity was used to identify cells with distinct temporal dynamics. The clustering method was performed on the averaged poststimulus time histogram (PSTH) in both MGB (n=779 SU, 5 animals) and AAF (n=346 SU, 6 animals) recordings pooled together. The analysis time window for the clustering was chosen to emphasize the offset rather than the onset responses (25 – 75 ms, bin size: 5ms). Davies Bouldin evaluation was used to determine the optimal number of clusters (Supplementary Figure 3.5). Nine clusters were identified, reflecting five main temporal categories of auditory evoked responses: *onset-only*, *late-onset*, *onset-offset*, *sustained,* and *suppressed* (Figure 12). Few clusters with the same temporal dynamic pattern were detected (e.g., D-G)

resulting from various latencies, width, and the ratio of offset/onset responses. These clusters were merged for further analysis. In the MGB, both *onset-only* and *onset-offset* cells represented the biggest clusters: 40.1 % and 33.0 %, respectively (Figure 12b). Cells with these two temporal response patterns also revealed separate anatomical clusters within the MGB (Supplementary Figure 3.6) (He, 2002). *Suppressed* responses were found in 12.3 %, *late-onset* responses in 10.2 %, and *sustained* in 4.4% of cells. In the AAF, most cells were *onset-offset* responsive (83.2 %). Other categories were represented by much smaller proportions: *onset-only* (3.2 %), *late-onset* (6.1 %), and *sustained* (7.5 %). In contrast to the MGB, no *suppressed* cells were recorded in the AAF. The overrepresentation of onset-offset responses in the AAF compared to the preceding nucleus of the auditory pathway indicates that the AAF is highly specialized in processing information on sound termination.

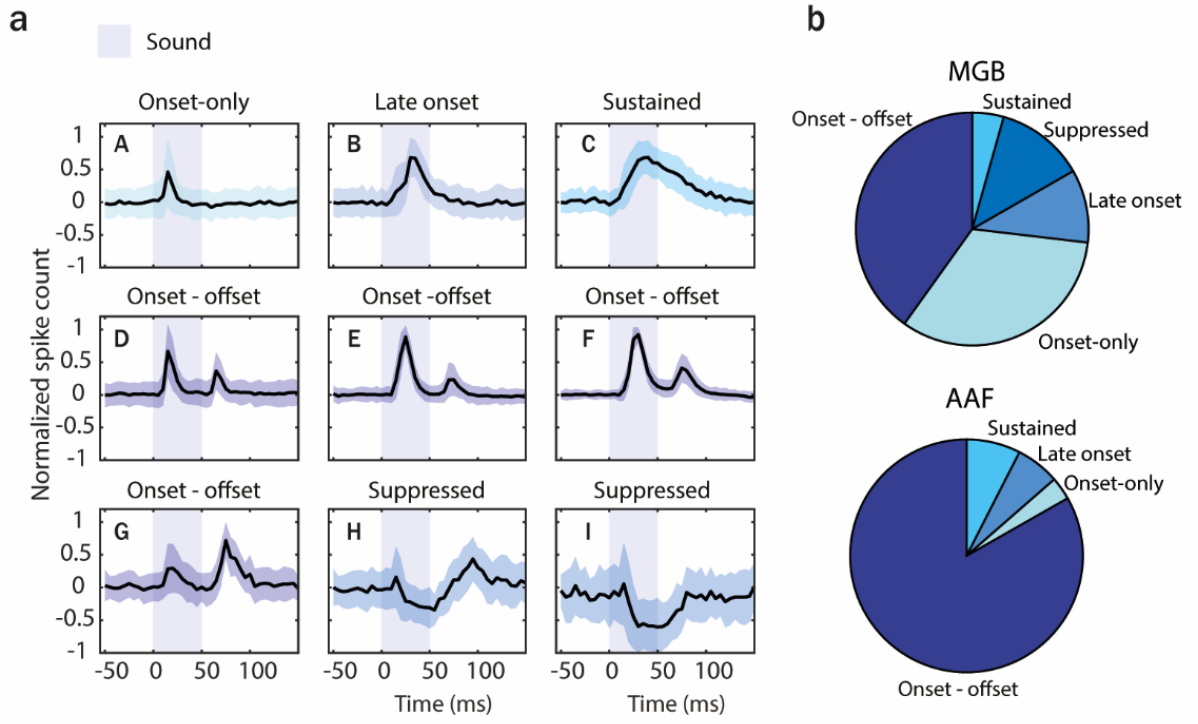


**Figure 12 The AAF has significantly more offset-responsive neurons than its input nucleus.** (**a**) Results of k-means clustering performed on both MGB (n=779) and AAF (n=346) neuron's responses (time window: 25-75 ms, bin size: 5ms) evoked by 50 ms PT with varied frequency (4 to 48.5 kHz) and sound level (0 to 80 dB SPL) presented with randomized ISI (500–1000 ms). Graphs represent the mean signal of cells belonging to each cluster. Data represent mean ± STD. The blue shaded bars represent the tone. (**b**) Representation of cells with the distinct temporal dynamic of responses in the MGB and the AAF. See also Supplementary Figure 3.5, 3.6.

### 3.4.5. Onset-offset responsive cells are the main inputs from the MGB to the AAF

As the AAF contains cells with mainly onset-offset responses - unlike the MGB or A1 (Solyga and Barkat, 2019), we asked whether these cortical offset responses were inherited from the MGB cells or whether they arose *de novo* in the AAF. We combined *in vivo* electrophysiological recordings in the MGB (n=1548 SU, 5 animals) with antidromic stimulation of the AAF, followed by pure tone

stimulation to characterize the temporal dynamics of cells projecting from the MGB to the AAF (Figure 13a, Supplementary Figure 3.7). A stimulating electrode was inserted into the previously functionally identified AAF (see methods). Pulse trains of monophasic square pulses were used for the electric stimulation (Figure 13b). We identified the MGB cells directly connected to the AAF by analyzing the percentage and latency of responses to the first stimulation pulse in each train. The MGB cells that fired as a response to the AAF stimulation in at least 50% of the trials with a first spike latency of 1 to 3 ms and a trial-to-trial latency jitter lower than 0.3 ms (Serkov, 1976) were considered to be sending direct inputs to the AAF (Figure 13c). These MGB cells were clustered mainly as onset-offset cells (83 %). We also identified some sustained (11 %) and suppressed (6 %) cells projecting from the MGB to the AAF, but their representation was significantly lower. Onset-only cells were not identified (Figure 13d). These results indicate that offset responses in the AAF are mainly inherited from the MGB. Whether further processing of these offset responses within the cortex took place is, however, still unclear.

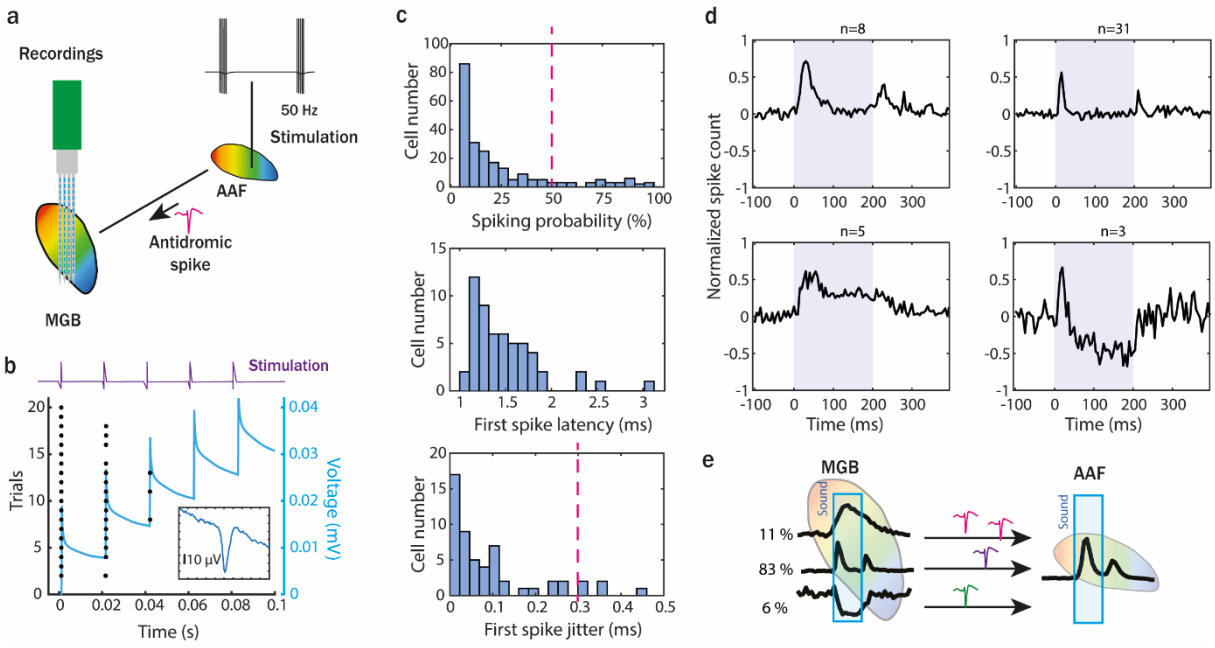


**Figure 13 Onset-offset responsive cells are the main inputs from the MGB to the AAF.** (**a**) Illustration of the experimental setup to perform an antidromic stimulation of MGB neurons projecting to the AAF. The stimulation tip was placed in the AAF after field identification (based on functional tonotopy). Monophasic electric pulses were delivered with 50 Hz at 30 µA. 64-channels electrode was inserted into MGB to record antidromic activity. (**b**) Example MBG unit spike raster of antidromic activity within 20 trials (5 pulses in each trial). The blue line represents increasing current injected during electric stimulation. (**c**) A number of recorded antidromic spikes in MGB neurons, where at least 1 spike following stimulation was detected in the time window from 1 to 5 ms after stimulation (*top*). Latency (*middle*) and jitter (*bottom*) of first antidromic spikes in MGB cells which were detected in at least half of the electric stimulation trials. (**d**) Temporal dynamic of clustered MGB cells (k-means) projecting to AAF identified during the antidromic experiment (mean± SEM). Three main temporal categories of auditory evoked responses were identified: onset-offset sustained and suppressed. MGB cells were considered AAF input if (1) in more than 50% of trials antidromic spikes were detected and (2) antidromic spikes jitter was lower than 0.3 ms. (**e**) Illustration of temporal dynamic and proportion of MGB cells projecting to AAF based on our antidromic results. See also Supplementary Figure 3.7.

### 3.4.6. Offset responses increase with sound duration, mainly in the AAF

Given the presence of offset responses in the MGB and the AAF, we asked whether their properties were similar in both regions. To reveal differences in offset processing, we decided to check how offset responses in the MGB and the AAF are affected by different sound properties such as sound duration, spectral content, or temporal complexity. We first addressed the question of the dependence of offset responses on sound duration (Scholl et al., 2010; Solyga and Barkat, 2019). We recorded responses in the MGB and the AAF offset cells (clustering based on Figure 12) to 60 dB SPL tones with durations varying between 50 and 500 ms and inter-stimulus intervals varying between 50 and 2000 ms (Figure 14a, d). For the MGB, the tone frequency was dependent on the offset BF of neurons in each session (because of narrow offset tuning of MGB neurons); for the AAF, a fixed PT of 9 kHz was used (as most of the widely tuned cells were responding to this frequency).

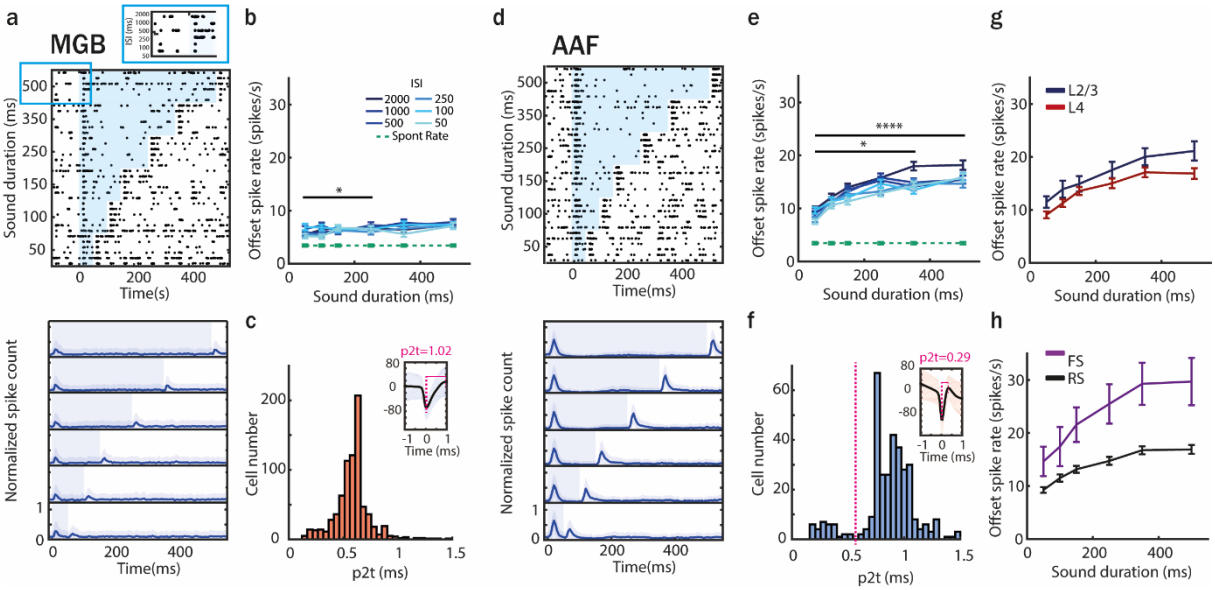


**Figure 14 Offset responses increase with sound duration, mainly in the AAF.** (**a**) Raster plot of an example MGB neuron's response to PT (frequency chosen based on offset tuning) with sound duration varying between 50 and 500 ms and ISI between 50 and 2000 ms (*top*) and PSTH (mean± STD) averaged over all neurons population (*bottom*). The blue shaded bars represent the tone. (**b**) MGB neurons offset responses (mean± SEM) to PT with increasing duration across all ISI of 2000 ms (correlation between sound duration and response rate: PT, $\rho$=0.05, p=0.02, n=307 SU, 5 animals, Spearman correlation). Comparison of offset responses: 50 ms vs. 100 ms: n.s. p=0.08; 50 ms vs 150 ms: n.s. p=1; 50 ms vs 250 ms: p=0.0318; 50 ms vs 350: n.s. p=0.7013; 50 ms vs 500 ms n.s. p=0.9064, Dunn's multiple comparisons test (**c**) Distribution of peak-to-trough times (p2t) of MGB neurons. (**d**) Raster plot of an example AAF neuron's response to PT (9 kHz) played at 60 dB SPL with sound duration varying between 50 and 500 ms and ISI between 500 and 2000 ms (*top*), and PSTH (mean± STD) averaged over all neurons population (*bottom*). The blue shaded bars represent the tone. (**e**) AAF neurons offset responses (mean± SEM) to PT with increasing duration across ISI of 2000 ms (correlation between sound duration and response rate: PT, $\rho$=0.25, p<0.0001, n=285 SU, 6 animals, Spearman correlation). Comparison of offset responses: 50 ms vs. 100 ms: n.s. p=0.5655; 50 ms vs 150 ms: n.s. p=0.9983; 50 ms vs 250 ms n.s. 0.0819; 50 ms vs 350: p<0.0411; 50 ms vs 500 ms p<0.0001, Dunn's multiple comparisons test. (**f**) Distribution of p2t of AAF neurons (**g**) Comparison of offset spike rate in L2/3 and L4 neurons in AAF for sounds with duration varying between 50 and 500 ms and longest tested ISI of 2000 ms (mean± SEM), L2/3: $\rho$=0.26, p<0.0001 $n_{2/3}$=87, L4: $\rho$=0.24, p<0.0001 $n_4$=198, Spearman correlation. (**h**) Comparison of offset spike rate of fast and regular spiking neurons in AAF for sounds with duration varying between 50 and 500 ms and longest tested ISI of 2000 ms (mean± SEM), FS: $\rho$=0.29, p=0.00012, $n_{FS}$=28, RS: $\rho$=0.24, p<0.0001, $n_{RS}$=257, Spearman correlation.

The correlation between sound duration and offset spike rate evoked by tones in onset-offset cells was very weak in the MGB but much stronger in the AAF (Figure 14b, e). In the MGB, population responses showed almost no difference in offset spike rate evoked by tones when durations changed between 50 ms and 500 ms (Figure 14b). However, in the AAF, differences in tone duration were significantly reflected by increased offset spike rates for the longest sounds (Figure 14e).

To explore whether the dependence of offset responses on sound duration is a result of AAF computations in layer 2/3 (L2/3) or is already present in the input layer 4 (L4), we compared the dependence of offset responses on sound duration in these layers (Figure 14g). Our recordings span the range of 150 to 600 μm from the pia surface, corresponding mainly to L2/3 (150-300 μm) and L4 (300-500 μm) (Meng et al., 2017). A significant correlation was present in L2/3 and L4, suggesting that the increase in offset response amplitude with sound duration is not unique to one layer.

As the MGB does not contain fast-spiking interneurons (FS) (Bartlett, 2013), we then asked whether their presence in the AAF could be driving the dependence of offset responses on sound duration in this cortical region (Figure 14c, f). We distinguished putative FS and regular spiking (RS) neurons based on the peak-to-trough times (p2t) of their spike waveforms (Figure 14f). Fast spiking units were defined as having a p2t smaller than the minimum between the two peaks of the p2t distribution (0.55 ms), in accordance with previous studies (Moore and Wehr, 2013). The unimodal distribution of p2t in the MGB confirmed the lack of FS in this region (Figure 14c). We found a significant correlation between offset spike rate and sound duration both in FS and RS (Figure 14h) neurons, ruling out the possibility that one of these cell populations is alone driving the dependence of offset responses on sound duration in the AAF.

Together, these results reveal an important difference between AAF and MGB offset encoding and demonstrate a clear amplification of the dependence of offset responses on sound duration in the AAF compared to the MGB.

### 3.4.7. Offset responses to white noise bursts are present in the AAF but not in the MGB

Next, we compared offset responses in the MGB and the AAF evoked by sounds with different spectral complexity. We recorded responses in both regions to 500 ms pure tones (PT), and white noise (WN) bursts played at 60 dB SPL (for the MGB, the PT frequency was chosen based on offset BF of neurons in each session; for the AAF, a fixed PT of 9 kHz was used). Our results showed distinct neuronal activity patterns in response to WN or the spectrally less complex PT, both in the MGB and in the AAF (Figure 15). In the MGB, 500 ms WN evoked no offset responses above spontaneous activity, unlike PT of the same length (Figure 15a, c). However, in the AAF, both PT and WN did evoke offset responses (Figure 15b, d). The lack of offset responses evoked by WN in the MGB, and their significant presence in the AAF, reveals offset responses generated *de novo* in the cortex.

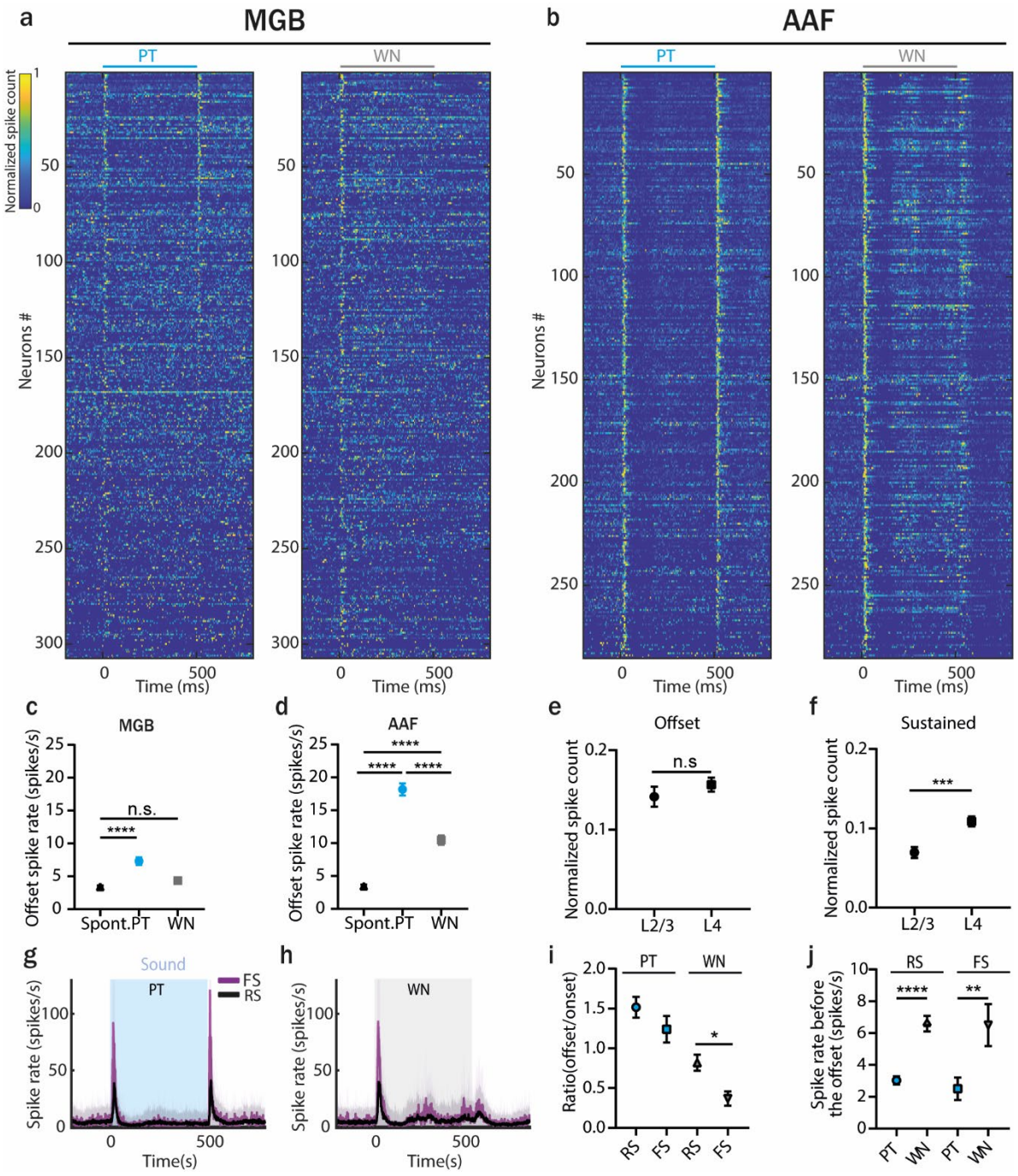


**Figure 15 Offset responses to white noise bursts are present in the AAF but not in the MGB.** (**a**) Normalized PSTH of MGB neurons to 500 ms PT or WN bursts, bin size: 5ms. Data are sorted by descending spike rate at the PT offset. (**b**) Normalized PSTH of AAF neurons to 500 ms PT or WN bursts, bin size: 5ms. Data are sorted by descending spike rate at the PT offset. (**c**) Comparison of MGB offset responses evoked by PT and WN for onset-offset cells. Data represent mean ± SEM, PT vs. spont. rate: $p<0.0001$; WN vs spont. rate: $p=0.071$, $n=307$, Wilcoxon test. (**d**) Comparison of AAF offset responses evoked by PT and WN for onset-offset cells. Data represent mean ± SEM, PT vs. spont. rate: $p<0.0001$; WN vs spont. rate: $p<0.0001$, PT vs WN: $p<0.0001$, $n=285$ Wilcoxon test. (**e**) Comparison of sustained responses (calculated in the window: 100-500 ms) for AAF cells from L2/3 and L4 evoked by 500 ms WN stimulation (mean± SEM), $p=0.0003$, $n_{2/3}=87$, $n_4=198$, Mann-Whitney test. (**f**) Comparison of offset responses for AAF cells from L2/3 and L4 evoked by 500 ms WN stimulation (mean± SEM), $p=0.2963$, $n_{2/3}=87$, $n_4=198$, Mann-Whitney test. (**g, h**) Averaged PSTH of fast (n=29) and regular (n=249) spiking AAF neuron's response to PT and WN bursts played at 60 dB SPL with sound duration 500 ms and ISI between 500 and 2000 ms. (**i**) Ratio of offset/onset responses evoked by 500 ms PT or WN in fast and regular spiking AAF neurons (mean± SEM), $p=0.0202$, $n_{FS}=28$, $n_{RS}=246$, Mann-Whitney test. (**j**) Spike rate preceding sound offset (calculated in window: 450-500ms) in AAF neurons for longest ISI of 2000 ms (mean± SEM), RS: $p<0.0001$, $n=257$; FS: $p=0.0013$, $n=28$ Wilcoxon test. See also Supplementary Figure 3.8.

We then asked whether offset responses to WN stimulation differed between different neuronal populations of the AAF. We found that responses to WN were significantly more sustained in L4 than in L2/3 (Figure 15e, calculated in a window of 100-500 ms following sound onset), despite having similar offset responses in both layers (Figure 15f). It seems that responses to WN stimulation, even if not present among MGB inputs, arise already in the AAF input layer. Next, we compared offset responses evoked by PT and WN in putative FS and RS neurons (Figure 15g, h). As expected, offset responses were bigger and faster in FS than RS neurons following PT termination (Figure 15i, Supplementary Figure 3.8a, b). In addition, there was not a significant difference in spike rate and latency between FS and RS neurons following WN termination (Supplementary Figure 3.8c). The comparison of ratios of offset/onset responses between cell and sound types showed that the ratio for FS neurons was significantly smaller than the ratio for regular spiking neurons with WN stimulation (Figure 15i). This relative decrease of offset responses in FS neurons could reduce inhibition and enhance excitatory cells' activity, leading to offset responses generated *de novo* in the AAF. These findings suggest that FS neurons could play an essential role in the cortical processing of WN offset responses.

The PSTHs of AAF neurons responding to PT and WN stimulation indicate that WN evokes more sustained activity than PT (Figure 15b). More specifically, WN gives rise to sharp onset responses followed by suppression, and then an activity rebound at around 200 ms, followed by a second suppression phase and another rebound. Could this specific response of neurons to WN stimulation influence the strength of AAF offset responses? Comparing the firing rate of FS and RS cells in the AAF 50 ms before the sound termination revealed that they were significantly bigger for WN than PT stimulation (Figure 15j). This extended firing could possibly affect the generation of offset for WN stimulation.

Studying offset responses evoked by WN bursts revealed two interesting differences between MGB and AAF processing. First, offset responses to WN stimulation are not present in the MGB but are present in the AAF. Second, cells in the AAF seem to follow ongoing WN stimulation with some kind of bursting activity happening every ~200 ms.

### 3.4.8. Offset responses to white noise stimulation do not increase with sound duration

Our results demonstrated that in AAF, offset responses increase as a function of PT duration and that responses to WN and PT are strikingly different in both AAF and MGB (Figure 15). Thus, we wondered if WN bursts with increasing durations would evoke higher responses than shorter bursts in either MGB or AAF. We recorded responses in both fields to 60 dB SPL WN bursts with durations varying between 50 and 500 ms and interstimulus intervals varying between 50 and 2000 ms. Offset responses to WN in both the MGB and the AAF were not increasing as a function of sound duration (Figure 16a-f). This data confirmed again that different mechanisms might be at play when WN or PT are heard.

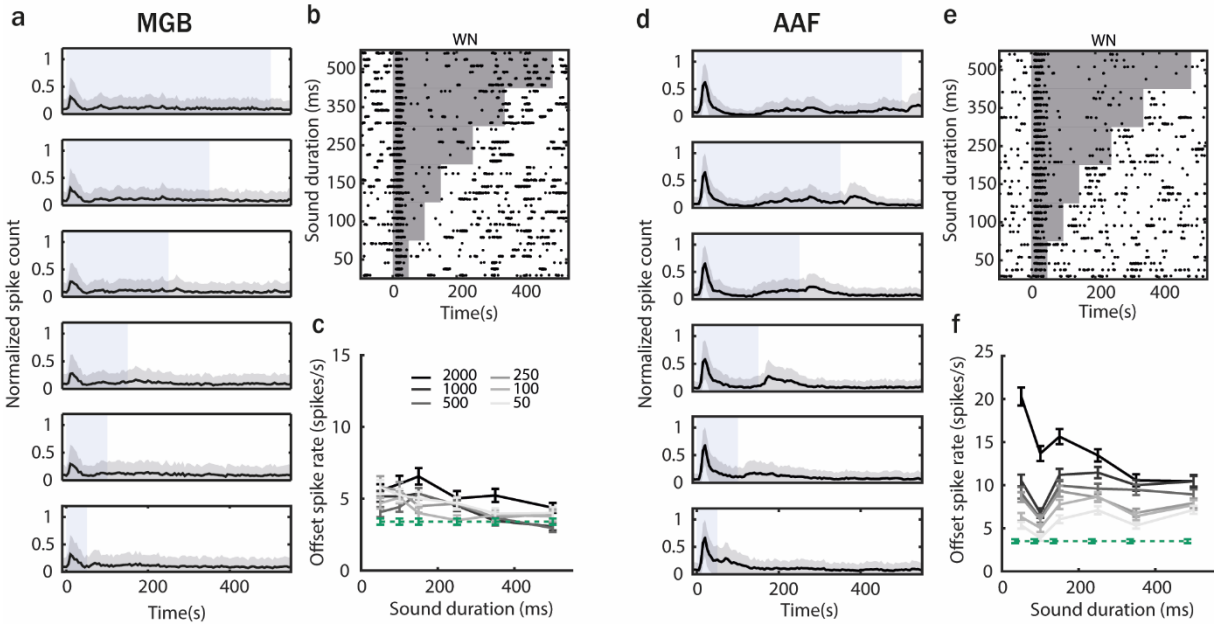


**Figure 16 Offset responses to white noise stimulation do not increase with sound duration** (**a**) PSTH (mean± STD) averaged over all MGB neuron's response to WN bursts played at 60 dB SPL with sound duration varying between 50 and 500 ms and ISI between 500 and 2000 ms. (**b**) Raster plot of an example MGB neuron's response to WN. The grey shaded bars represent the tone. (**c**) MGB neurons offset responses to WN with increasing duration across all ISI (correlation between sound duration and response rate $\rho$= -0.08, $p<0.0001$, Spearman correlation). (**d**) PSTH (mean± STD) averaged over all AAF neuron's response to WN bursts played at 60 dB SPL with sound duration varying between 50 and 500 ms and ISI between 500 and 2000 ms. (**e**) Raster plot of an example AAF neuron's response to WN. The grey shaded bars represent the tone. (**f**) AAF neurons offset responses to WN with increasing duration across all ISI (correlation between sound duration and response rate $\rho$= -0.01, $p<0.0001$, Spearman correlation).

### 3.4.9. Offset responses encode more than just silence

The precise detection of fast changes in sound frequency and level is crucial for gap detection and vocalization (Kopp-Scheinpflug et al., 2018; Sollini et al., 2018). We asked if offset responses in the MGB and the AAF could encode more than silence - i.e., sound termination - such as important changes within temporally discontinuous sounds (Lu et al., 2001). We recorded responses to a multi-frequency component sound in the MGB (n=275 SU, 5 animals) and in the AAF (n=284 SU, 6 animals). The complex sound consisted of three frequency components (20 kHz, 14 kHz, and 9 kHz) played at 60 dB SPL, which had a common onset but ended at different time points (300 ms, 400 ms, 500 ms). The offset responses evoked by removing one or two frequency components demonstrate that neurons can encode the disappearance of a frequency component in an ongoing sound, especially in the AAF (Figure 17a-f).

A single MGB neuron usually encoded the removal of one or two frequency components. In contrast, most AAF neurons encoded the removal of all frequency components. However, at the population level, the termination of all three components was significantly encoded in both MGB and AAF activities (Figure 17g, h). Interestingly, removing the first frequency component (20 kHz) evoked the smallest offset response, which, in the MGB, was close to spontaneous activity. Removal of the last component (9 kHz), followed by silence, evoked the highest offset response within MGB neurons. In contrast, the

highest offset response was present in the AAF after removing the second component (14 kHz). AAF neurons seem to have a stronger ability to integrate information over spectrally and temporally complex ongoing sounds and not only to respond to simply silence. This ability to encode important changes within continuous sound could be crucial for processing temporally discontinuous sounds, making the AAF an interesting field to study the encoding of vocal calls.

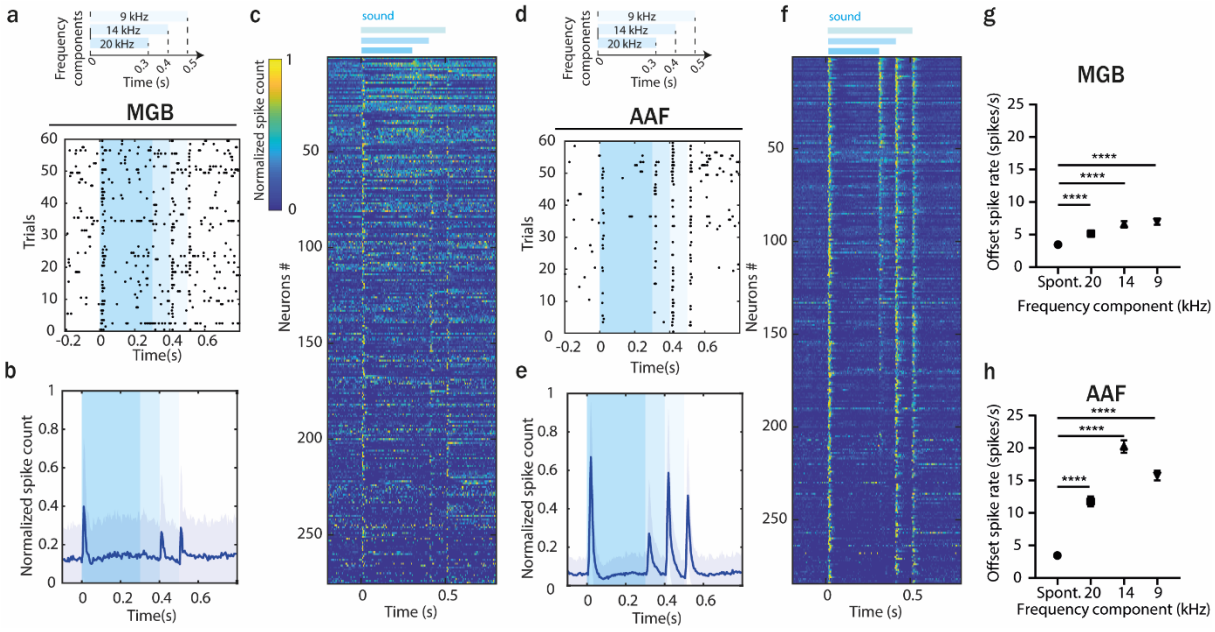


**Figure 17 Offset responses encode more than just silence.** (**a**) Raster plot of an example MGB neuron's response to 3-components stimuli. (**b**) Averaged PSTH (mean ± STD) of MGB neuron's response to 3-components stimuli, n=275, n=5 animals (**c**) Normalized PSTH of MGB neuron's response to 3-components stimuli, bin size: 5ms. Data are sorted by descending spike rate at the first component termination. (**d**) Raster plot of an example AAF neuron's response to 3-components stimuli. (**e**) Averaged PSTH (mean ± STD) of AAF neuron's response to 3-components stimuli, n=284, n=6 animals. (**f**) Normalized PSTH of AAF neuron's response to 3-components stimuli, bin size: 5ms. (**g**) Comparison of spiking rate of MGB neurons following removal of each frequency component. Data represent mean ± SEM, $p<0.0001$, n=275, n=5 animals Wilcoxon test. (**h**) Comparison of spiking rate of AAF neurons following removal of each frequency component. Data represent mean ± SEM, $p<0.0001$, n=284, n=6 animals Wilcoxon test.

## 3.5. Discussion

As the auditory system very robustly represents timing information, it is a model of choice to study neural offset responses evoked by the disappearance of a stimulus. This study shows that minimizing AAF offset responses decreases the mouse performance to detect sound termination, revealing their importance at the behavioral level. By combining *in vivo* electrophysiology recordings in the AAF and the MGB of awake mice, we also demonstrate that the AAF inherits, amplifies, and sometimes even generates *de novo* offset responses. These results are of high importance for all studies on sensory processing. The mechanisms determining specificities in cortical versus thalamic processing revealed by our studies could be common between the different sensory areas.

The functional significance of offset responses was long under debate (Saha et al., 2017). Here we show that minimizing AAF offset responses significantly decreases the performance of mice to detect sound termination (Figure 9, Figure 10). In addition, sounds terminating with a fast fall ramp and therefore triggering a bigger offset response are significantly easier to detect at the beginning of a behavioral session when the task is still new and more difficult than after exposure to more trials. A possible explanation for this dependence on task difficulty could be related to the distinct involvement of the ACx during more or less challenging tasks. Previous studies have shown that the cortex could be required for complex tasks but less so for easier tasks or when the task is learned well (Ceballo et al., 2019; Christensen et al., 2019; Dalmay et al., 2019; Kawai et al., 2015). When the task is easy or familiar, high and low amplitude offset responses seem to be informative about sound termination to a similar extent. Finally, we used logistic regression to show that AAF activity during a single trial could be predictive of the animal's performance (Figure 11). The neural activity during hit trials in the AAF could be influenced by the animal's general motivation (Fritz et al., 2003), motor-related inputs (Schneider, 2020), or reward expectations (De Franceschi and Barkat, 2020).

Another approach to understanding the behavioral role of auditory offset responses could be to study where the AAF is projecting and what could be the use of offset responses in these areas. It was previously shown that offset responses in the secondary auditory cortex are plastic and can enhance the representation of a newly acquired, behaviourally relevant sound category (Chong et al., 2020). Whether the activity of AAF neurons is crucial for this plasticity to happen remains to be elucidated. Only recently, Nakata et al. revealed direct AAF connections to the secondary motor cortex, the primary somatosensory cortex, the insular auditory cortex, and the posterior parietal cortex (Nakata et al., 2020). What the role of auditory offset responses in these fields could be and whether they provide any information for association with the somatomotor system remain unanswered.

Spectro-temporal tuning properties of auditory neurons differ during the presentation of natural and synthetic stimuli (David et al., 2007; Theunissen et al., 2001). Additionally, natural sounds commonly start abruptly, but their termination is obscured by sound reverberations, which is not the case for synthetic stimuli. In most of our experiments, we used a sharp 0.01 ms sinusoidal offset ramp while keeping the onset ramp at 4 ms. We checked if any significant onset response could be mixed with the actual offset responses due to spectral splatter. We measured with an ultrasensitive microphone, acceleration traces of 9 kHz pure tone played at 60 dB SPL with 0.01 ms and 1 ms rise and fall-ramp (Supplementary Figure 3.3a, b). We detected a weak spectral splatter present for less than 0.5 ms covering a frequency range between 6 and 30 kHz (Supplementary Figure 3.3c, d). At the same time, we did not see increased offset responses in neurons tuned to the frequencies corresponding to the spectrum of the artifact (Supplementary Figure 3.3e). The peak amplitude of offset responses evoked by 0.01 ms fall-ramp was highly correlated with the peak amplitude of offset responses evoked by 1 ms ramp (Supplementary Figure 3.3f), suggesting that our protocol allows us to identify real offset

responsive cells. We also found that onset responses are suppressed by preceding onset responses but not affected by preceding offset responses (Supplementary Figure 3.3g), even when the interval was as short as 50 ms. This suggests that offset responses we recorded are driven by a different set of synapses that onset responses, confirming parallel processing streams (Scholl et al., 2010). In the future, the role of offset responses in detecting sound termination in natural environments, using, for example, vocalization calls (Chong et al., 2020), should be studied. This would answer if the auditory system, and the MGB or the AAF more specifically, evolved to meet the challenges of detecting naturally terminating sounds.

Our results demonstrate that cortical offset responses are not only inherited from the periphery (Figure 12, Figure 13) but also amplified by sounds with longer duration (Figure 14). Could the presence of FS interneurons in the AAF, but not in the MGB (Bartlett, 2013), be driving the dependence of offset responses on sound duration in this cortical region? The strength of the correlation between offset responses and sound duration was similar between FS and RS cells in the AAF (Figure 14). However, FS neurons showed a significantly bigger amplitude of offset responses in comparison to RS neurons. The AAF was previously shown to have more PV+ cells than the other auditory primary region A1 (Reinhard et al., 2019). Mechanistically, we suggest that such a prominent PV network in the AAF and the big amplitude offset responses they exhibit could be crucial for evoking duration-dependent offset responses in the AAF but not in the A1 (Solyga and Barkat, 2019) or the MGB (Figure 14). With our antidromic experiments, we also show that some of the AAF cells receive inputs from sustained and suppressed MGB cells (Figure 12). Whether or not the inputs from these cells are involved in the duration dependence of offset response in the AAF should be explored further.

What could be the role of the cortex in tracking subtle differences in sound duration? At the behavioral level, one could speculate that the amplitude of offset responses would be needed to better track subtle differences in sound duration, especially for sounds shorter than 500 ms, covering a spectrum of most mouse calls (Geissler and Ehret, 2002). Nevertheless, if the increase in the amplitude of offset responses with sound duration is a carrier of useful information or just a result of cortical cells being unable to handle short sounds remains unclear.

The spectral complexity of sounds is significantly modulating offset responses in the central auditory system in several ways. First, the lack of offset responses to WN in the MGB onset-offset cells and their presence in the AAF reveals offset responses generated *de novo* in the cortex (Figure 15). How could the differences in offset responses to WN stimulation be explained? The large spectral integration of thalamic inputs (Supplementary Figure 3.9) in individual cortical neurons (Liu et al., 2007; Vasquez-Lopez et al., 2017) should not play a role, as no firing upon WN termination was observed in the thalamus. Interestingly, offset responses to WN stimulation were present in the AAF both in L4 and L2/3, suggesting that it is a general property of the AAF network to generate offsets *de novo* and not only an exclusive property of the superficial layer. What mechanisms could drive offset responses to

WN in the AAF? FS and RS neurons exhibit similar offsets responses to WN stimulation, thus not allowing us to speculate on their particular involvement in *de novo* generated offset responses. The potential role played by other types of cortical neurons, like the somatostatin interneurons previously suggested to be involved in offset response generation (Liu et al., 2019), remains to be elucidated. It is also possible that information on sound termination arises from non-lemniscal areas projecting to the AAF. Such possible projections and their potential contributions have not been described yet.

Second, the activity during WN stimulation in the AAF shows a clear pattern of bursting activity, where a transient onset is followed by a suppression phase, then rebound activity around 200 ms, followed by another suppression and rebound phase. Does this reflect an internal clock allowing the AAF to follow sound duration irrespectively from inputs coming from the MGB? What could be the role of such bursting activity in the AAF, and how could it be generated? Bursts are thought to be emitted by many subcortical and cortical areas of the brain, but their hypothesized functions differ across brain areas (Zeldenrust et al., 2018). It has previously been shown in marmosets that the auditory cortex can use a combination of temporal and rate representation to encode the wide range of complex, time-varying sounds (Lu et al., 2001). The offset responses and bursting activity we see in the mouse AAF could play these multiple roles in encoding different temporal features such as ongoing sound and its termination. Human linguistic studies reported that certain timescale of acoustic-energy modulation is more relevant than others for conveying conspecific vocalizations such as speech (Rosen, 1992). It would be most efficient if these modulations could be matched to mean syllable length (125–250 m) across languages (Greenberg and Ainsworth, 2006) and if they would only occur after stimulus presentation but not being present in the network otherwise. The reoccurring activity we recorded in the AAF was triggered by stimuli and had a frequency of ~5 Hz thus fitting to the mean syllable length. Therefore, although entirely speculative at this time, it is tempting to suggest that similar reoccurring activity could also exist in the human primary auditory cortex and serve an important function in speech comprehension. If the bursting and offset activity observed in the AAF is a common feature of other primary sensory cortices is unclear.

Finally, we demonstrate that offset responses to WN or PT are strikingly different in the central auditory system (Figure 15). This could have multiple origins. First, the significantly increased activity of AAF neurons preceding WN termination could, in turn, result in a decreased ability of neurons to respond properly to the end of the sound (Figure 15j). Second, the lack of proper inhibition - excitation balance (Figure 15i) could decrease the offset responses evoked by WN burst. WN stimulation is widely used in auditory research, especially for the gap in noise detection (Syka et al., 2002; Threlkeld et al., 2008; Weible et al., 2014a; Weible et al., 2014b) and for offset responses studies (Anderson and Linden, 2016). It is an attractive auditory stimulus to study purely temporal information as it ensures an effective stimulation of the auditory system irrespectively of neuronal tuning. However, one has to be careful about generalizing results obtained with this stimulus to all auditory inputs. Our observations indicate that different mechanisms might be at play when WN or PT, and by extension natural sounds, are heard.

The experiments with multi-frequency component sounds show that within both the MGB and the AAF, offset responses indicate not only when a sound ends but also all-important changes that occur within a temporally discontinuous sound (Figure 17), emphasizing their possible relevance for behavior and perception. The temporal integration of offset responses is crucial for perceptual grouping of communication sounds, in which rapid changes in intensity and frequency occur (Sollini et al., 2018). Our results suggest that this integration is accentuated in the cortex, making it an interesting hub to look for the mechanisms that might explain impairments in sound-offset sensitivity, and by extension, deficits in temporal processing arising both in aging and disease. A deeper knowledge of the cellular and circuit mechanisms of cortical offset responses could be crucial to develop new strategies to prevent abnormal auditory perceptual grouping.

## 3.6. Methods

### Surgical procedures

All experimental procedures were carried out in accordance with Basel University animal care and use guidelines and were approved by the Veterinary Office of the Canton Basel-Stadt, Switzerland. 35 C57BL/6J mice were used in this study, procured from Janvier LABS, France. Mice were a mixture of males and females and aged between 7 and 12 weeks of age at the time of behavioral training or electrophysiological recording.

Awake electrophysiology recordings and behavior experiments were performed on adult (7–12 weeks) male and female C57BL/6J mice (Janvier, France). For surgeries, mice were anesthetized with isoflurane (4% for induction, 1.5 to 2.5% for maintenance), and subcutaneous injection of bupivacain/lidocain (0.01 mg/animal and 0.04 mg/animal, respectively) was used for analgesia. A custom-made metal head post was fixed with super glue (Henkel, Loctite) on the bone on top of the left hemisphere and used to head-fix the animals. Their body temperature was kept at 37°C with a heating pad (FHC, ME, USA), and lubricant ophthalmic ointment was applied on both eyes. Craniotomy (~2×2 $mm^2$) was performed with a scalpel just above the right auditory cortex and covered with silicone oil and silicone casting compound (Kwik cast, World Precision Instruments, Inc. FL, USA) during the 2 h recovery period from the anesthesia.

### Recordings

The electrophysiological recordings were performed in awake mice (AAF: n=6; MGB: n=5). Mice were head-fixed and placed in the cardboard tube for recordings inside a sound box. Extracellular recordings were conducted in AAF (identified based on the functional tonotopy: ventro-dorsal increase in BF) and MGB (centered 0.8 mm anterior and 2 mm lateral to Lambda). Multi-channel extracellular electrodes with 32 channels (A4×8-5 mm-50-200-177-A32 or A1x32-5mm-25-177-A32 Neuronexus, MI, USA)

or 64 channels (A4x16-5mm-50-200-177-A64, Neuronexus, MI, USA) were inserted orthogonally to the brain surface with a motorized stereotaxic micromanipulator (DMA-1511, Narishige, Japan) at a constant depth (AAF: the tip of the electrode at 556±9 µm from pia; MGB: the tip of the electrode at 3575±300 µm from pia). Responses from extracellular recordings were digitized with a 32- or 64-channel recording system (RZ5 Bioamp processor, Tucker Davis Technologies, FL, USA) at 24414 Hz. Single unit clusters were identified from raw voltage traces using kilosort (Pachitariu et al., 2016) (CortexLab, UCL, London, England) followed by manual corrections based on the inter-spike-interval histogram and the consistency of the spike waveform (phy, CortexLab, UCL, London, England) and further analyzed in MATLAB (Mathworks, MA, USA).

**Auditory stimulation**

Sounds were generated with a digital signal processor (RZ6, Tucker Davis Technologies, FL, USA) at 200 kHz sampling rate and played through a calibrated MF1 speaker (Tucker Davis Technologies. FL, USA) positioned at 10 cm from the mouse's left ear. Stimuli were calibrated with a wide-band ultrasonic acoustic sensor (Model 378C01, PCB Piezotronics, NY, USA).

**Antidromic stimulation**

To identify temporal dynamics of cells projecting from MGB to AAF, *in vivo* electrophysiology recordings in MGB were combined with antidromic stimulation of AAF (n=5 animals). First, Mice were anesthetized with an intraperitoneal injection of ketamine/xylazine (80 mg/kg and 16 mg/kg, respectively), and subcutaneous injection of bupivacain/lidocain (0.01 mg/animal and 0.04 mg/animal, respectively) was used for analgesia. Ketamine (45 mg/kg) was supplemented during surgery as needed. For surgery, mice were head-fixed, and their body temperature was kept at 37 °C with a heating pad (FHC, ME, USA). Two separate craniotomies (~2 × 2 $mm^2$) were performed with a scalpel above the right MGB and auditory cortex and covered with silicone oil. AAF was mapped with electrophysiology recordings based on the ventro-dorsal increase in BF to identify the target area for stimulus pipette insertion. Then both craniotomies were covered with silicone casting compound (Kwik cast, World Precision Instruments, Inc. FL, USA) during the 2 h recovery period from the anesthesia. Electric stimulator (Master-8, A.M.P.I., Israel) was connected to a stimulation isolator (ISO-Flex, A.M.P.I, Israel), which was then connected to the wire electrode. Wire electrode was fixed in pulled capillary glass (tip:<10 µm) filled with saline and then inserted into AAF (~300 µm). Monophasic square wave pulses were generated with an electronic stimulator as pulse train (pulse duration: 0.1 ms; frequency: 50 Hz; train number: 20; intensity: 30 uA (similar to the method described in (Peng et al., 2017)). At the same time, electrophysiology recordings with 64-channels electrodes were performed in MGB. As described in the recordings section, spike sorting was performed using kilosort (Pachitariu et al., 2016), followed by manual corrections in phy and further analysis in MATLAB. The mean cluster waveform

from raw data was calculated for each antidromicaly-identified cluster to ensure the absence of electrical artifacts. Clusters containing any high amplitude electric artifacts were removed from the analysis.

**Offset detection task**

*Headplate implant.* Mice were implanted with a custom-made metal head post at 7-8 weeks after birth under isoflurane anesthesia (4% induction, 1.2 to 2.5% maintenance). Local analgesia was provided with subcutaneous injection of bupivacaine/lidocaine (0.01 mg/animal and 0.04mg/animal, respectively). A head post and a ground screw were fixed to the skull with dental cement (Super-Bond C&B; Sun Medical, Shiga, Japan). The portion of the skull above the target recording site was left free from cement and covered with a thick layer of Kwik-Cast Sealant (WPI, Sarasota, FL, USA). Post-operative analgesia was provided with an intraperitoneal injection of buprenorphium (0.1 mg/kg). After recovery from the surgery for a couple of days, mice were food restricted. *Training.* Mice were then placed in the cardboard tube and adapted to the head restraint. The speaker was placed 10 cm away from the left ear of the animals. Next, they were taught to associate a sound offset with a reward availability. Mice were trained to detect sound offset of pure tones (9 kHz) played at 80 dB SPL (training) with varied duration (1 s, 1.5 s, 2 s). The rise ramp of the tones was always fixed to 10.0 ms, while at the offset fast (0.01 ms) or slow (10.0 ms) ramp was used and varied randomly. During the beginning of the training, mice had to lick within 3 s after sound offset to receive a drop of soya milk as a reward, and the trial was considered a correct hit. If the animal did not lick within and after, the tone trial was considered as missed. If the mice licked while the tone was ongoing, they received a mild air puff oriented toward the right eye and a time out (2-3 s) until the next trial could start. These trials were removed from the analysis as the target (sound offset) could not be correctly delivered. Sounds were delivered without preceding cues at random interstimulus intervals ranging from 3 to 5 s. Licks were detected with a piezo sensor attached to the reward spout. Within consecutive training days, the reward window was shortened down to 1 s. *Craniotomy.* Once animals performed at least 30 % of correct hits, they were considered initially trained and had a craniotomy performed under ketamine/xylazine (80 mg/kg) and AAF mapping on the same day. *Recordings.* The following day, mice were moved on to a tasting phase where behavior training was coupled with acute electrophysiology recordings in AAF. During the testing phase, tones were played at 60 dB SPL, and laser was added unilaterally above right-AAF and activated for 200 ms following sound termination in half of the trials. All experiments were performed in a soundproof box (IAC acoustics, Hvidovre, Denmark) and monitored outside the sound box with a camera (C920, Logitech, Switzerland). Laser power was set around 4.2 mWat and adjusted every day, so it is causing a robust suppression of offset responses in PV- cells. The testing phase was carried out for up to 6 days. Behavioral control and data collection were carried out with custom-written programs using a complex auditory processor (RZ6, Tucker Davis Technology, FL, USA) and further analyzed with MATLAB (MathWorks, MA, USA).

**Data Analysis**

All data analysis was performed using custom-written MATLAB (2019) (Mathworks) code.

**Tuning receptive fields**. To determine BF and tuning receptive fields (TRF), we used PT (50 ms duration, randomized ISI distributed equally between 500 and 1000 ms, 2 repetitions, 4 ms cosine on, and 0.01 ms cosine off-ramps) varying in frequency from 4 to 48.5 kHz in 0.1 octave increments and level from 0 to 80 dB SPL in 5 dB increments. Tuning receptive fields, best frequency, and spiking rates were calculated in fixed time windows: onset: 6-56 ms, offset: 56–106 ms. TRFs were smoothed with a median filter (4×4 sampling window) and thresholded to 0.2 of peak amplitude. Onset and offset BF was defined as the frequency that elicited maximal response across all sound levels. Onset and offset peak latency was determined as the time point in which the smooth PSTH (kernel=hann (9)) collapsed across all tested stimuli showed a maximum response (binning size: 5 ms). Spontaneous activity was calculated based on activity preceding sound onset (150-50 ms, binning size: 5 ms).

**Tone duration responses.** To study responses to tones with different durations, we used 10 repetitions of PT (AAF: 9 kHz; MGB: frequency adapted to offset BF of recorded neurons) with 4 ms cosine on and 0.01 ms cosine off-ramps, which were varied in duration (50, 100, 150, 250, 350, 500 ms), ISI (the gap between 2 stimuli of 50, 100, 250, 500, 1000, 2000 ms) and played at 60 dB SPL. For AAF, the frequency was fixed to 9 kHz because 9 kHz PT evoked significant offset responses in almost all tested AAF. Offset spike rates were calculated in a fixed time window of 6-56 ms following sound termination.

**Spectral complexity.** To study offset responses in MGB and AAF evoked by sounds with different spectral complexity, we recorded responses in both regions to 500 ms pure tones (PT), and white noise (WN) bursts played at 60 dB SPL with 4 ms cosine on and 0.01 ms cosine off-ramps (for MGB the PT frequency was chosen based on offset BF of neurons in each session; for the AAF, a fixed PT of 9 kHz was used). WN bursts were not fixed but consisted of randomly chosen noise samples. Offset spike rates were calculated in a fixed time window of 6-56 ms following sound termination.

**Sound rise-fall time study.** To study the dependence of onset and offset responses on the temporal profile of a tone, we varied rise and fall time at sound onset and offset (0.01, 1, 2, 4, 10, 50, 100, 200 ms). PT (AAF: 9 kHz; MGB frequency adapted to offset BF of recorded neurons) was played at 60 dB SPL for 500 ms and repeated 50 times. The peak amplitude of offset responses was defined in the first 100 ms after stimulus onset or offset.

**Offset detection in ongoing sound.** To check if offset responses encode changes within ongoing sound, we used tone consisting of 3 frequency components (20 kHz, 14 kHz, and 9 kHz) played at 60 dB SPL and repeated 60 times. All frequency components had common onset but were terminated at different

time points (300 ms, 400 ms, and 500 ms). Offset spike rates were calculated after every component removal in fixed windows: 306-356 ms; 406 – 456 ms; 506 – 556 ms.

**Sound termination detection task.** To compare the hit rate for trials with and without laser or for different tested ramps, a moving average was calculated with a window size of 10 trials. The data for each condition was calculated separately. For the average, 10 adjacent trials were taken, and only the behavior corresponding to the specific condition was used (meaning that each average is made of a maximum of 10 trials but usually of less). This allows a comparison of performance over time across the tested conditions.

**Decoding population activity**. The logistic regression model was used to decode animal performance from neural responses (code from Neuromatch Academy W1D4, www.neuromatchacademy.org). Spontaneous activity (50 – 100 ms before sound onset), onset response (0-50 ms from sound onset), sustained response (500 – 450 ms before sound offset), offset response (0-50 ms from sound offset), or late response (500 – 550 ma after sound offset) were used to train and test the model. L2 regularization was used to avoid over-fitting. 8-fold cross-validation was performed by leaving out a random 12,5 % subset of trials to test the classifier performance, and the remaining trials were used to train the classifier. A range of regularization values was tested (0.0001 to 10000 log spaced), and the one that gave the smallest error on the validation dataset was chosen as the optimal regularization parameter. Classifier accuracy was computed as the percentage of testing trials in which the animal's choice was accurately predicted by the classifier and summarized as the average across the 10 repetitions of trial subsampling. The spiking activity of each neuron was z-scored before running the logistic regression model. Trial labels were shuffled to confirm that decoding is not working for random data. This procedure was repeated 10 times. Then the average across the 10 repetitions was used to assess classifier accuracy for randomized data. To remove all the sessions with too few trials or too few offset cells, only the sessions with a significant difference classification accuracy between real and shuffled data based on the late response (0.5 s after sound offset) were used.

**Statistical analysis**

The sample size was determined based on standards established by previous publications studying single-neuron activity with in vivo recording, which have been adequate to demonstrate significant population effects. A traditional power analysis is not possible because noise properties of neural data are difficult to estimate a priori. Based on norms for the field, we acquired data from at least five animals, except for Figure 10a (n=2 animals), and numbering at least 14 behavioral sessions or 50 neurons per group, except for the number of putative fast-spiking neurons in Figure 14 and Figure 15 (n=28). Statistical tests were performed with GraphPad Prism software version 7.03 (GraphPad Software, USA). The standard error of the mean was calculated to quantify the amount of variation between responses from different populations. A Nonparametric, unpaired Mann-Whitney test was used to calculate

whether there were any significant differences between medians of recordings in AAF and MGB. Wilcoxon paired test was used to compare differences between paired values obtained in different treatments. Two-way ANOVA was used to test the main effects of sound duration and intervals on offset responses and their interaction effect. Dunn's multiple comparisons test was used to perform multiple pairwise comparisons. Spearman correlation tests were used to test for significant associations between pairs of variables measured with ranking. The effects were named significant if the p-value was smaller than 0.05 (*), 0.01 (**), 0.001 (***) or 0.0001(****), for a confidence interval of 95, 99 or 99.9%, respectively.

## 3.7. Supplementary data

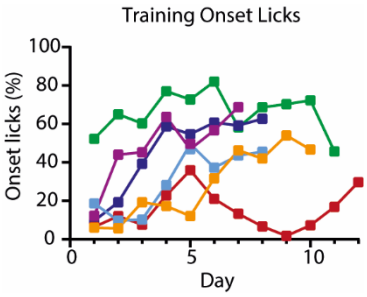


**Supplementary Figure 3.1 Occurrence of offset licks during training.**

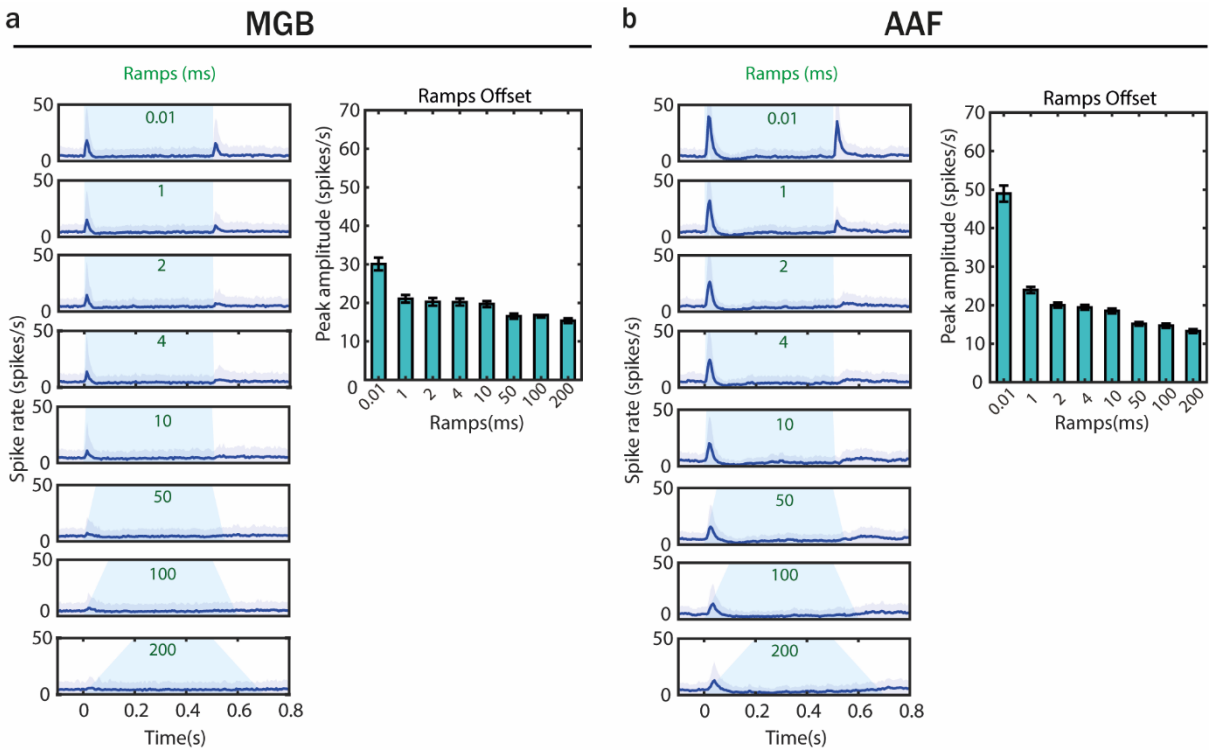


**Supplementary Figure 3.2 Offset responses evoked by sounds terminated with different fall ramps emerge already in MGB.** (**a**) (Left) averaged PSTH (mean± STD) of MGB neuron's response to PTs (9 kHz) played at 60 dB SPL with varied on and off-ramps: 0.01, 1, 2, 4, 10, 50, 100, 200 ms. (Right) comparison of offset peak amplitude evoked by PTs with the different onset and offset ramps. (**b**) (Left) averaged PSTH of AAF neuron's response to PTs (frequency adapted to offset BF of recorded neurons) played at 60 dB SPL with varied on and off-ramps. (Right) comparison of offset peak amplitude evoked by PTs with the different onset and offset ramps.

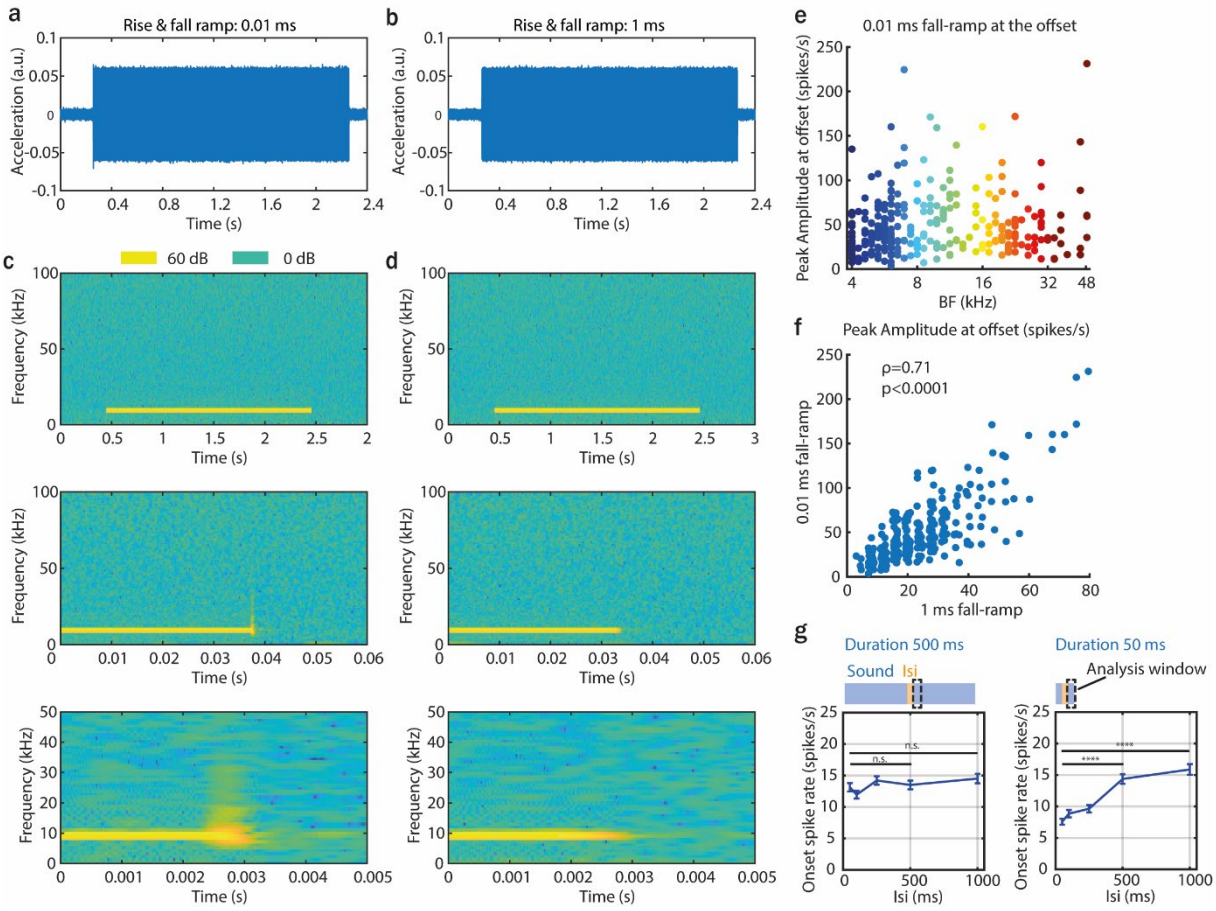


**Supplementary Figure 3.3 Properties of 9 kHz pure tones played at 60 dB SPL with different rise and fall ramps.** (**a, b**) Acceleration traces of 9 kHz pure tone played at 60 dB SPL with 0.01 ms (a) and 1 ms (b) rise and fall-ramp measured with an ultrasensitive microphone (Avisoft-Bioacoustics CM16/CMPA). (**c, d**) Spectrograms of a 9 kHz pure tone played at 60 dB SPL with 0.01 ms (c) and 1 ms (d) rise and fall-ramp. (**e**) The peak amplitude of offset responses evoked by 0.01 ms fall ramp as a function of onset best frequency. (**f**) Comparison of the peak amplitude of offset responses evoked by 0.01 ms and 1 ms fall ramp (ρ=0.71, p<0.0001, Spearman correlation). (**g**) Modulation of onset responses by preceding offset (left) or onset (right) responses.

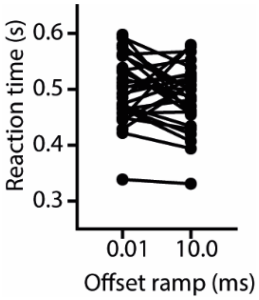


**Supplementary Figure 3.4 Comparison of reaction times in sound termination detection task for two tested fall-ramps: 0.01 ms and 10.0 ms.**

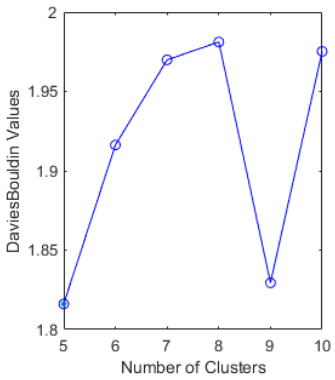


**Supplementary Figure 3.5 Davies-Bouldin index for the different number of clusters. The minimum value is reached for 5 and 9 clusters.**


**Supplementary Figure 3.6 2D representation of temporal dynamics of MGB cells recorded during 4 experiments with the 64-channel electrode (16x4).**

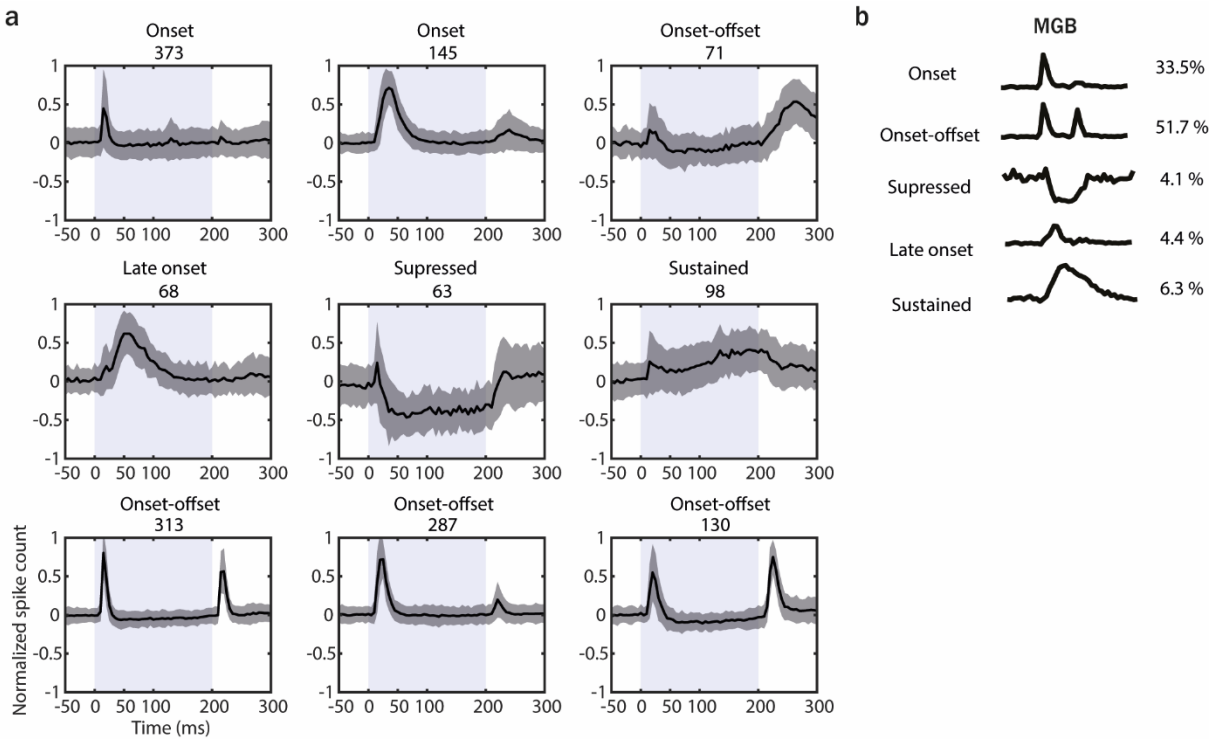


**Supplementary Figure 3.7 Response dynamics of MGB cells recorded during antidromic stimulation experiment.** (**a**) Results of k-means clustering performed on MGB cells recorded during antidromic stimulation experiments (n=1548) evoked by 200 ms PT with varied frequency (4 to 48.5 kHz) and sound level (0 to 80 dB SPL) presented with randomized ISI (500–1000 ms). The graphs represent the mean temporal dynamic of cells belonging to each cluster. Data represent mean ± SD. The grey shaded bars represent the tone. (**b**) Percentage of cells with a distinct temporal dynamic of responses in the MGB cells recorded during the antidromic experiment.

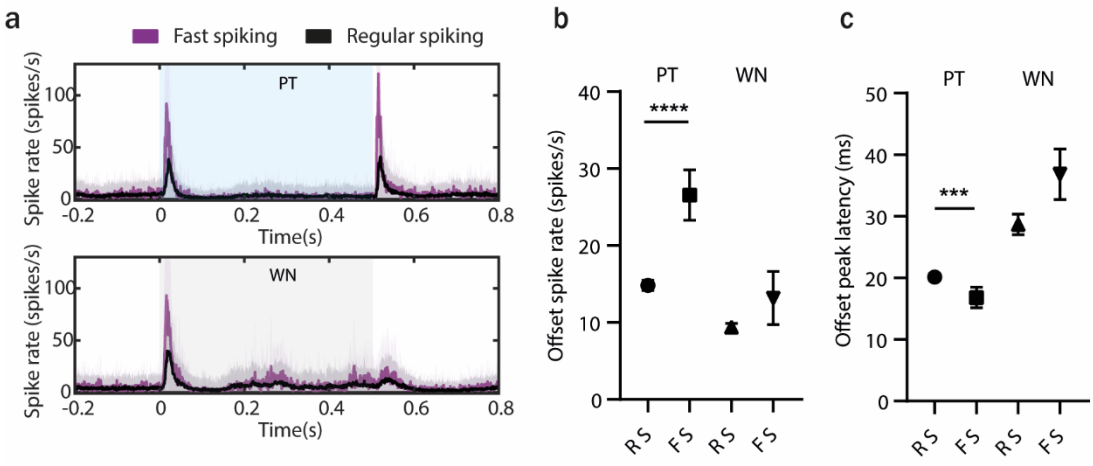


**Supplementary Figure 3.8 Offset processing in fast and regular spiking AAF neurons.** (**a**) Averaged PSTH (mean±STD) of fast and regular spiking AAF neuron's response to PTs (9 kHz) or WN bursts played at 60 dB SPL with a sound duration of 500 ms and ISI between 500 and 2000 ms. (**b**) Comparison of offset spike rate for RS and FS units in response to termination of 500 ms PT or WN, $p<0.0001$, Mann-Whitney test. (**c**) Comparison of offset response latencies of RS and FS units in response to termination of 500 ms PT or WN, $p=0.0006$, Mann-Whitney test.

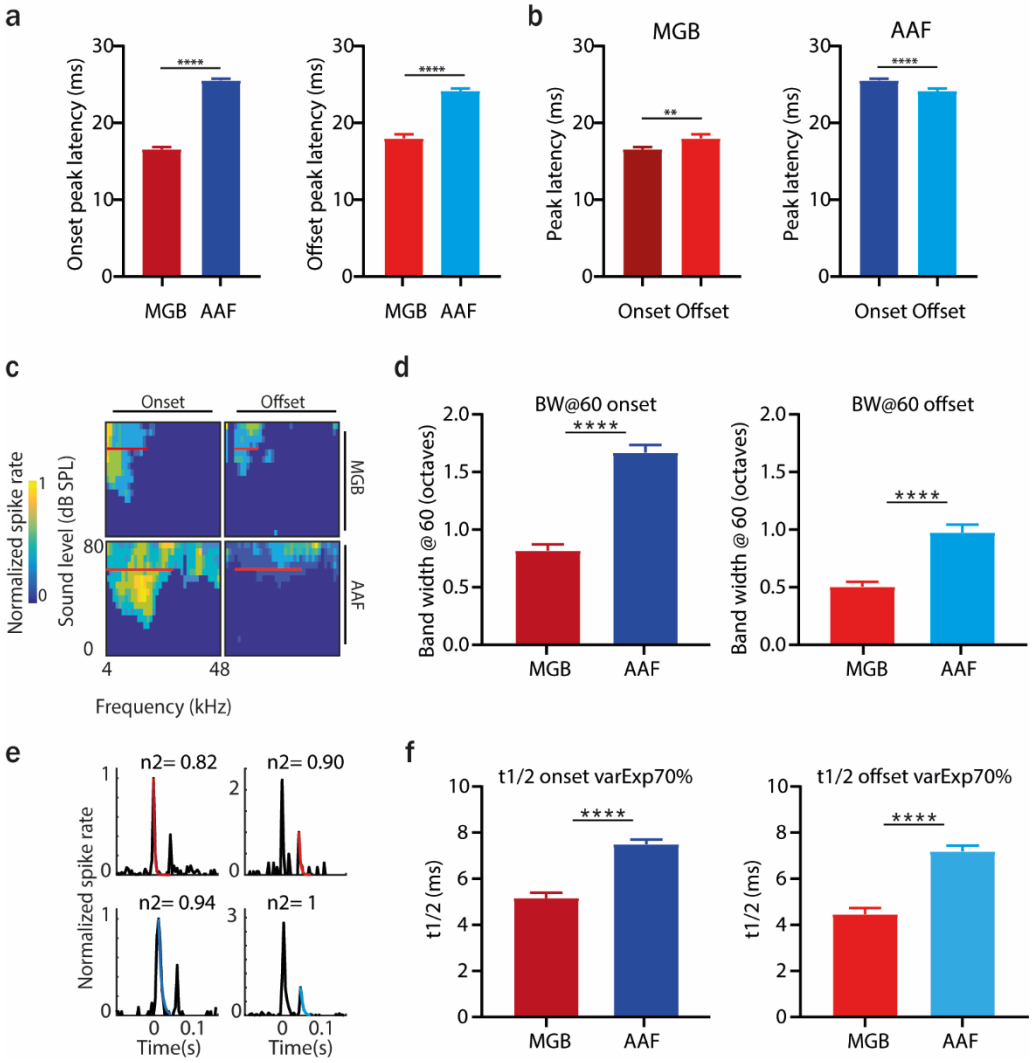


**Supplementary Figure 3.9 Distinct spectral and temporal tuning properties of MGB and AAF cells.** (**a**) Comparison of onset (left) and offset (right) peak latency between MGB and AAF neurons. Data represent mean ± SEM. (**b**) Comparison of onset and offset peak latency within MGB (left) and AAF (right) neurons. Data represent mean ± SEM. (**c**) Example of tuning receptive fields (TRF) of onset and offset responses of an MGB and AAF neuron. (**d**) Comparison of tuning bandwidth at 60 dB SPL of onset and offset responses in MGB and AAF neurons. (**e**) Example fit of exponential decay model to PSTH of MGB and AAF neurons' onset and offset responses (n2: the amount of variance explained). (**f**) Comparison of half decay time (t1/2) of onset and offset responses in MGB and AAF neurons. Data represent mean ± SEM.

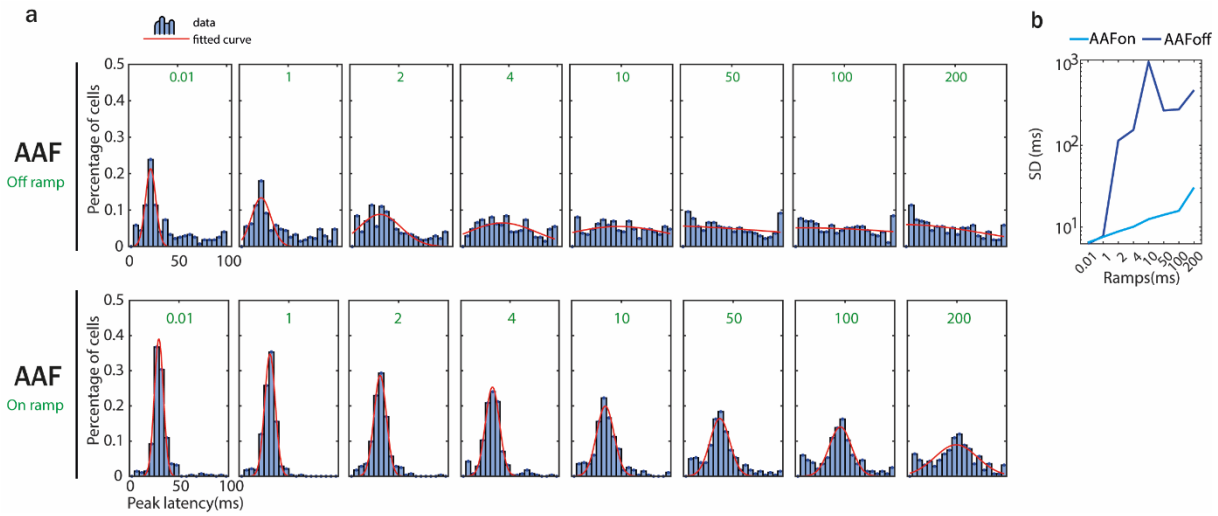


**Supplementary Figure 3.10 Jitter of onset and offset response latencies in AAF neurons** (**a**) Distribution of offset (top) and onset (bottom) response's peak latency in and AAF neurons evoked by sounds with varied ramps. The redline is a Gaussian fit. (**b**) Comparison of distribution width (STD) of Gaussian fits for peak latencies of offset and onset responses in AAF neurons.

# Chapter 4

# Distinct integration of spectrally complex sounds in primary auditory cortices in mice

## 4.1. Abstract

The standard hierarchical signal transmission along the lemniscal auditory pathway changes in the cortex, where two tonotopically organized auditory regions receive thalamic inputs in parallel: the primary auditory cortex (A1) and the anterior auditory field (AAF). These fields show distinct properties of auditory evoked responses, where A1 responds robustly to sound onset and AAF exhibits faster, more transient responses following both sound onset and offset. Many reports showed a strong involvement of AAF in temporal processing, revealing its particular role in encoding sound timing. More regular tonotopy, narrower tuning receptive fields, and more robust direction selectivity led to the speculation that A1 codes better information on the frequency spectrum of a sound than AAF. However, potential mechanisms explaining why A1 favors spectral processing have not been previously described. Using *in vivo* electrophysiological recordings in the mouse auditory cortex, we found that A1 neurons, unlike AAF neurons, respond stronger and faster to spectrally complex tones than pure tones. Next, we show that both regular and putative fast-spiking neurons in A1, but not in AAF, respond more robustly to spectrally complex tones than to pure tones. Finally, we use laminar analysis to demonstrate that A1 neurons in layer 2/3 respond stronger to harmonic sounds than neurons in layer 4, indicating an important transformation of harmonic sound processing between thalamo-recipient and supragranular layers in A1 but not in AAF. Our study reveals circuit features contributing to distinct processing of spectrally simple and complex sounds in the two primary auditory cortices and supports dual-stream processing in the core auditory cortex.

## 4.2. Graphical abstract

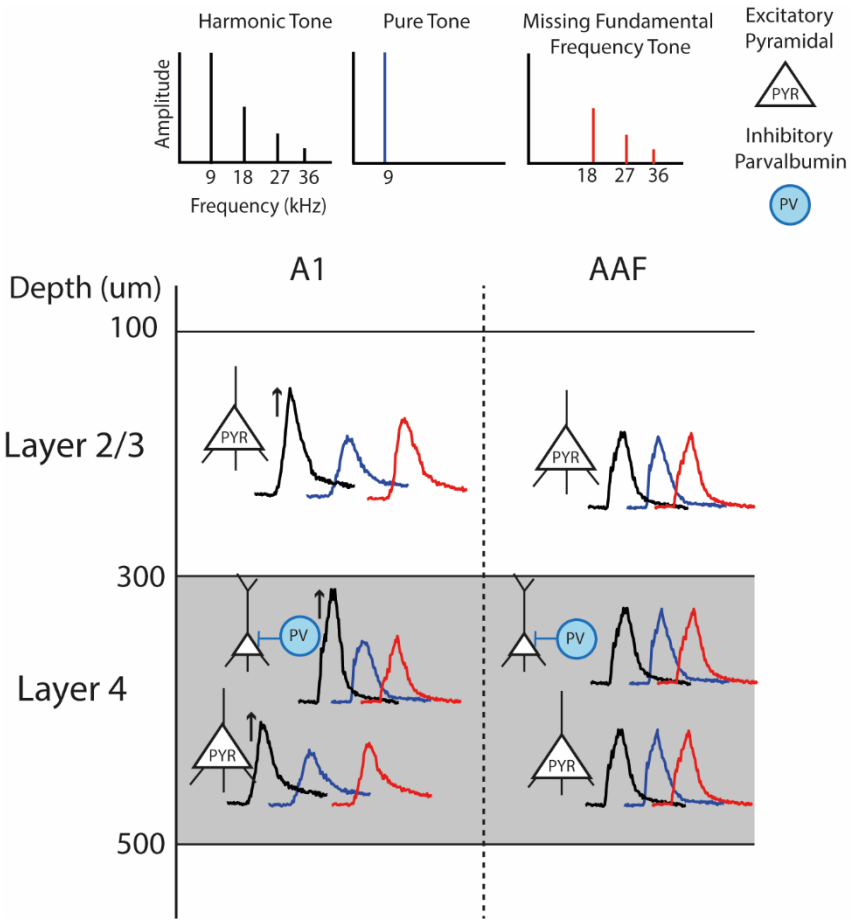


**Highlights:**

- A1 neurons respond stronger and faster to spectrally complex tones than to pure tones.
- Regular and fast-spiking neurons are highly activated by harmonic tones in the A1 but not in the AAF.
- Layer 2/3 neurons in A1, but not in AAF, can further process harmonic sounds.
- This data unfold which circuit features contribute to distinct processing of spectrally simple and complex sounds within two primary auditory cortices and underpin dual-stream processing in the primary auditory cortex.

## 4.3. Introduction

Comparative views of the brain lead to the observation of several canonical properties across sensory cortices. Models of auditory processing at the cortical level can be directly compared to other sensory cortices, such as the visual cortex, as both regions share response properties like direction selectivity, bandwidth selectivity, receptive fields, or on-off subregions (Rauschecker, 2015). However, in contrast to the visual system, the auditory system has two primary cortical regions, raising an interesting question about the relevance of this division. The primary auditory cortex (A1) and the anterior auditory field (AAF) have early been distinguished as two separate primary auditory fields in mice (Stiebler et al., 1997). They both receive direct input from the medial geniculate body (MGB): A1 receives 80% of projections from the tonotopically organized ventral division of MGB and AAF 40 and 35% from ventral division and rostral pole, respectively (Lee et al., 2004; Morel and Imig, 1987). The parallel projections from the thalamus to both A1 and AAF were confirmed in later studies (Kishan et al., 2008; Lee and Winer, 2008a, 2011; Takemoto et al., 2014), strengthening the statement that both fields are primary cortical regions and that they should be considered as two independent processing centers.

Another reason to treat A1 and AAF as separate regions is that their cells show distinct temporal patterns of auditory evoked responses. A1 neurons respond robustly to sound onset, whereas AAF neurons exhibit faster, more transient responses following both sound onset and offset (Solyga and Barkat, 2019). Additionally, AAF neurons show faster temporal modulation than A1 neurons (Schreiner and Urbas, 1988), significantly shorter spectro-temporal receptive field durations and latencies (Linden et al., 2003), better timing precision (Christianson et al., 2011) and fast-pass selectivity for the rate of frequency-modulated sweeps (Trujillo et al., 2011). It was also previously shown that AAF is highly specialized for processing information on sound termination and that minimizing its offset responses decreases the mouse performance to detect when a sound ends (Solyga and Barkat, 2021). All these reports confirm a strong involvement of AAF in temporal processing, revealing its unique role in encoding stimulus timing.

Neurons in both A1 and AAF display frequency tuning and a tonotopic organization (Guo et al., 2012; Kelly et al., 1986; Kowalski et al., 1995; Phillips et al., 1988) but differ in the tonotopy gradient direction and proportion of cortical area tuned to specific frequencies (Bizley et al., 2005; Carrasco and Lomber, 2009a; Imaizumi et al., 2004). Neurons in A1 tuned to different frequencies are evenly distributed, while tonotopy in AAF is more irregular with an underrepresentation of cells tuned to mid-range frequencies (Carrasco and Lomber, 2009b). Also, upward and downward frequency-modulated sweeps lead to distinct responses within A1 and indistinguishable responses within AAF, suggesting that A1 neurons have more robust direction selectivity (Bhumika et al., 2020). Together, the more regular tonotopy, narrower tuning receptive fields, and more robust direction selectivity suggest that A1 may code better than AAF the information about the frequency spectrum of a sound. However, putative mechanisms explaining how A1 favors spectral processing over AAF have not previously been described.

Here we show that the spectral complexity of a sound significantly influences responses in A1 but not in AAF. By studying neural responses evoked by spectrally simple and complex sounds in A1 and AAF, we found that A1 activity is significantly higher and faster for spectrally complex tones than pure tons. We show that both regular and putative fast-spiking neurons are highly activated by harmonic tones in A1 but not in AAF. We also report that layer 2/3 neurons in A1, but not in AAF, respond stronger to harmonic tones than cells in the input layer 4, indicating the processing of harmonic tones between the thalamo-recipient and superficial layers. Our data reveal vastly different processing of spectrally complex sounds within two primary auditory cortices and emphasize the complexity of the sound processing at the cortical level.

## 4.4. Results

### 4.4.1. Increasing a sound's spectral complexity significantly amplifies neuronal responses in A1 but not in AAF

We first asked how the frequency content of a sound is encoded in A1 and AAF. To do so, A1 and AAF were identified based on their functional tonotopy. Pure tones (PT) varying in frequency from 4 to 48.5 kHz and in level from 0 to 80 dB SPL were used to determine tuning receptive fields (TRFs). Using a 4 shank electrode (200 µm distance between shanks in a 4x8 electrode configuration), we identified A1 and AAF based on their caudo-rostral and diagonal ventro-dorsal increase in best frequency (BF, defined as the frequency that elicited maximal response across all sound levels; see methods), respectively (Figure 18a, b). We then assessed how A1 and AAF code information on the frequency content of a sound. We investigated neuronal processing in response to PT and harmonic tones (HT) and missing fundamental frequency tones (MFFT). The HT was composed of 4 frequency components (f0, f1, f2, f3), where each component was an integer multiple of a fundamental frequency (f0). We also tested responses to MFFT, which consisted only of the three harmonically related higher frequency components (f1, f2, f3). Using *in vivo* electrophysiological recordings, we compared neuronal responses in both regions evoked by HT (9+18+27+36 kHz), PT (9 kHz), and MFFT (18+27+36 kHz) (Figure 18c). For this experiment, the frequencies of tones were fixed and not adjusted to the recorded neuron's BF. Sounds were played at 60±5 dB SPL with varied duration (0.1 s and 0.5 s) and inter-stimulus intervals (ISIs, 0.5-2 s). The population response evoked by sounds with different spectral complexity showed that A1 responses were very distinct, while AAF responses were highly similar for all tested sounds (Figure 18d, e). Comparing peak amplitudes normalized to the responses to HT revealed significant differences between responses evoked by HT in comparison to PT or MFFT in A1. In contrast, no difference was observed in AAF (Figure 18f left). The normalized spike rates, calculated in a window of 5-55 ms following the sound onset, were also distinct in A1 but not in AAF (Figure 18f right). These analyses show that both peak amplitude and spike rate allow the distinction of the three sounds played based on A1 activity. In contrast, these parameters do not allow distinguishing which sound was played in AAF. If the auditory cortex uses neural information encoded in the firing rate on

the population level to assign a category to a sound, A1 activity would be much more informative about the frequency content of a sound than the activity of AAF.

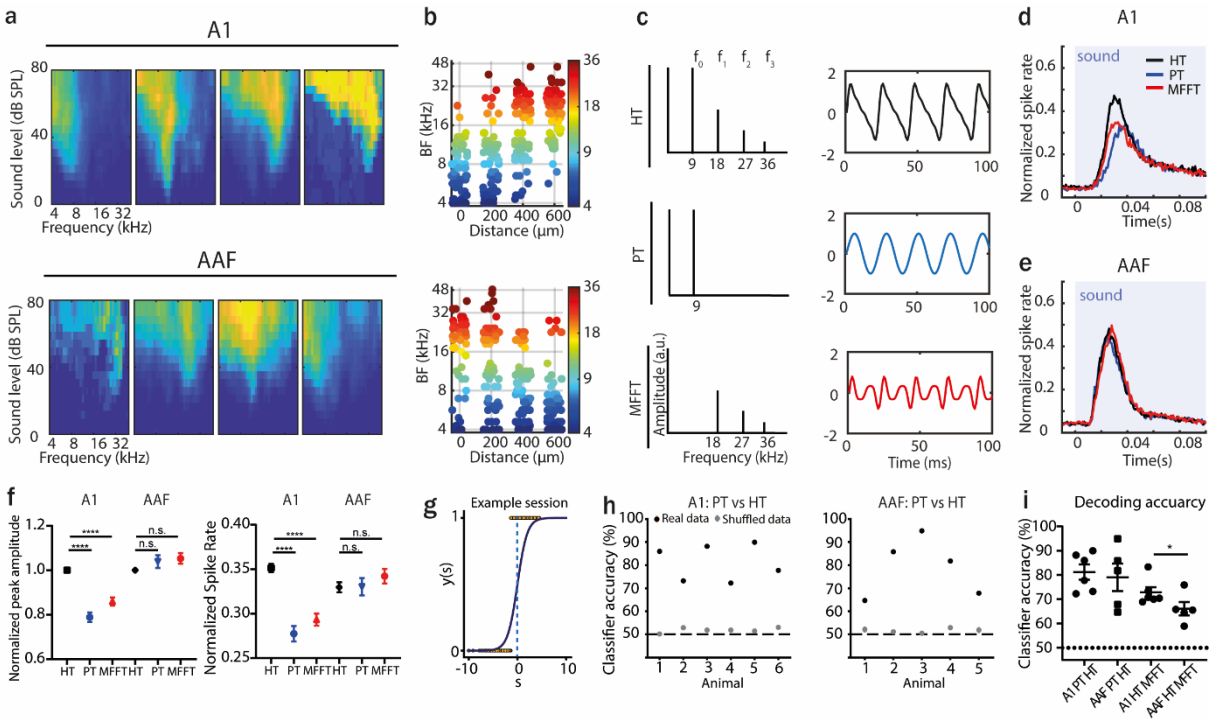


**Figure 18 Increasing a sound's spectral complexity significantly amplifies neuronal responses in A1 but not in AAF.** (**a**) Average TRFs of cells recorded in A1 or AAF tuned to low, middle, high, and very high frequencies. (**b**) BF of A1 neurons (n=304 cells, 6 animals) and AAF neurons (n=271 cells, 5 animals) displayed as a relative distance between electrode shafts. Responses are color-coded to BF. (**c**) Frequency spectra and waveforms of tones used in this experiment. (**d**) Average PSTH of A1 response to HT, PT, or MFFT, normalized to the maximum response evoked by HT. (**e**) Average PSTH of AAF response to HT, PT, or MFFT, normalized to the maximum response evoked by HT. (**f**) Comparison of peak amplitude and normalized spike rate (analysis window: 5-55 ms) of A1 and AAF responses evoked by HT, PT, and MFFT. Peak amplitude: A1: HT vs PT: $p<0.0001$, HT vs MFFT: $p<0.0001$; AAF: HT vs PT: $p=0.9323$, HT vs MFFT: $p=0.2860$, Wilcoxon test. Spike rate: A1: HT vs PT: $p<0.0001$, HT vs MFFT: $p<0.0001$; AAF: HT vs PT: $p=0.1059$, HT vs MFFT: $p=0.2559$, Wilcoxon test. (**g**) Example classification of responses to HT and PT based on spike rate with the use of logistic regression. s – weighted spike rates, y(s) – the probability of HT, dotted line – threshold. (**h**) Classification accuracy based on A1 (left) or AAF (right) responses for real and shuffled data. (**i**) Comparison of classifier accuracy of decoders trained and tested on A1 or AAF responses to sounds with different spectral complexity, *, $p=0.0476$, Kolmogorov-Smirnov test. Data show mean ± SEM.

We then asked if A1 and AAF activity could be predictive of the sound stimulus. We used a logistic regression model to predict which stimulus was presented from the single-trial population activity (cross-validated, L2 penalty, see methods). We examined the classifier accuracy for the model trained and tested on HT vs. PT responses and HT vs. MFFT responses for both A1 and AAF cells (Figure 18g). We compared the classifier accuracy and found that both A1 and AAF responses allowed for good stimulus decoding (significant above the chance level, Figure 18h). However, A1 responses were more informative than AAF responses if HT or MFFT sounds were played (Figure 18i). These results suggest that A1 encodes significantly better than AAF, the absence of fundamental frequency component within a tone.

If A1 and AAF analyze spectral complexity of the sound by combining information from multiple neurons into a population code then A1 activity is significantly more informative on which stimulus was presented (Figure 18f). If information of spike rate activity of each single neuron is used then responses within both regions can be informative about spectral complexity of the sound (Figure 18i).

### 4.4.2. A1 cells respond faster to spectrally complex sounds than to pure tones

Recent physiological experiments suggested that apart from spiking rate, many parts of the nervous system operate on the timing of individual action potentials (Ponulak and Kasinski, 2011). In auditory research, the first spike latency has been suggested to be a source of information required for fast sound discrimination (Zohar et al., 2011). We asked if response latencies evoked by sounds with different spectral complexity vary in either A1 or AAF network and could convey information about the identity of the presented stimulus. Comparing response onset latencies at the population level revealed significant differences between responses evoked by HT and PT in A1, whereas no difference was observed in AAF (Figure 19a-c). HT and MFFT, which differ only by one frequency component, did not lead to distinct response latencies in any field (Figure 19c).

At the core cortical regions level, response onset latencies of individual neurons result mainly from the integration of thalamocortical inputs. Whether a frequency component can be integrated within a neuron is to some extent reflected by its TRF. Suppose many frequency components of the sound fall within the neuron's TRF. In that case, the integration of thalamocortical inputs can contribute to the faster crossing of the firing threshold, resulting in shorter onset response latencies. To understand the relation between the tuning of A1 and AAF cells and their response latencies evoked by sounds with different complexity, we analyzed onset latencies of responses evoked by HT, PT, and MFFT in neurons tuned to low (BF<8 kHz), middle (8 kHz<BF<16 kHz) and high (BF>16 kHz) frequencies (Figure 19d). Neurons with low BF responded equally fast to HT, PT, and MFF in A1 and AAF (Figure 19e, f). This was surprising as we expected PT to evoke the fastest responses in the group of cells which tuning fields include 9 kHz. Similarly, latencies of both A1 and AAF cells tuned to middle frequencies were also not affected by additional frequency components. Interestingly, A1 cells tuned to high frequencies responded significantly faster to HT than the PT, unlike AAF neurons. Onset latencies evoked by HT and MFFT were not different, neither in A1 nor in AAF. Our data reveal that the response threshold of A1 cells is crossed faster when spectrally complex sounds are presented compared to a simple one. If the auditory cortex uses temporal coding to discriminate different sound categories, distinct latencies of responses in A1 would be more informative at whether simple or spectrally complex stimuli were presented.

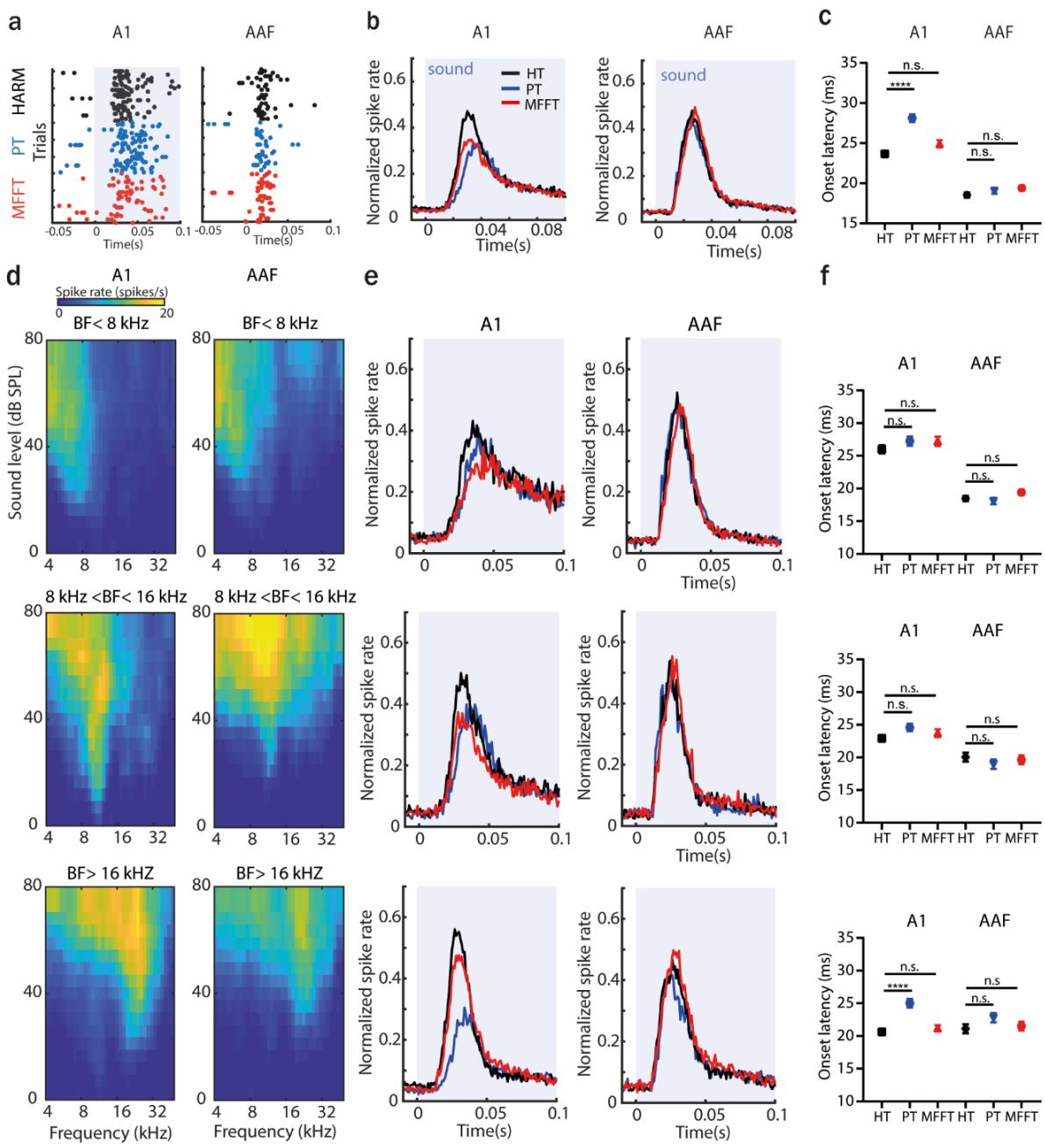


**Figure 19 A1 cells respond faster to spectrally complex sounds (a)** Raster plots of example A1 and AAF cell in response to HT, PT and MFFT (30 trials). (**b**) Average PSTH of A1 and AAF response to HT, PT, or MFFT, normalized to maximum response evoked by HT. (**c**) Comparison of onset latencies of A1 and AAF neurons in response to HT, PT or MFFT. A1: HT vs PT: $p<0.0001$, HT vs MFFT: $p=0.2324$, $n_{HT}=290$ cells, $n_{PT}=269$ cells, $n_{MFFT}=276$ cells, AAF: HT vs PT: $p=0.5917$, HT vs MFFT: $p=0.1964$ $n_{HT}=263$ cells, $n_{PT}=265$ cells, $n_{MFFT}=268$ cells, Kolmogorov-Smirnov test. (**d**) Average TRF of neurons tuned to low (BF<8), middle (8<=BF<16) or high (BF>=16) frequencies recorded in A1 and AAF. (**e**) Average PSTH of A1 and AAF neurons tuned to low, middle or high frequencies in response to HT, PT or MFFT, normalized to maximum response evoked by HT, 1ms bin. (**f**) Comparison of onset latencies of A1 and AAF neurons tuned to low, middle or high frequencies in response to HT, PT or MFFT. Low BF: A1: HT vs PT: $p=0.2545$, HT vs MFFT: $p=0.3762$, $n_{HT}=77$ cells, $n_{PT}=61$ cells, $n_{MFFT}=62$ cells, AAF: HT vs PT: $p=0.5920$, HT vs MFFT: $p=0.2288$ $n_{HT}=112$ cells, $n_{PT}=113$ cells, $n_{MFFT}=114$ cells. Middle BF: A1: HT vs PT: $p=0.0533$, HT vs MFFT: $p=0.5410$, $n_{HT}=82$ cells, $n_{PT}=67$ cells, $n_{MFFT}=79$ cells; AAF: HT vs PT: $p>0.9999$, HT vs MFFT: $p=0.8186$, $n_{HT}=45$ cells, $n_{PT}=45$ cells, $n_{MFFT}=45$ cells. High BF: A1: HT vs PT: $p<0.0001$, HT vs MFFT: $p=0.3788$, $n_{HT}=102$ cells, $n_{PT}=81$ cells, $n_{MFFT}=102$ cells. AAF: HT vs PT: $p=0.3315$, HT vs MFFT: $p=0.8063$, $n_{HT}=84$ cells, $n_{PT}=85$ cells, $n_{MFFT}=86$ cells, Kolmogorov-Smirnov test. Data show mean ± SEM.

### 4.4.3. Both regular and putative fast-spiking neurons are significantly more activated by harmonic than pure tones in A1 but not in AAF

We next asked what neuronal circuit features could explain such distinct processing of simple and complex sounds within A1 and AAF. It has previously been shown that A1 has fewer parvalbumin-positive (PV+) fast-spiking (FS) cells than AAF (Reinhard et al., 2019). Could a lower level of inhibition contribute to distinct A1 responses to spectrally complex sound? To answer this question, we distinguished putative FS and regular spiking (RS) neurons based on the peak-to-trough times (p2t) of their spike waveforms (Figure 20a). Fast spiking units were defined as having a p2t smaller than the minimum between the two peaks of the p2t distribution (0.6 ms), in accordance with previous studies (Moore and Wehr, 2013) and based on the bimodal distribution of p2t parameter of A1 and AAF cells (Figure 20b).

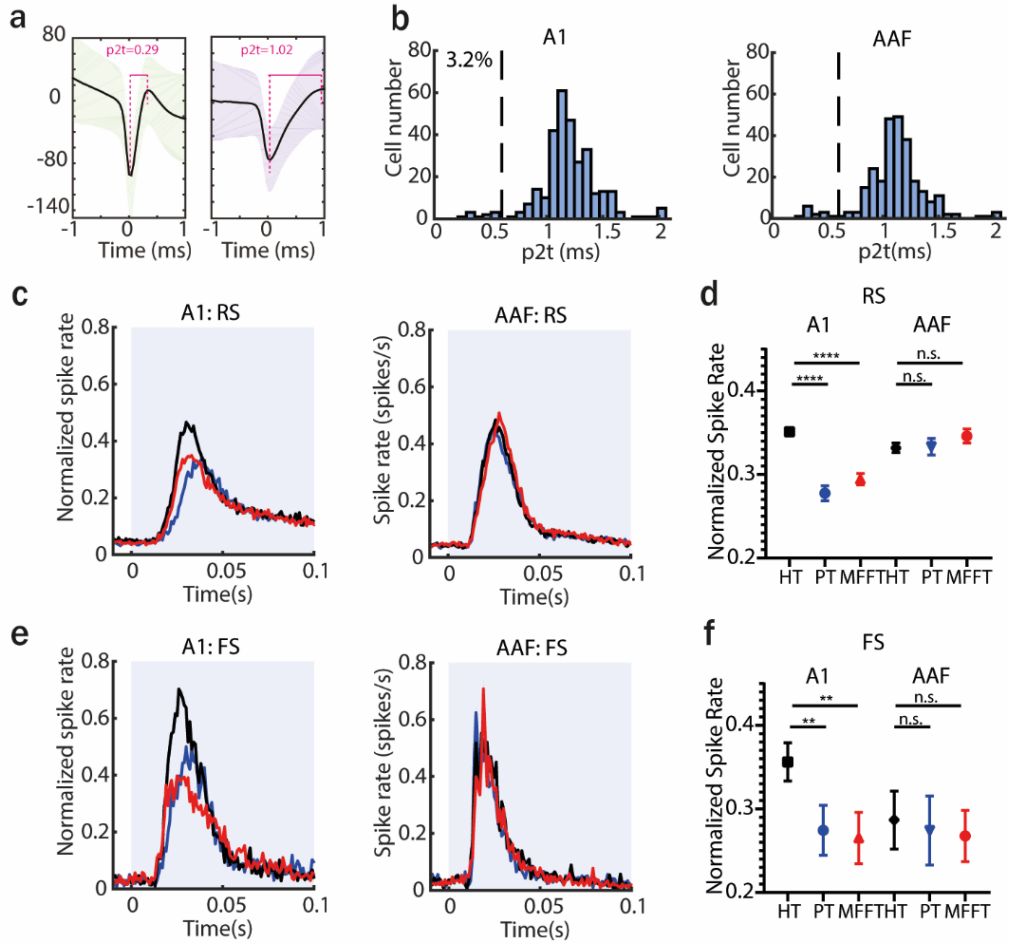


**Figure 20 Both regular and putative fast-spiking neurons are significantly more activated by harmonic than pure tones in A1 but not in AAF.** (**a**) Example of fast and regular spiking unit waveforms. (**b**) Distribution of peak-to-trough times of A1 and AAF neurons. The dashed line defines the middle of the bimodal distribution (p2t=0.6). (**c**) Average PSTH of A1 or AAF regular spiking neurons response to HT, PT or MFFT, normalized to the maximum response evoked by HT. (**d**) Comparison of spike rates of A1 and AAF regular spiking neurons evoked by HT, PT and MFFT (A1: HT vs. PT: $p<0.0001$, HT vs. MFFT: $p<0.0001$, n=294 cells, AAF: HT vs. PT: $p=0.1319$, HT vs. MFFT: $p=0.1633$, n=258 cells, Wilcoxon test). (**e**) Average PSTH of A1 or AAF fast-spiking neuron responses to HT, PT or MFFT, normalized to the maximum response evoked by HT. (**f**) Comparison of spike rates of A1 and AAF fast-spiking neurons evoked by HT, PT, and MFFT (A1: HT vs. PT: $p=0.0098$, HT vs. MFFT: $p=0.0039$, n=10 cells, AAF: HT vs. PT: $p=0.5417$, HT vs. MFFT: $p=0.0803$, n=13 cells, Wilcoxon test). Data show mean ± SEM.

RS neurons showed a distinct spike rate in A1 evoked by HT, PT, and MFFT, whereas in AAF, responses evoked by these three tones were indistinguishable (Figure 20c, d). Similarly, FS neurons responded significantly stronger to HT than PT or MFFT in A1 but not in AAF (Figure 20e, f). We confirmed that this was not due to different distributions of BFs of A1 and AAF RS and FS cells (Supplementary Figure 4.1a). These results reveal that both RS and FS neurons within A1 and AAF have distinct involvement in processing simple and complex sounds. Still, this distinct processing cannot be attributed to one cell type in particular.

### 4.4.4. Additional computation of harmonic sound response is observed in supragranular layers of A1 but not AAF

The differences observed in spectrally complex sound processing between A1 and AAF cannot be explained by the different involvement of RS and FS neurons. We thus asked if other neuronal circuit features could play a role. As our recordings span the range of 150 to 600 µm from the pia surface, corresponding mainly to layer 2/3 (L2/3, 150-300 µm) and layer 4 (L4, 300-500 µm), we explored the dependence of responses to sounds with different spectral complexity in those layers (Figure 21a, b). We evaluated evoked spike rates (baseline removed) to HT in A1 and found a significant signal amplification in L2/3 compared to the input L4 (Figure 21c, d). This amplification was not present between L4 and L2/3 responses in AAF, where the strength of the response did not differ between both layers. We confirmed that this was not due to different distributions of BFs of A1 and AAF L4 and L2/3 cells (Supplementary Figure 4.1b). This result suggests that A1 neurons compute further and integrate information on frequency components of spectrally complex sounds. In contrast, AAF seems to convey information received from the thalamus without any additional processing.

What could be the neural circuit feature allowing layer 2/3 in A1 to compute further and integrate information on frequency components of spectrally complex sounds? It could be a result of different bandwidths of the tuning of cells in L2/3 and L4. Our data did not reveal any significant difference in the width of tuning between A1 L2/3 and L4 cells (Supplementary Figure 4.2c). This suggests that the integration capacity of A1 cells is not fully reflected in the width of their tuning and that it is probably a consequence of other network features.

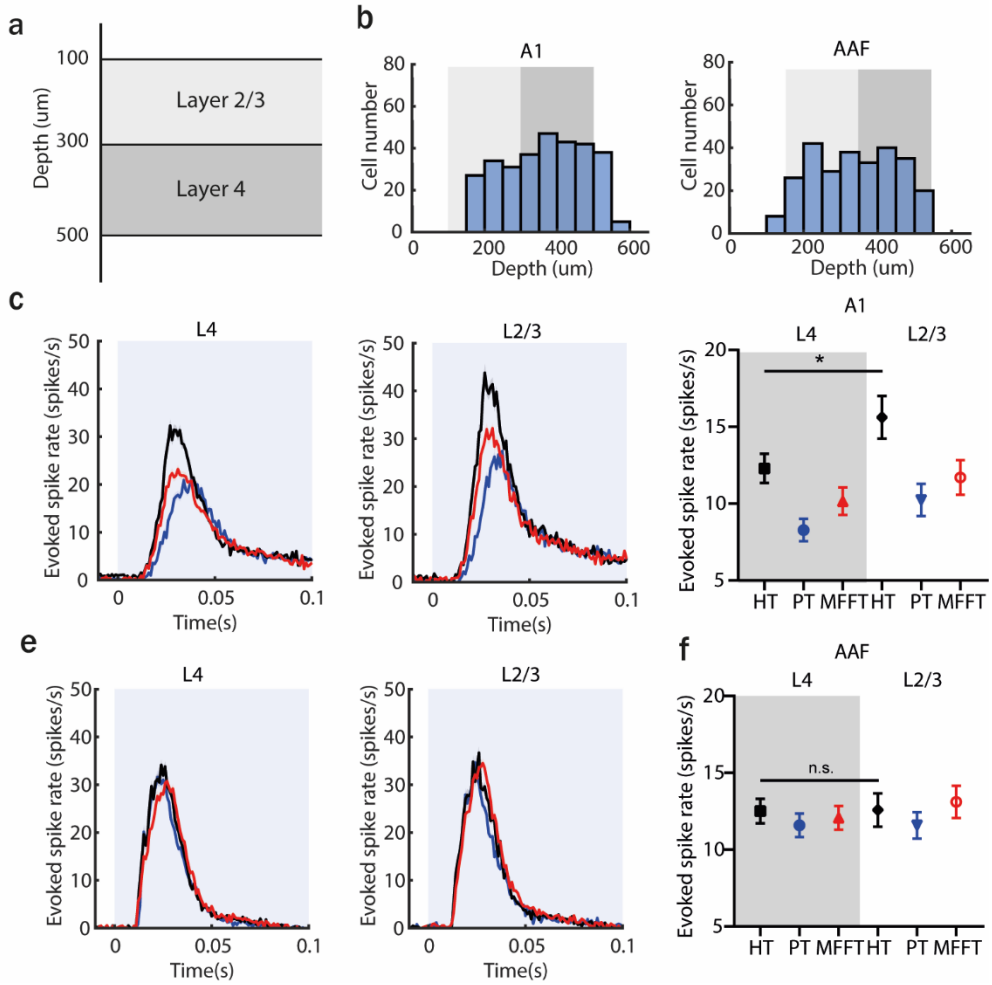


**Figure 21 Additional computation of harmonic sound response is observed in supragranular layers of A1 but not AAF** (**a**) Schematic showing depth of layer 2/3 and layer 4 within auditory cortex. (**b**) Distribution of A1 and AAF cells recorded within different cortical depths. (**c**) Average PSTH of A1 layer 4 or layer 2/3 neuron responses evoked by HT, PT, or MFFT. (**d**) Comparison of evoked spike rates in different cortical layers in A1 by HT, PT, and MFFT. A1: HT: L2/3 vs. L4: p=0.0241, $n_{L4}$=172 cells, $n_{L2/3}$=92 cells, Mann-Whitney test. (**e**) Average PSTH of A1 layer 4 or layer 2/3 neurons responses evoked by HT, PT, or MFFT. (**f**) Comparison of evoked spike rates in different cortical layers in AAF by HT, PT, and MFFT. AAF: HT: L2/3 vs L4: p=0.7803, $n_{L4}$=158 cells, $n_{L2/3}$=105 cells, Mann-Whitney test. Data show mean ± SEM.

## 4.5. Discussion

Understanding the specific roles of different brain regions - what a structure is "for" - is a fundamental question in neuroscience. Here we present new evidence that A1 has its unique role in sound processing which distinguishes it from AAF. By studying neural responses in A1 and AAF evoked by spectrally simple and complex sounds, we found that neurons process sounds of different spectral complexity in a distinct way in A1 but less so in AAF. We reveal two mechanisms that could contribute to this distinct processing in the two primary auditory cortices: (1) distinct involvement of regular and fast-spiking interneurons within both fields and (2) different integration of the information on the frequency components in the computational layer 2/3.

Many reports have previously shown that A1 cells are more narrowly tuned than AAF cells in different species (Guo et al., 2012; Imaizumi et al., 2004; Kowalski et al., 1995; Rutkowski et al., 2003). Thus, one could expect that additional frequency components would not highly influence responses in A1 due to higher frequency selectivity. In AAF, where cells are more broadly tuned, we would expect the additional frequency components to increase the neuronal response. Our results reveal the opposite pattern, where A1 responses are significantly more influenced by the presence of additional frequency components than AAF, allowing for better decoding of the presented stimuli (Figure 18, Figure 19). By contrast to the previous reports (Guo et al., 2012), but consistent with Linden et al. (Linden et al., 2003), we find that neurons in mouse A1 and AAF share a similar range of TRF bandwidths (Supplementary Figure 4.2a). As the measured bandwidth is dependent on the type and range of stimulus used to evoke the neuronal response, it is expected to have subtly different spectral characteristics across studies. Yet, despite a similar bandwidth, spike rates and latencies of A1 neurons reveal much better the spectral complexity of tones than AAF neurons, pointing to the more informative encoding of the spectral complexity of the sound within this field.

The excitatory neurons selectivity is shaped by interactions with inhibitory populations and is determined by inhibitory-excitatory connectivity patterns (Isaacson and Scanziani, 2011; Natan et al., 2017). It has previously been shown that there are more PV+ cells and perineuronal nets (PNNs) surrounding cell bodies in AAF than in A1 (Reinhard et al., 2019) and that the spectrotemporal selectivity in A1 is shaped differently by putative excitatory than by inhibitory interneurons (Atencio and Schreiner, 2008). Thus, the robustness of PNNs may be contributing to differences in firing properties of PV+ cells to simple and spectrally complex sounds in A1 and AAF. PV+ cells could also be differentially embedded within the cortical network of A1 and AAF, allowing for complementary sound processing within those two fields. Comparing tuning widths revealed that FS neurons have wider bandwidths than RS neurons in A1 but not in AAF (A1: $p=0.0227$; AAF: $p=0.1307$; Mann-Whitney test; Supplementary Figure 4.2b). Whether this broader tuning arises due to inputs coming from differentially tuned MGB cells projecting to PV+ cells in the cortex or whether it is a consequence of cortical information exchange in the A1 network remains to be elucidated. Other inhibitory populations could also influence differential processing of HTs within A1 and AAF circuits. It was previously shown that PV+ and SOM+ cells differentially shape frequency tuning following adaptation (Natan et al., 2017) and that SOM+ cells have a dominant role in the integration of information across multiple frequencies (Lakunina et al., 2020). Even if there are no significant differences in the number of somatostatin expressing cells (SOM+) between A1 and AAF (Reinhard et al., 2019), they could be differentially embedded within the network and thus responsible for distinct processing of HTs in A1 and AAF. If SOM+ cells contribute to distinct processing of complex tones within A1 and AAF remains to be elucidated.

It has recently been shown that in the human primary auditory cortex, deep and middle layers are equally well represented by simple frequency model, and superficial layers can be significantly better represented by frequency-specific spectrotemporal modulation model (Moerel et al., 2019). This suggested that a relevant transformation of natural sound processing takes place between thalamo-recipient and superficial layers. Our results demonstrate that A1 cells in layer 2/3 respond stronger to HTs than cells in the input layer 4. This amplification was not significant for PT or MFFT responses. It is possible that the A1 population further computes only more natural and behaviorally relevant sounds such as HTs. This processing step in A1 could be crucial for integrating spectral components belonging to the same auditory object and may be a first computational step towards complex sounds perception. As our data did not reveal any significant difference in the width of tuning between A1 and AAF L2/3 and L4 cells (Supplementary Figure 4.2c), this integration property in A1 cannot be fully explained by the wider bandwidth, and other network features probably contribute to this integration.

Another interesting finding pointing to the distinct network architecture of A1 and AAF are late responses to low-frequency components recorded within the population of A1, but not within AAF cells (Figure 19) (Guo et al., 2012; Linden et al., 2003; Solyga and Barkat, 2019). Our data reveal that the responsiveness threshold of A1 cells is crossed faster when spectrally complex sounds are presented, which results in smaller latencies and reflects better integration capacity in A1 cells. As first spike latency has been suggested to be a source of information required for fast sound discrimination (Zohar et al., 2011), A1 response latency seems to be more informative on the stimulus identity than response latencies in AAF (Figure 19). As these delayed responses in A1 to low-frequency sounds are more robust in input layer 4 than in superficial layer 2/3 (Supplementary Figure 4.3a), it seems that a relevant integration of the thalamic inputs driven by different frequency components occurs already at the level of thalamo-recipient cells in A1. However, latencies of responses in AAF cells evoked by sounds with different spectral complexity are invariable. This confirms reliable temporal processing in AAF, which is not affected by the frequency components present within the sound. What are the network mechanisms driving response delay in A1 and lack of any latency differences in AAF? Invariable and fast onset responses in AAF could be driven by a high number of PV+ cells and robust PNNs (Reinhard et al., 2019). Therefore, although completely speculative at this time, it is tempting to suggest that the lack of such a robust inhibitory network allows A1 to combine information over many frequency components, thus resulting in variable latencies following sound with distinct spectral complexity. An alternative mechanism accounting for these latency differences could also be the distinctive architecture of local connectivity within A1 and AAF or the different integration of thalamocortical inputs at the cell level.

The more predictable responses in A1 to sounds with different complexity suggests that A1 could enroll the function of spectral processing. This is in agreement with speculation from previous studies that A1 codes better information on the frequency content of a sound than AAF because of a more accurate tonotopic map (Carrasco and Lomber, 2009a; Imaizumi et al., 2004), narrower tuning of neurons

(Imaizumi et al., 2004), and stronger frequency-modulated sweep directionality (Bhumika et al., 2020). Consistently, our results on reliable temporal processing irrespective of the frequency content of a sound combined with previous results (Bhumika et al., 2020; Guo et al., 2012; Hackett et al., 2011; Linden et al., 2003; Polley et al., 2007; Solyga and Barkat, 2019) point to the higher involvement of AAF in temporal processing. These different but complementary functions of A1 and AAF emphasize the complexity of sound processing at the cortical level.

Do A1 and AAF have a distinct implementation into brain function beyond sound processing? It has previously been shown that noise exposure reduces the density of perineuronal nets in A1 but not in AAF and that A1 and AAF inhibitory cells are differently sensitive to developmental experience (Reinhard et al., 2019). Furthermore, in early-deafened cats, AAF neurons become responsive to somatosensory and visual stimuli (Meredith and Lomber, 2011), while A1 neurons do not (Kral et al., 2003), indicating a functional distinction between these core auditory cortical areas. It was also lately shown that A1 and AAF have different projection targets, where A1 projects more to visual fields and AAF to motor and somatosensory cortices (Nakata et al., 2020). These vastly different sensitivities to developmental experience, cross-modal plasticity, and projection targets ultimately provide further support to the notion that the existence of parallel streams of processing at the auditory cortex level is not only a consequence of the high complexity of sound processing but could also have an important implication beyond it.

## 4.6. Methods

**Surgical procedures.** All experimental procedures were carried out in accordance with Basel University animal care and use guidelines and were approved by the Veterinary Office of the Canton Basel-Stadt, Switzerland. They were performed on adult (7-9 weeks) male or female C57BL/6J mice (Janvier, France).

Mice were anesthetized with an intraperitoneal injection of ketamine/xylazine (80 mg/kg and 16mg/kg, respectively), and subcutaneous injection of bupivacain/lidocain (0.01mg/animal and 0.04mg/animal, respectively) was used for analgesia. Ketamine (45 mg/kg) was supplemented during surgery as needed. For surgery, mice were head-fixed, and their body temperature was kept at 37°C with a heating pad (FHC, ME, USA). Craniotomy (~2x2 mm2) was performed with a scalpel just above the auditory cortex and covered with silicone oil. For awake recordings, the surgery was performed under isoflurane (4% for induction, 1.5 to 2.5% for maintenance), and the brain was additionally covered with a silicone casting compound (Kwik cast, World Precision Instruments, Inc. FL, USA) during the 2h recovery period from the anesthesia.

**Recordings.** The electrophysiological recordings were performed in anesthetized mice (A1: n=6, AAF: n=5). Mice were head-fixed and placed on a heating pad (or in the cardboard tube for awake recordings) inside a sound box. The body temperature was kept at 37°C. Extracellular recordings were conducted in

A1 and AAF, which were identified based on the functional tonotopy (caudal-rostral increase in BF for A1, and ventro-dorsal increase in BF for AAF). Multi-channel extracellular electrodes with 32 channels (A4x8-5mm-50-200-177-A32, Neuronexus, MI, USA) were inserted orthogonal to the brain surface with a motorized stereotaxic micromanipulator (DMA-1511, Narishige, Japan) at a constant depth (tip of the electrode at 575 ± 25 µm from pia). Responses from extracellular recordings were digitized with a 32-channel recording system (RZ5 Bioamp processor, Tucker Davis Technologies, FL, USA) at 24414 Hz. The single unit cluster was identified from raw voltage traces using kilosort (Pachitariu et al., 2016) (CortexLab, UCL, London, England) followed by manual corrections based on the inter-spike-interval histogram and the consistency of the spike waveform (phy, CortexLab, UCL, London, England) and further analyzed in MATLAB (Mathworks, MA, USA). Neural activity was considered as auditory responsive when it exceeded twice the standard deviation of the spontaneous activity.

**Auditory stimulation.** Sounds were generated with a digital signal processor (RZ6, Tucker Davis Technologies, FL, USA) at a 200 kHz sampling rate and played through a calibrated MF1 speaker (Tucker Davis Technologies. FL, USA) positioned at 10 cm from the mouse's left ear. Stimuli were calibrated with a wide-band ultrasonic acoustic sensor (Model 378C01, PCB Piezotronics, NY, USA).

*Tuning receptive fields:* To determine BF and tuning receptive fields, we used PTs (50 ms duration, randomized ISI distributed equally between 500 and 1000 ms, 2 repetitions, 4 ms cosine on, and 0.01 ms cosine off-ramps) varying in frequency from 4 to 48.5 kHz in 0.1-octave increments and level from 0 to 80 dB SPL in 5 dB increments. Tuning receptive fields, BF, and spiking rates were calculated in fixed time windows: A1: 10-60 ms, AAF: 8-58 ms. TRFs were smoothed with a median filter (4x4 sampling window) and thresholded to 0.2 of peak amplitude. Onset BF was defined as the frequency that elicited maximal response across all sound levels.

*Frequency integration*: To study frequency integration properties of A1 and AAF neurons, we compared neuronal responses in both regions evoked by HT (9+18+27+36 kHz), PT (9 kHz), and MFFT (18+27+36 kHz, Figure 18c). Frequencies of tones were fixed for this experiment, independently of the neuron's BF. Independent sound complexity tones were played at 60±5 dB SPL with varied duration (0.1 s and 0.5 s) and intersounds intervals (0.5-2 s). Sound level ratio (in V) of harmonic components was as follow: HT: 1f0:1/2f1:1/4f2:1/8f3; PT 1f0; MFFT: 1/2f1:1/4f2:1/8f3; Figure 18c). Onset latency was determined as the first time point in which the smooth PSTH (kernel=hann(9)) collapsed across all tested stimuli exceeded with 2 standard deviations the spontaneous activity (binning size: 1ms). Peak latency was defined as the time at which the maximum number of driven spikes occurred within the PSTH in window 5-55 ms following stimulus onset. Peak amplitude was defined as the maximum number of driven spikes that occurred within the PSTH in window 5-55 ms following stimulus onset. Spike rates were calculated in a fixed time window of 5-55 ms following stimulus onset.

**Decoding population activity.** The logistic regression model was used to decode which stimulus was presented from neural responses within one trial (code from Neuromatch Academy W1D4,

www.neuromatchacademy.org). Spike rates evoked by HT, PT or MFFT, in a fixed window following sound onset (5-55 ms) were used to train and test the model. L2 regularization was used to avoid over-fitting. 8-fold cross-validation was performed by leaving out a random 12,5% subset of trials to test the classifier performance, and the remaining trials were used to train the classifier. A range of regularization values was tested (0.0001 to 10000 log spaced), and the one that gave the smallest error on the validation dataset was chosen as the optimal regularization parameter. Classifier accuracy was computed as the percentage of testing trials in which the presented sound was accurately predicted by the classifier and summarized as the average across the 10 repetitions of trial subsampling. The spiking activity of each neuron was z-scored before running the logistic regression model. Trial labels were shuffled to confirm that decoding is not working for random data. This procedure was repeated 10 times. Then the average across the 10 repetitions was used to assess classifier accuracy for randomized data.

**Statistical Analysis.** Statistical tests were performed with GraphPad Prism software version 7.03 (GraphPad Software, USA). The standard error of the mean was calculated to quantify the amount of variation between responses from different populations. A Nonparametric, unpaired Mann-Whitney test was used to calculate whether there were any significant differences between latencies of responses evoked by sounds with different spectral complexity and between responses recorded within layer4 and layer2/3. Wilcoxon paired test was used to compare differences between paired values obtained in different treatments which did not have Gaussian distribution.

**Data availability.** Data are available upon reasonable request.

## 4.7. Supplementary data

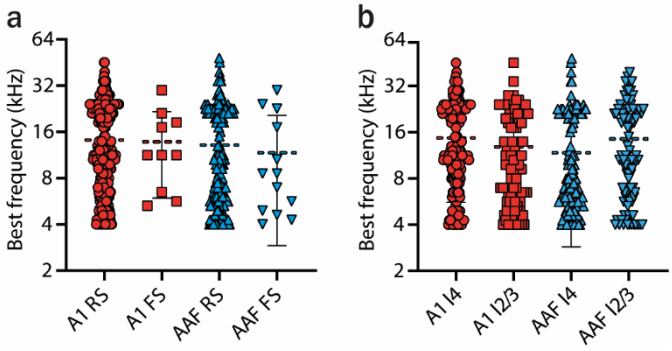


**Supplementary Figure 4.1** Distribution of best frequencies of (**a**) fast and regular spiking neurons recorded in A1 and AAF, (**b**) of neurons recorded within layer 2/3 and layer 4 in A1 and AAF.

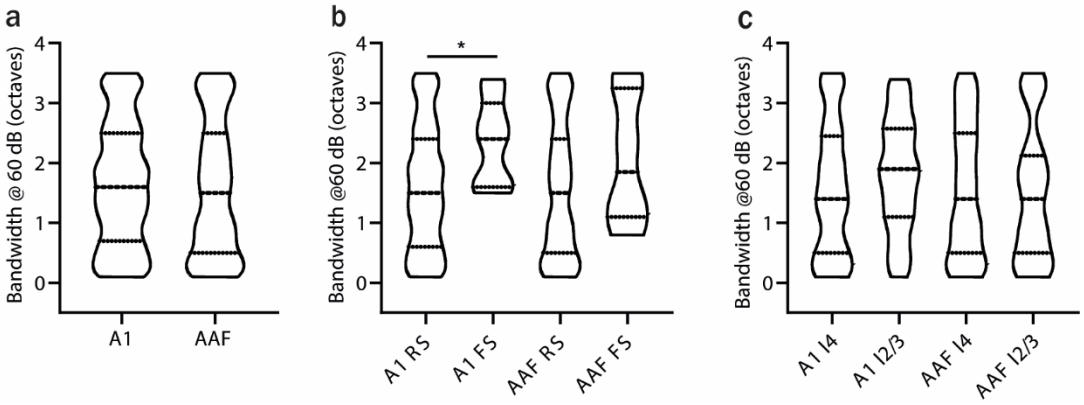


**Supplementary Figure 4.2** (**a**) Comparison of the tuning bandwidth of A1 and AAF cells at 60dB SPL. (**b**) Comparison of tuning bandwidth of fast-spiking and regular spiking neurons in A1 and AAF, A1: p=0.0227; AAF: p=0.1307, Mann-Whitney Test. (**c**) Comparison of tuning bandwidth of l2/3 and l4 neurons in A1 and AAF.

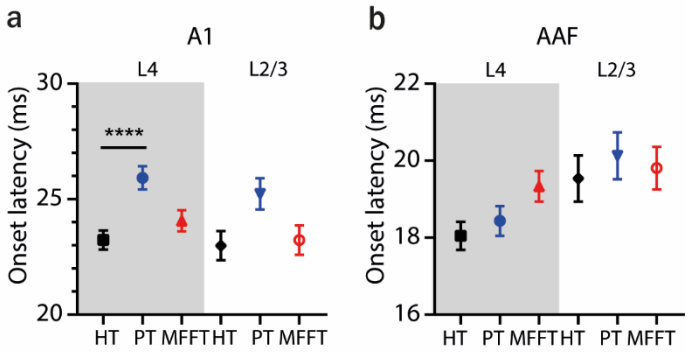


**Supplementary Figure 4.3** (**a**) Comparison of onset latencies of A1 and AAF L4 and L2/3 neurons in response to HT, PT or MFFT. A1 L4: HT vs PT: p<0.0001, HT vs MFFT: p=0.3430, $n_{HT}$=153 cells, $n_{PT}$=117 cells, $n_{MFFT}$=146 cells, A1 L2/3: HT vs PT: p=0.1367, HT vs MFFT: p=0.9891 $n_{HT}$=86 cells, $n_{PT}$=71 cells, $n_{MFFT}$=78 cells. AAF L4: HT vs PT: p=0.9587, HT vs MFFT: p=0.0803, $n_{HT}$=153 cells, $n_{PT}$=154 cells, $n_{MFFT}$=157 cells, AAF L2/3: HT vs PT: p=0.7519, HT vs MFFT: p=0.6716 $n_{HT}$=102 cells, $n_{PT}$=103 cells, $n_{MFFT}$=103 cells, Kolmogorov-Smirnov test.

# Chapter 5

# General discussion

Understanding the specific roles of different brain regions - what each structure is "for" - is a fundamental question in neuroscience. This question is especially relevant for the auditory cortex, consisting of two primary fields operating in parallel. Previous reports described that parameters of auditory evoked responses in A1 and AAF neurons do not fully overlap, providing support for the idea that these two fields have distinct roles in sounds processing (Bizley et al., 2005; Carrasco and Lomber, 2009a; Guo et al., 2012; Linden et al., 2003; Polley et al., 2007). On the other hand, neurons within both fields have frequency tuning fields with similar thresholds and bandwidths, overlapping range of latencies, comparable amplitudes, and similar temporal dynamics of sound-evoked responses. Thus, it was challenging to understand whether minor differences in response parameters reflect the distinct involvement of these fields in sound processing. The results of our study emphasize the specific processing in A1 and AAF by revealing the existence of response characteristics unique to each area. We found that a high percentage of neurons responding to sound termination are present in AAF but not in A1 (Chapter 2). In parallel, we show that A1 responses are highly influenced by the spectral content of the sound, whereas AAF responses remain mostly invariable (Chapter 4). These two fundamental findings reveal a unique encoding of sounds in A1 and AAF and provide direct evidence for their distinct involvement in sound processing.

## 5.1. Functional differences

While comparing A1 and AAF responses, we found that neurons in AAF have significantly stronger responses to tone termination than cells in A1 (Figure 5, Figure 6). It was recently stated that, within the auditory cortex, there is no anatomical clustering of cells showing offset responses and that they seem to be scattered over the whole auditory cortex (Kopp-Scheinpflug et al., 2018). Our study contradicts this and provides the first evidence for the existence of clustering of offset responsive cells within the auditory cortex and shows that the majority of this cluster belongs to AAF (Solyga and Barkat, 2019). Further, LFP and laminar analysis suggested that differences in offset responses between A1 and AAF are both of subcortical and intracortical origin (Figure 7). In agreement with previous studies, we also showed that AAF neurons display faster and more transient responses than A1 neurons (Figure 5). Additionally, we found that offset responses in AAF, unlike in A1, increase with sound duration (Figure

6). These results reveal the existence of a cortical cluster of offset responsive cells and emphasized the potentially critical role of AAF for temporal processing, consistently with previous reports (Bhumika et al., 2020; Guo et al., 2012; Hackett et al., 2011; Linden et al., 2003; Polley et al., 2007).

Our results demonstrate that A1 is highly enrolled in spectral processing. First, we found that A1 responses are significantly more influenced by the frequency spectrum of a sound than AAF (Figure 18, Figure 19). Second, we showed that both regular and fast-spiking neurons are highly activated by harmonic tones in A1 but not in AAF (Figure 20). Third, we revealed that A1 cells in layer 2/3 respond stronger to harmonic sounds than cells in the input layer 4, indicating an important transformation of harmonic sound processing between thalamo-recipient and superficial layer in A1 (Figure 21). This data suggests which circuit features contribute to distinct processing of spectrally simple and complex sounds within the two primary auditory cortices and support dual-stream processing in the primary auditory cortex. Our findings are in agreement with speculations from previous studies that A1 represents better the frequency of the sound than AAF as a consequence of a more accurate tonotopic map (Carrasco and Lomber, 2009a; Imaizumi et al., 2004), narrower tuning of neurons (Imaizumi et al., 2004), and stronger frequency-modulated sweep directionality (Bhumika et al., 2020).

Why does the primary auditory cortex need two separate processing centers? One can speculate that auditory stimuli, as compared to other sensory stimuli, have more complex and challenging temporal characteristics. Based on the connectivity patterns and a well-defined model of the sequential information flow in the visual system, it was suggested that primary sensory regions are involved in processing fundamental stimulus features, such as intensity, duration, or frequency. In contrast, the secondary auditory field (A2) or the dorsal posterior auditory field (DP), which receive inputs mainly from A1 and AAF, were thought to be responsible for the integration of more complex sounds, such as processing of harmonic or rhythmic patterns, melodies, or for the storage of complex sound patterns (Zatorre et al., 1994). Even if A1 and AAF work as two separate sound analysis centers, we expect information from these two regions to be combined in one of the higher-order auditory fields. Previous studies conducted on cats have shown that A1 and AAF are highly interconnected (Lee and Winer, 2008b). However, the lack of prominent offset responses in A1 (Figure 4, Figure 5) and the invariable responses to sounds with different spectral complexity in AAF (Figure 18, Figure 19) suggest that the integration of signals from the two primary fields happens mainly at a higher level. We believe that the distinct roles of A1 and AAF are likely to be used complementarily. If and how other sound features are differentially encoded in A1 and AAF, and where information from those two parallel processing centers diverges, remains to be elucidated.

Our studies highly contributed to the general knowledge on the behavioral importance of cortical offset responses and the mechanisms driving them (Chapter 3). First, we showed that experimentally minimizing auditory cortical offset responses decreases the mouse performance to detect sound termination (Figure 9, Figure 10). Second, we found that cortical offset responses are inherited from the

periphery, amplified, and generated *de novo* (Figure 13, Figure 14, Figure 15*)*. De novo generated offset responses suggest that some computations are performed in the AAF when the longer sound stimulus is presented. Until now, only context-dependent modulation was shown to change responses in A1 according to the recent stimulus history, which indeed leads to *de novo* generation of responses within local auditory circuits (Chen et al., 2015; Natan et al., 2015; Natan et al., 2017). Which cell types or network interactions contribute to *de novo* generated offset responses in AAF remains an important open question.

We barely experience complete silence in our everyday life and are constantly surrounded by many sounds. Our present results demonstrate that offset responses code more than silence, including relevant changes in sound trajectories (Figure 17). This reveals the importance of cortical offset responses in encoding sound termination and detecting changes within temporally discontinuous sounds. What could be the role of offset response in sound encoding, apart from tracking sound duration? Sound offset responses are likely necessary for perceptual grouping, gap detection, and consonant identification, thus crucial for speech and vocalization (Kopp-Scheinpflug et al., 2018). The relevance of cortical offset responses should be further studied with more behaviourally relevant paradigms to investigate if offsets are crucial for vocalization processing.

### 5.2. Dual-stream processing

The segregation of neural pathways for the processing of increasing and decreasing intensity of the stimuli is common between different sensory modalities (Gjorgjieva et al., 2014). The presence of separate populations of cells that are excited by either stimuli increments or decrements was described in vision (Wassle, 2004), chemosensation (Chalasani et al., 2007), audition (Scholl et al., 2010), and thermosensation (Gallio et al., 2011). However, most previous studies investigated how a complete splitting of onset and offset pathways implicates efficient encoding of the stimuli. It was shown that segregation of onset-offset pathways provides a better code for extracting information at low average metabolic costs under a broad set of conditions, with the most pronounced benefits appearing for sparse but ecologically important stimuli (Gjorgjieva et al., 2014; Westheimer, 2007). It is interesting to think how parallel processing in A1 and AAF fits within this framework, as we are trying to understand the possible benefits of separation of onset (A1) from onset-offset (AAF) auditory pathways. The on-off system provides a better code for extracting information about the stimulus or reducing the number of spikes required for the same information compared with two neurons of the same polarity (on-on), especially when the input is noisy (Gjorgjieva et al., 2014). One possibility could be that AAF, with its onset-offset responsive cells and precise temporal resolution, encodes that there is something important to attend to when A1, with its onset responsive cells population and better analytical abilities, is more involved in encoding exact spectral content or identity of the presented stimuli. The evidence supporting the existence of at least two processing streams, ‘where’ and ‘what’ in the non-primary auditory cortex, has been identified in cats (Lomber and Malhotra, 2008). A spatial position of the sound source

corresponding to the ‘where’ stream is determined based on the delay between sounds arriving at the two ears, represented by the time difference on the neural level (van der Heijden et al., 2019). One could think that AAF, with its high temporal precision and ability to detect stimulus beginning and termination, plays a role in the ‘where’ or ‘when’ stream, determining temporally and spatially that relevant sound stimuli appeared. On the other hand, slower and more sustained responses in A1 could be a part of the ‘what’ stream, determining what an object is and assigning a meaning to it. Our speculations are in contrast to previous studies in cats, where AAF was considered more as a modulatory center for handling the frequency content of sound (Lomber and Malhotra, 2008; Shi et al., 2019), and A1 was speculated to be a part of the “where” pathway for localization of targets (Nakata et al., 2020). Thus, stream processing in primary auditory cortices still requires more studies to fully define the functions of individual cortices and their involvement in sound processing.

The periods of high cortical plasticity are critical for developing higher-order executive functions of specialized cortical regions (Baum et al., 2020). Distinct sensitivity of brain regions during development to the influence of experience reflects distinct functional specialization of those networks. It was previously shown that noise exposure reduces the density of perineuronal nets in A1 but not in AAF and that A1 and AAF inhibitory cells are differently sensitive to developmental experience (Reinhard et al., 2019). In other words, A1 processing would be more influenced by specific exposure during development than AAF. If A1 works as a ‘what’ stream, where it is involved in analyzing the stimulus and assigning it a meaning, we would expect it to be more plastic and thus more susceptible to the influence of experience. If AAF works as a ‘where’, ‘when’ pathway, it should not be affected to such a high extend by developmental experience as other brain regions could rely on its ability to precisely encode timing and source of the sound.

### 5.3. A functional role beyond sound processing

Sensory cortices are not working in isolation, but they are organized into complex circuits allowing us to perform everyday tasks such as the detection, localization, and discrimination of external stimuli. What could be the implementation of A1 and AAF in brain function and the relevance of these divisions beyond sound processing? It was previously shown that A1 and AAF have different projection targets, where A1 projects more to visual fields and AAF to motor and somatosensory cortices (Nakata et al., 2020). What could be the functional consequence of these distinct projection targets? Suppose A1 serves more as a ‘what’ pathway. In that case, it is important that it exchanges information with the visual cortex to combine visual and auditory inputs to identify objects and understand their meaning correctly. In parallel, information from AAF, potentially serving as a ‘where’ or ‘when’ stream, could be useful for driving motor action to focus on the source of sound or quickly react to the relevant auditory inputs. It was previously shown that, in early-deafened cats, AAF is responsive to somatosensory and visual stimuli (Meredith and Lomber, 2011), whereas A1 does not (Kral et al., 2003). If AAF is part of the ‘where’ or ‘when’ stream, it cannot perform its primary function after early deafening. Thus, it is not

surprising that AAF is involved in adaptive or compensatory plasticity by replacing lost inputs with other sensory modalities. A1, as a part of the 'what' stream, possibly being involved in more complex sound features analysis, would not be affected to the same extent as possibly computations performed there are dependent on the thalamic inputs and integrate, e.g., visual or AAF inputs.

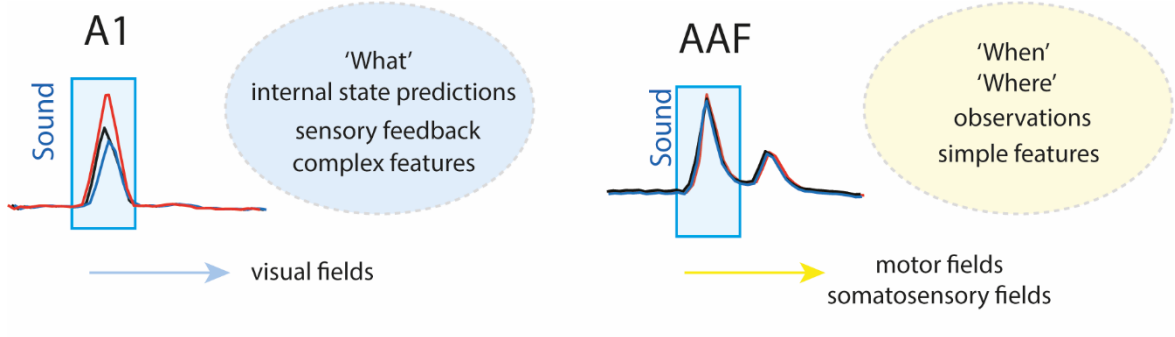


**Figure 22** Proposed structure of stream processing in primary auditory cortices.

### 5.4. Predictions and top-down modulation

For a long time, it was thought that activity in primary sensory cortices is mainly driven by sensory inputs following the feedforward processing hierarchy. However, evidence from awake experiments showed that non-sensory signals strongly influence activity in the primary sensory cortex. In 2012, Keller et al. combined neural recordings in the visual cortex with feedback manipulations during locomotion in a virtual reality environment. They showed that processing in the primary visual cortex might be based on predictive coding strategies (Keller et al., 2012). This would mean that the primary sensory cortices are not only operating based on sensory inputs but also that these inputs interact with an internal model created based on the predictions. Different sensory signals would then be used to detect mismatches between predicted and actual sensory information. An interesting question is whether similar predictive coding exists in the primary auditory cortices. To directly answer this question, it would be worth examining if one field plays a more important role in predictive processing than the other. The prediction field would have to store information on the world's internal representation, thus being highly involved in creating expectations. The other region would then possibly be involved more in simple stimulus feature analysis and thus should be less invariant to the context, to the animal's attention, or mismatches between expectation and experience. Therefore, although entirely speculative at this time, it is tempting to suggest that A1 would play the role of prediction center. The activity in this region should thus reflect a reweighting of sensory cues based on the predictions. With its robust temporal responses, AAF could be involved in simple sound parameters processing like sound onset, termination, duration, loudness, or location. A recent study showed a higher level of response modulation by task engagement in A1 than in AAF (De Franceschi and Barkat, 2020). Future experiments should address if cells within both regions are to the same extend sensitive to mismatches between expectation and experience.

Understanding processing in primary auditory cortices requires a deeper investigation of the nature of information exchanged between them and other sensory cortical regions. The implementation of parallel processing of A1 and AAF in functions beyond sound processing could be studied by comparing how other modalities, such as movement or vision, affect responses in both fields. Investigating to what extent both regions are modulated by attention, context, and involvement in a behaviourally relevant paradigm will help us understand if A1 plays a crucial role in complex sound features extraction and AAF in processing time and space, representing two classical facets of sensory perception. The next obvious step is to identify which network mechanisms drive this differential processing in A1 and AAF. Finally, understanding how other brain regions use these two streams of information and where they merge will be highly relevant. Thus, how A1 and AAF interact with each other and with other cortical and subcortical areas will be essential to understand how they mediate sensation, perception, and finally, orchestrate sound-driven behavior.

# Chapter 6

# Experimental prospects

This chapter combines a set of preliminary data paving the way for future experiments. It describes the potential of the voltage-sensitive dye imaging approach for studies of the function of adjacent cortical regions. Then it presents preliminary recordings from IC, suggesting that a significant encoding transformation of temporally dynamic sounds happens between different nuclei on the central auditory pathway. Finally, it shows that AAF cells respond to vocalization, making it an exciting stimulus for further studies of how temporally dynamic sounds in AAF are encoded.

## 6.1. Studying auditory cortex activity with voltage-sensitive dye imaging

Voltage-sensitive dye imaging (VSDI) offers the possibility to visualize, in real-time, the cortical activity of large neuronal populations with high temporal resolution. Imaging a few cortical areas simultaneously is very beneficial for comparing properties of responses within two or more fields. We performed a set of VSDI experiments to test if some of our electrophysiology results could also be obtained with this technique. After the opening of the skull above the auditory cortex, a cement wall was built, the dura mater was removed, and dye molecules were applied on the surface of the cortex (Figure 23a-d).

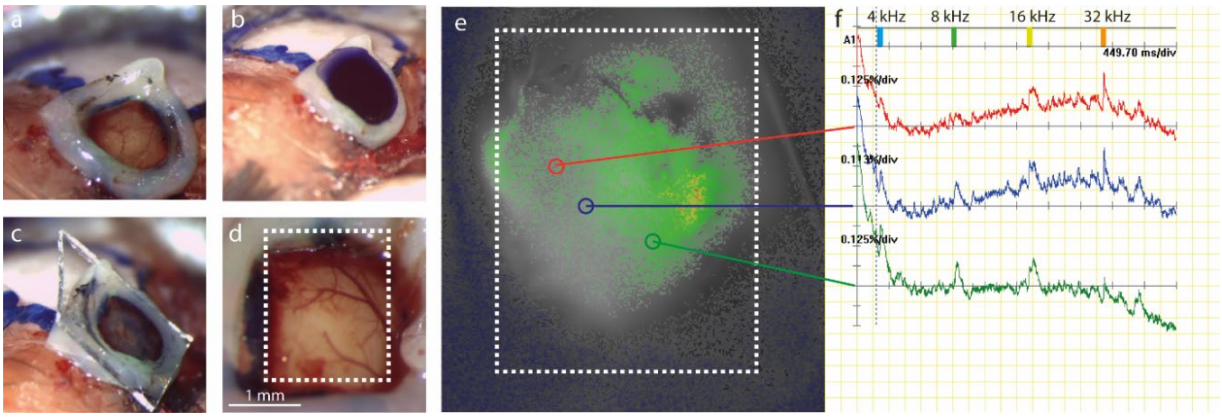


**Figure 23 Studying auditory cortex activity with VSDI.** Preparation steps: (**a**) Craniotomy over the auditory cortex with dura removal and a temporary staining chamber made with cement (**b**) Application of the dye solution (RH1691) into the chamber for 90 minutes. (**c**) Application of low-melt agarose on the brain surface and sealing with the cover glass. (**d**) Imaging window. (**e**) Imaging window with an indication of the analyzed region of interests (ROI). Green ROI – a low-frequency region in A1, Blue ROT – a middle-frequency region in A1. Red ROI – a high-frequency region in A1. (**f**) Individual time-course traces recorded in A1 during tonotopy mapping.

Upon imaging, the molecules of the dye transformed changes in membrane potential into changes in optical signal. After revealing tonotopy over A1 or AAF (Figure 23e-f), VSDI recordings were used to confirm the presence of bigger offset responses in AAF compared to A1 (Figure 24a). We also used this technique to verify that PT stimulation evokes higher offset responses in AAF neurons than WN bursts (Figure 24b). Thus, the VSDI technique is a promising tool to compare processing in adjacent cortical regions. In the future, it could be used to study if and how features other than sound termination or spectral complexity are differentially encoded in A1 and AAF.

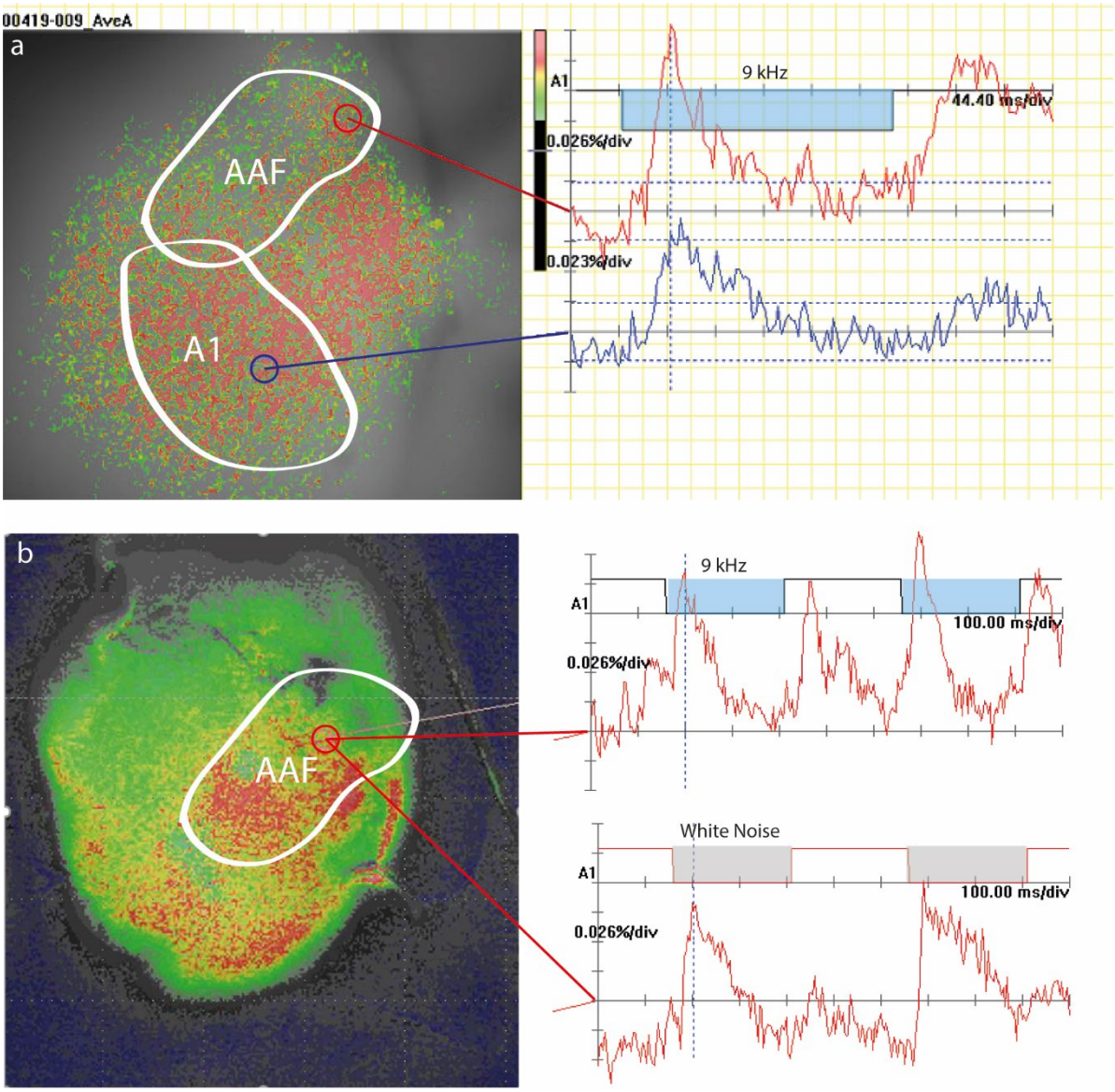


**Figure 24 VSDI recordings confirm the presence of bigger offset responses in AAF compared to A1** (**a**) Individual time-course traces recorded within A1 (blue ROI) and AAF (red ROI) in response to 250 ms 9 kHz pure tones. (**b**) Individual time-course traces recorded in AAF in response to 250 ms 9 kHz pure tone or white noise burst.

## 6.2. Transformation of offset responses on the central auditory pathway

One of the most striking results of our study was the lack of offset responses to WN stimulation in MGB and their presence in AAF. These vastly different responses could be a result of different neural processing in purely excitatory (MGB) in contrast to excitatory-inhibitory (AAF) networks (Figure 25a).

As IC comprises both excitatory and inhibitory neurons, we expected this region to encode offset responses of terminated WN bursts similarly to AAF. Surprisingly, we did not see any significant increase in the spike rate following sound termination (Figure 25b). On the other hand, many IC cells exhibited sustained responses and a substantial decrease of firing when the sound stopped. (Figure 25c). Comparing offset responses evoked by 9 kHz PT revealed a wide variety of firings in the IC population. We found onset-offset responsive cells, cells with sustained firing, and a big cluster of cells showing onset responses and suppression precisely at the offset.

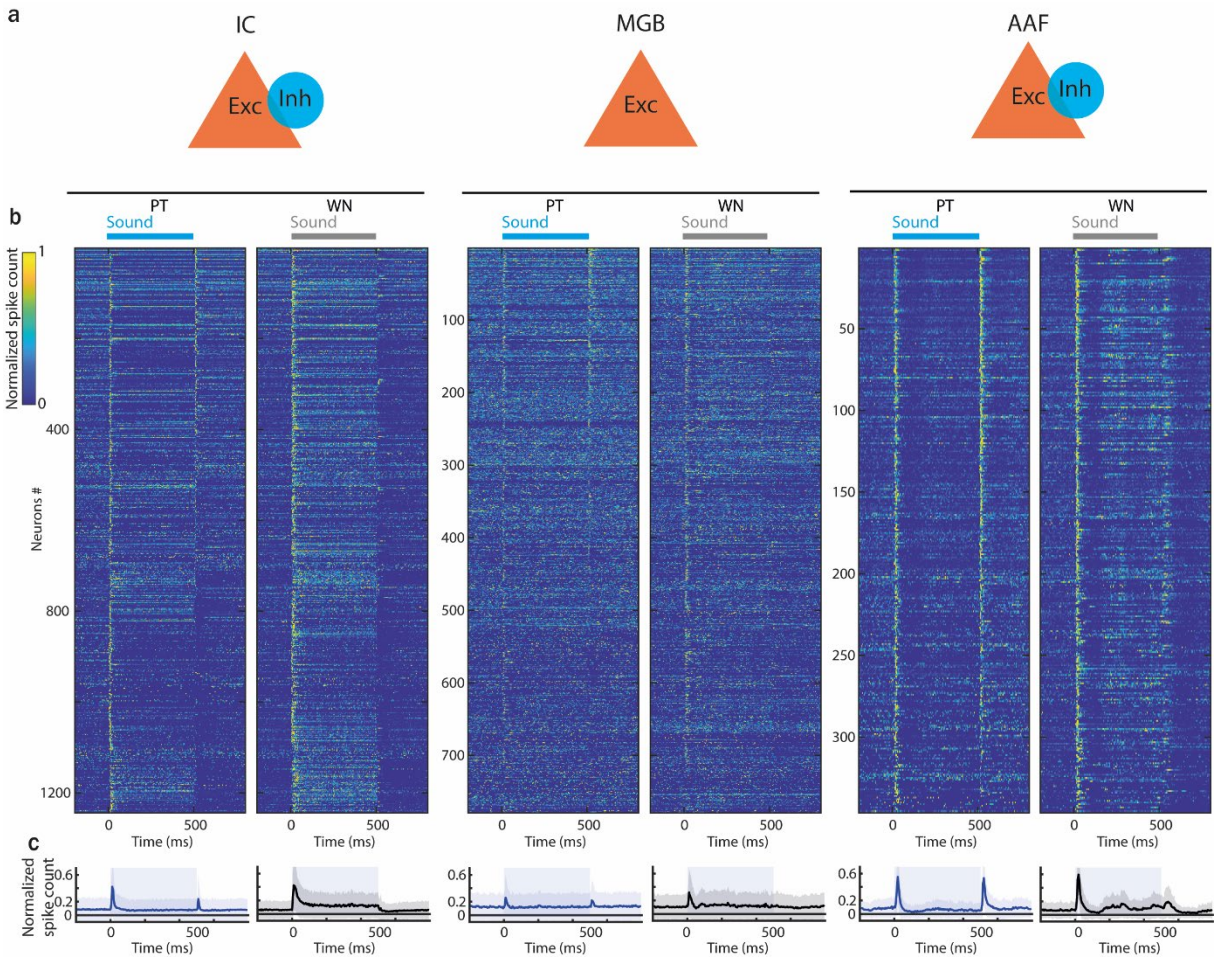


**Figure 25 Transformation of offset responses on the central auditory pathway (a)** Schematic representation of excitatory-inhibitory or purely excitatory neural networks of different nuclei of central auditory pathway (**b**) Normalized PSTH of IC, MGB, and AAF neurons in response to 500 ms PT or WN bursts, bin size: 5ms. Data are sorted by descending spike rate at the PT offset. (**c**) Averaged PSTH of IC, MGB, or AAF neuron's normalized response to PT and WN bursts played at 60 dB SPL with sound duration 500 ms and ISI between 500 and 2000 ms.

Our results show that both AAF and MGB could encode important changes within ongoing sounds with multiple offset responses (Chapter 3, Figure 17). Based on the very distinct encoding of sound termination in IC (Figure 25) in comparison to MGB and AAF, we wondered which strategy for encoding the presence and disappearance of multiple frequency components would be used by its population. Multi-frequency component sounds evoked very distinct responses within IC (Figure 26a, b). Some neurons showed offset responses following the removal of each frequency component. Other cells were suppressed or sustained throughout the duration of only specific frequency components. This data revealed a very complex encoding of changes in frequency within a temporally discontinuous sound in IC.

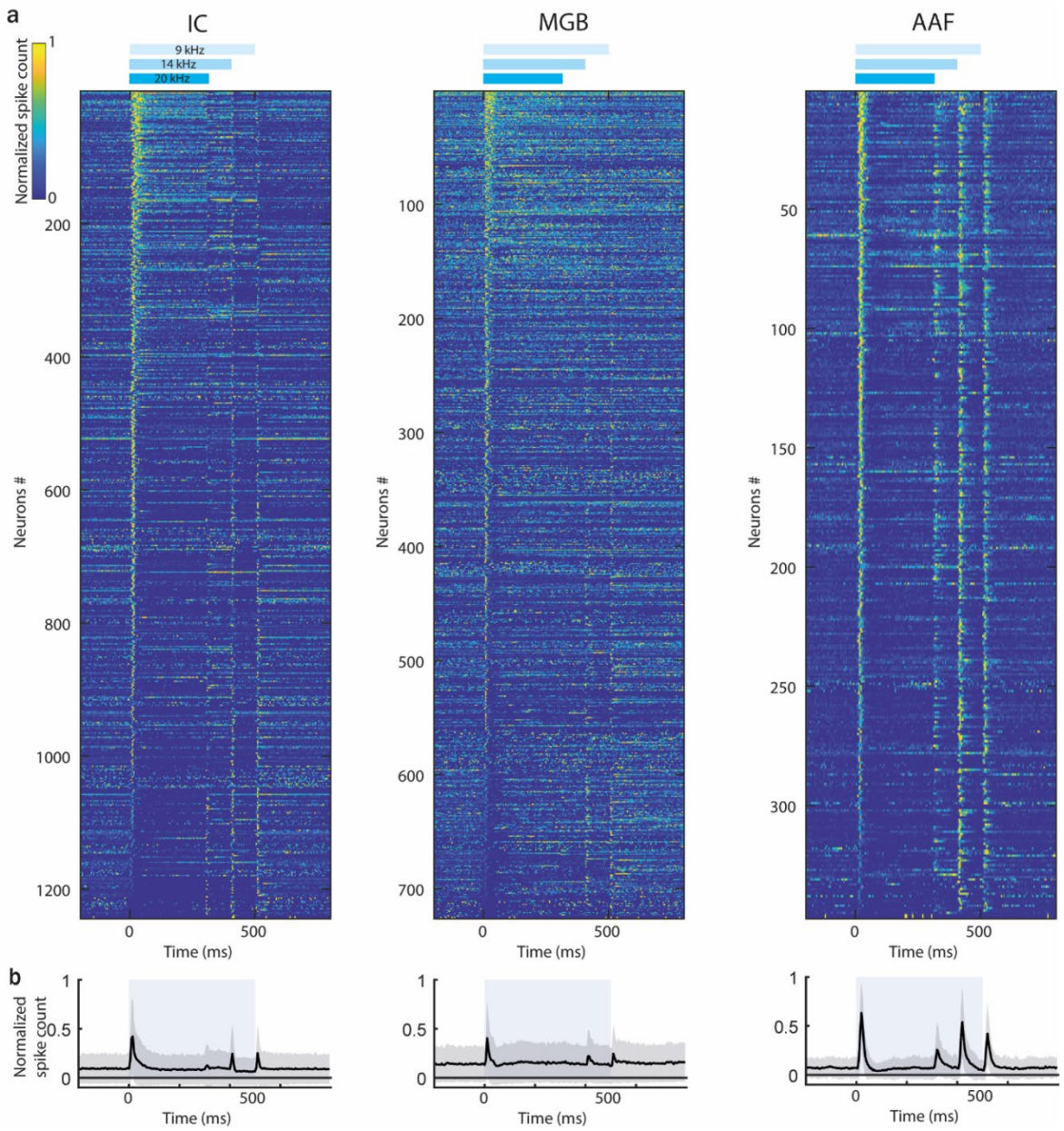


**Figure 26 Multi-frequency component sounds evoked very distinct responses within IC (a)** Normalized PSTH of IC, MGB, or AAF neuron's response to 3-components stimuli, bin size: 5ms. Data are sorted by descending spike rate at the onset. (b) Averaged PSTH (mean ± STD) of IC, MGB, or AAF neuron's response to 3-components stimuli.

These observations highlight different IC, MGB, and AAF strategies to encode important changes within a temporally discontinuous sound. There is an important transformation of signal between those nuclei, which cannot be captured with the analysis of onset responses only. Thus studying more temporally dynamic sounds, which more closely reassemble what we hear in the natural settings, is the key to reveal a specific role in sound processing for each nucleus on the central auditory pathway. Future experiments should improve the understanding of how complex patterns of IC responses are transformed into more homologous responses in MGB and AAF upon processing temporally dynamic sounds.

### 6.3. Encoding of ultrasonic vocalizations in AAF

Offset responses are thought to be crucial for perceptual grouping, sound duration discrimination, consonant identification, and, in general, for processing temporally discontinuous sounds such as those in speech or vocalization. To test if onset-offset cells in AAF respond to temporal changes present within natural vocalization calls, we performed *in vivo* electrophysiology recordings in an anesthetized mouse while presenting multi-jump mice vocalization. Multi-jump calls contain both frequency-modulated sweeps and gaps between different syllables, and their spectrum of frequencies varies between 60 and 80 kHz. We found that AAF cells respond to specific frequency modulation and gaps in between syllables (Figure 27a-c). Regardless of the very high frequencies of the tested ultrasonic vocalization, some cells within AAF still responded to such high frequencies possibly outside of their tuning receptive field. These observations underscore the ability of AAF to process temporally complex sounds such as mouse calls.

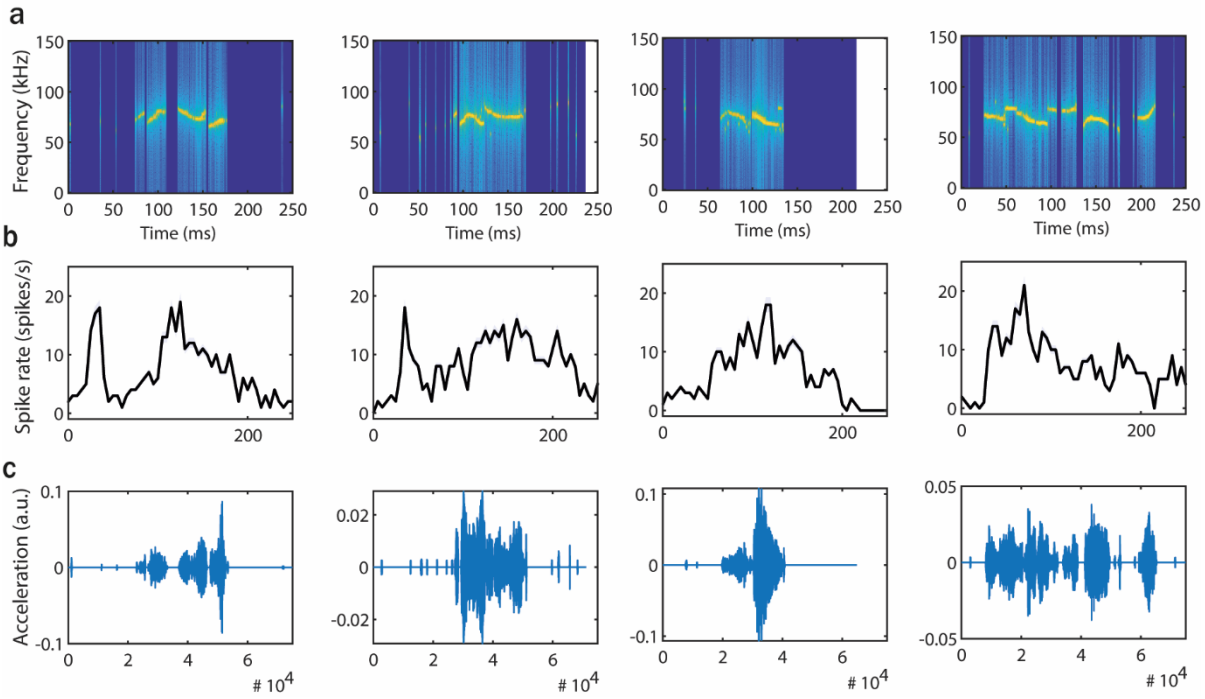


**Figure 27 Encoding of ultrasonic vocalizations in AAF.** (**a**) Spectrograms of four ultrasonic vocalization calls of the mouse. (**b**) PSTH of an example neuron's response to multi-jumps vocalization calls. (**c**) Acceleration traces of ultrasonic vocalization calls (same as in a).

As a control, we recorded responses to reverse playback of multi-jump vocalizations that maintain the same statistics of spectral amplitude distribution as the original vocalizations, but their higher-level features are modified (e.g., upward frequency sweep, when reversed, becomes a downward frequency sweep). Again, we saw some AAF cells encoding specific frequency modulations or gaps within the jumps (Figure 28a-c). Further studies could test a rich library of ultrasonic vocalizations to understand which temporal features are predominantly encoded within AAF and if, in general, there is any vocalization selectivity across auditory cortical fields in mice.

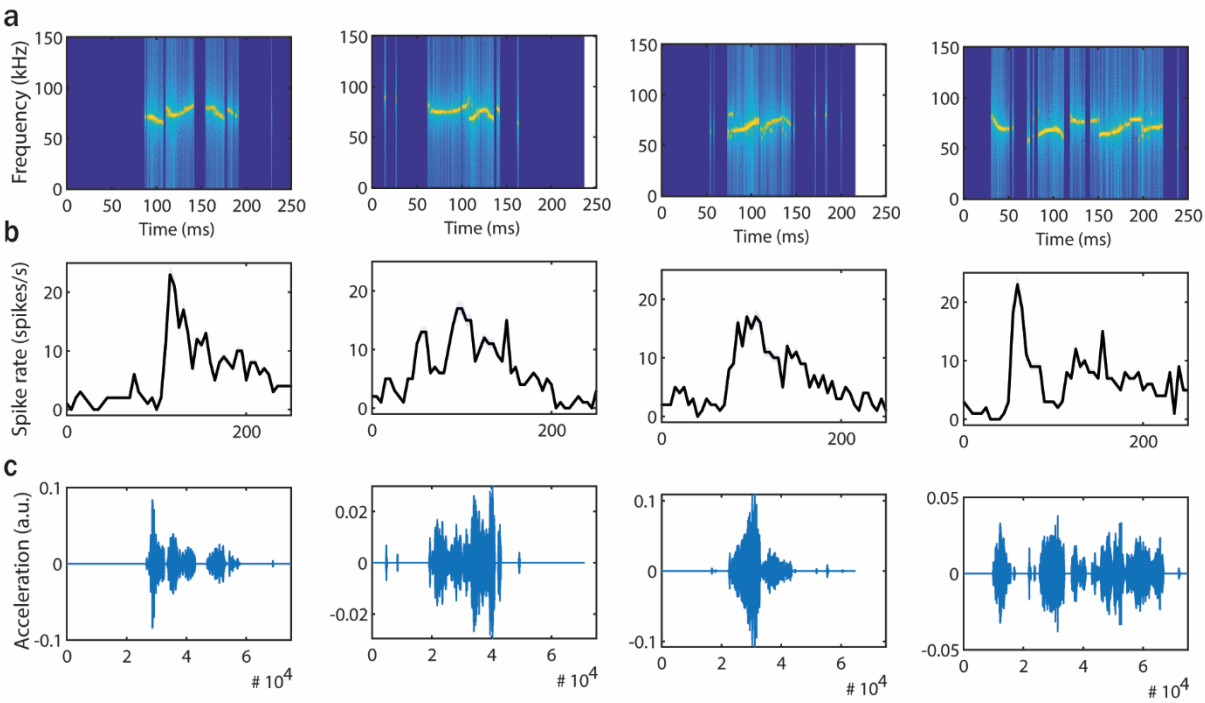


**Figure 28 Encoding of inverted ultrasonic vocalizations in AAF.** (**a**) Spectrograms of four inverted ultrasonic vocalization calls of the mouse. (**b**) PSTH of an example neuron's response to inverted multi-jumps vocalization calls. (**c**) Acceleration traces of inverted ultrasonic vocalization calls (same as in a).

# Chapter 7

# Conclusion

Identifying distinct roles for different auditory circuits is crucial to understand how an auditory signal is processed at the cortical level and ultimately leads to its perception. Our findings suggest distinct sound processing in the two primary auditory cortices of mice. The distinct offset responses in A1 and AAF and the different responses to spectrally complex and simple sounds emphasize the complexity of sound processing at the cortical level. Our data indicate that A1 and AAF should be clearly defined and distinguished during experiments as they process sound parameters differently. But why does the auditory cortex need two primary regions? One can speculate that auditory stimuli, as compared to other sensory stimuli, have more complex and challenging temporal characteristics. This suggests that the auditory cortex employs unique operating principles compared to other sensory systems and that assumptions about similar processing within different primary sensory fields can be misleading. Identification of distinct sound feature representation within A1 and AAF is just the first insight into how information flows within and between two primary auditory areas. If and how other sound features are differently encoded in A1 and AAF, and the relevance of these divisions beyond sound processing remains to be elucidated. It could be the basis of the two classical facets of the “where” and “what” processing streams.

# References


Adesnik, H., Bruns, W., Taniguchi, H., Huang, Z.J., and Scanziani, M. (2012). A neural circuit for spatial summation in visual cortex. Nature 490, 226-231.

Akimov, A.G., Egorova, M.A., and Ehret, G. (2017). Spectral summation and facilitation in on- and off-responses for optimized representation of communication calls in mouse inferior colliculus. Eur J Neurosci 45, 440-459.

Andersen, R.A., Knight, P.L., and Merzenich, M.M. (1980). The thalamocortical and corticothalamic connections of AI, AII, and the anterior auditory field (AAF) in the cat: evidence for two largely segregated systems of connections. J Comp Neurol 194, 663-701.

Anderson, L.A., and Linden, J.F. (2016). Mind the Gap: Two Dissociable Mechanisms of Temporal Processing in the Auditory System. The Journal of neuroscience : the official journal of the Society for Neuroscience 36, 1977-1995.

Asokan, M.M., Williamson, R.S., Hancock, K.E., and Polley, D.B. (2021). Inverted central auditory hierarchies for encoding local intervals and global temporal patterns. Curr Biol 31, 1762-1770 e1764.

Atencio, C.A., and Schreiner, C.E. (2008). Spectrotemporal processing differences between auditory cortical fast-spiking and regular-spiking neurons. The Journal of neuroscience : the official journal of the Society for Neuroscience 28, 3897-3910.

Barbour, D.L., and Callaway, E.M. (2008). Excitatory local connections of superficial neurons in rat auditory cortex. The Journal of neuroscience : the official journal of the Society for Neuroscience 28, 11174-11185.

Bartlett, E.L. (2013). The organization and physiology of the auditory thalamus and its role in processing acoustic features important for speech perception. Brain Lang 126, 29-48.

Baum, G.L., Cui, Z., Roalf, D.R., Ciric, R., Betzel, R.F., Larsen, B., Cieslak, M., Cook, P.A., Xia, C.H., Moore, T.M., *et al.* (2020). Development of structure-function coupling in human brain networks during youth. Proc Natl Acad Sci U S A 117, 771-778.

Bhumika, S., Nakamura, M., Valerio, P., Solyga, M., Linden, H., and Barkat, T.R. (2020). A Late Critical Period for Frequency Modulated Sweeps in the Mouse Auditory System. Cereb Cortex 30, 2586-2599.

Bizley, J.K., Bajo, V.M., Nodal, F.R., and King, A.J. (2015). Cortico-Cortical Connectivity Within Ferret Auditory Cortex. J Comp Neurol 523, 2187-2210.

Bizley, J.K., Nodal, F.R., Nelken, I., and King, A.J. (2005). Functional organization of ferret auditory cortex. Cereb Cortex 15, 1637-1653.

Bondanelli, G., Deneux, T., Bathellier, B., and Ostojic, S. (2019). Population coding and network dynamics during OFF responses in auditory cortex. BioRxiv [Preprint].

Caras, M.L., and Sanes, D.H. (2017). Top-down modulation of sensory cortex gates perceptual learning. Proc Natl Acad Sci U S A 114, 9972-9977.

Carrasco, A., and Lomber, S.G. (2009a). Differential modulatory influences between primary auditory cortex and the anterior auditory field. The Journal of neuroscience : the official journal of the Society for Neuroscience 29, 8350-8362.

Carrasco, A., and Lomber, S.G. (2009b). Evidence for hierarchical processing in cat auditory cortex: nonreciprocal influence of primary auditory cortex on the posterior auditory field. The Journal of neuroscience : the official journal of the Society for Neuroscience 29, 14323-14333.

Ceballo, S., Piwkowska, Z., Bourg, J., Daret, A., and Bathellier, B. (2019). Targeted Cortical Manipulation of Auditory Perception. Neuron.

Chalasani, S.H., Chronis, N., Tsunozaki, M., Gray, J.M., Ramot, D., Goodman, M.B., and Bargmann, C.I. (2007). Dissecting a circuit for olfactory behaviour in Caenorhabditis elegans. Nature 450, 63-70.

Chechik, G., Anderson, M.J., Bar-Yosef, O., Young, E.D., Tishby, N., and Nelken, I. (2006). Reduction of information redundancy in the ascending auditory pathway. Neuron 51, 359-368.

Chen, F., Takemoto, M., Nishimura, M., Tomioka, R., and Song, W.J. (2021). Postnatal development of subfields in the core region of the mouse auditory cortex. Hear Res 400, 108138.

Chen, I.W., Helmchen, F., and Lutcke, H. (2015). Specific Early and Late Oddball-Evoked Responses in Excitatory and Inhibitory Neurons of Mouse Auditory Cortex. The Journal of neuroscience : the official journal of the Society for Neuroscience 35, 12560-12573.

Chong, K.K., Anandakumar, D.B., Dunlap, A.G., Kacsoh, D.B., and Liu, R.C. (2020). Experience-Dependent Coding of Time-Dependent Frequency Trajectories by Off Responses in Secondary Auditory Cortex. The Journal of neuroscience : the official journal of the Society for Neuroscience 40, 4469-4482.
Christensen, R.K., Linden, H., Nakamura, M., and Barkat, T.R. (2019). White Noise Background Improves Tone Discrimination by Suppressing Cortical Tuning Curves. Cell Rep 29, 2041-2053 e2044.
Christianson, G.B., Sahani, M., and Linden, J.F. (2011). Depth-dependent temporal response properties in core auditory cortex. The Journal of neuroscience : the official journal of the Society for Neuroscience 31, 12837-12848.
Dalmay, T., Abs, E., Poorthuis, R.B., Hartung, J., Pu, D.L., Onasch, S., Lozano, Y.R., Signoret-Genest, J., Tovote, P., Gjorgjieva, J., and Letzkus, J.J. (2019). A Critical Role for Neocortical Processing of Threat Memory. Neuron.
David, S.V., Mesgarani, N., and Shamma, S.A. (2007). Estimating sparse spectro-temporal receptive fields with natural stimuli. Network 18, 191-212.
De Franceschi, G., and Barkat, T.R. (2020). Task-induced modulations of neuronal activity along the auditory pathway. bioRxiv [Preprint].
Dehmel, S., Kopp-Scheinpflug, C., Dorrscheidt, G.J., and Rubsamen, R. (2002). Electrophysiological characterization of the superior paraolivary nucleus in the Mongolian gerbil. Hear Res 172, 18-36.
Ding, J., Benson, T.E., and Voigt, H.F. (1999). Acoustic and current-pulse responses of identified neurons in the dorsal cochlear nucleus of unanesthetized, decerebrate gerbils. J Neurophysiol 82, 3434-3457.
Doucet, J.R., Molavi, D.L., and Ryugo, D.K. (2003). The source of corticocollicular and corticobulbar projections in area Te1 of the rat. Exp Brain Res 153, 461-466.
Eggermont, J.J. (2015). Animal models of auditory temporal processing. Int J Psychophysiol 95, 202-215.
Fader, S.M., Imaizumi, K., Yanagawa, Y., and Lee, C.C. (2016). Wisteria Floribunda Agglutinin-Labeled Perineuronal Nets in the Mouse Inferior Colliculus, Thalamic Reticular Nucleus and Auditory Cortex. Brain Sci 6.
Felix, R.A., 2nd, Gourevitch, B., and Portfors, C.V. (2018). Subcortical pathways: Towards a better understanding of auditory disorders. Hear Res 362, 48-60.
Fritz, J., Shamma, S., Elhilali, M., and Klein, D. (2003). Rapid task-related plasticity of spectrotemporal receptive fields in primary auditory cortex. Nat Neurosci 6, 1216-1223.
Gallio, M., Ofstad, T.A., Macpherson, L.J., Wang, J.W., and Zuker, C.S. (2011). The coding of temperature in the Drosophila brain. Cell 144, 614-624.
Geissler, D.B., and Ehret, G. (2002). Time-critical integration of formants for perception of communication calls in mice. Proc Natl Acad Sci U S A 99, 9021-9025.
Genon, S., Reid, A., Langner, R., Amunts, K., and Eickhoff, S.B. (2018). How to Characterize the Function of a Brain Region. Trends Cogn Sci 22, 350-364.
Gjorgjieva, J., Sompolinsky, H., and Meister, M. (2014). Benefits of pathway splitting in sensory coding. The Journal of neuroscience : the official journal of the Society for Neuroscience 34, 12127-12144.
Greenberg, S., and Ainsworth, W. (2006). Listening to Speech: An Auditory Perspective (Psychology Press).
Guo, W., Chambers, A.R., Darrow, K.N., Hancock, K.E., Shinn-Cunningham, B.G., and Polley, D.B. (2012). Robustness of cortical topography across fields, laminae, anesthetic states, and neurophysiological signal types. The Journal of neuroscience : the official journal of the Society for Neuroscience 32, 9159-9172.
Hackett, T.A., Barkat, T.R., O'Brien, B.M., Hensch, T.K., and Polley, D.B. (2011). Linking topography to tonotopy in the mouse auditory thalamocortical circuit. The Journal of neuroscience : the official journal of the Society for Neuroscience 31, 2983-2995.
Happel, M.F., Niekisch, H., Castiblanco Rivera, L.L., Ohl, F.W., Deliano, M., and Frischknecht, R. (2014). Enhanced cognitive flexibility in reversal learning induced by removal of the extracellular matrix in auditory cortex. Proc Natl Acad Sci U S A 111, 2800-2805.
He, J. (2001). On and off pathways segregated at the auditory thalamus of the guinea pig. The Journal of neuroscience : the official journal of the Society for Neuroscience 21, 8672-8679.
He, J. (2002). OFF responses in the auditory thalamus of the guinea pig. J Neurophysiol 88, 2377-2386.
He, J.F. (2003). Corticofugal modulation on both ON and OFF responses in the nonlemniscal auditory thalamus of the guinea pig. Journal of Neurophysiology 89, 367-381.

Imaizumi, K., Priebe, N.J., Crum, P.A., Bedenbaugh, P.H., Cheung, S.W., and Schreiner, C.E. (2004). Modular functional organization of cat anterior auditory field. J Neurophysiol 92, 444-457.
Isaacson, J.S., and Scanziani, M. (2011). How inhibition shapes cortical activity. Neuron 72, 231-243.
Ito, T., Bishop, D.C., and Oliver, D.L. (2016). Functional organization of the local circuit in the inferior colliculus. Anat Sci Int 91, 22-34.
Jabaudon, D. (2017). Fate and freedom in developing neocortical circuits. Nat Commun 8, 16042.
Joachimsthaler, B., Uhlmann, M., Miller, F., Ehret, G., and Kurt, S. (2014). Quantitative analysis of neuronal response properties in primary and higher-order auditory cortical fields of awake house mice (Mus musculus). Eur J Neurosci 39, 904-918.
Kasai, M., Ono, M., and Ohmori, H. (2012). Distinct neural firing mechanisms to tonal stimuli offset in the inferior colliculus of mice in vivo. Neurosci Res 73, 224-237.
Kawai, R., Markman, T., Poddar, R., Ko, R., Fantana, A.L., Dhawale, A.K., Kampff, A.R., and Olveczky, B.P. (2015). Motor Cortex Is Required for Learning but Not for Executing a Motor Skill. Neuron 86, 800-812.
Keller, C.H., Kaylegian, K., and Wehr, M. (2018). Gap encoding by parvalbumin-expressing interneurons in auditory cortex. J Neurophysiol 120, 105-114.
Keller, G.B., Bonhoeffer, T., and Hubener, M. (2012). Sensorimotor mismatch signals in primary visual cortex of the behaving mouse. Neuron 74, 809-815.
Kelly, J.B., Judge, P.W., and Phillips, D.P. (1986). Representation of the cochlea in primary auditory cortex of the ferret (Mustela putorius). Hear Res 24, 111-115.
King, A.J., and Nelken, I. (2009). Unraveling the principles of auditory cortical processing: can we learn from the visual system? Nat Neurosci 12, 698-701.
King, A.J., Teki, S., and Willmore, B.D.B. (2018). Recent advances in understanding the auditory cortex. F1000Res 7.
Kishan, A.U., Lee, C.C., and Winer, J.A. (2008). Branched projections in the auditory thalamocortical and corticocortical systems. Neuroscience 154, 283-293.
Kopp-Scheinpflug, C., Sinclair, J.L., and Linden, J.F. (2018). When Sound Stops: Offset Responses in the Auditory System. Trends Neurosci 41, 712-728.
Kopp-Scheinpflug, C., Tozer, A.J., Robinson, S.W., Tempel, B.L., Hennig, M.H., and Forsythe, I.D. (2011). The sound of silence: ionic mechanisms encoding sound termination. Neuron 71, 911-925.
Kowalski, N., Versnel, H., and Shamma, S.A. (1995). Comparison of responses in the anterior and primary auditory fields of the ferret cortex. J Neurophysiol 73, 1513-1523.
Kral, A., Schroder, J.H., Klinke, R., and Engel, A.K. (2003). Absence of cross-modal reorganization in the primary auditory cortex of congenitally deaf cats. Exp Brain Res 153, 605-613.
Kulesza, R.J., Jr., and Berrebi, A.S. (2000). Superior paraolivary nucleus of the rat is a GABAergic nucleus. J Assoc Res Otolaryngol 1, 255-269.
Kulesza, R.J., Jr., Spirou, G.A., and Berrebi, A.S. (2003). Physiological response properties of neurons in the superior paraolivary nucleus of the rat. J Neurophysiol 89, 2299-2312.
Lakunina, A.A., Nardoci, M.B., Ahmadian, Y., and Jaramillo, S. (2020). Somatostatin-Expressing Interneurons in the Auditory Cortex Mediate Sustained Suppression by Spectral Surround. The Journal of neuroscience : the official journal of the Society for Neuroscience 40, 3564-3575.
Lee, C.C., Imaizumi, K., Schreiner, C.E., and Winer, J.A. (2004). Concurrent tonotopic processing streams in auditory cortex. Cereb Cortex 14, 441-451.
Lee, C.C., and Winer, J.A. (2008a). Connections of cat auditory cortex: I. Thalamocortical system. J Comp Neurol 507, 1879-1900.
Lee, C.C., and Winer, J.A. (2008b). Connections of cat auditory cortex: III. Corticocortical system. J Comp Neurol 507, 1920-1943.
Lee, C.C., and Winer, J.A. (2011). Convergence of thalamic and cortical pathways in cat auditory cortex. Hear Res 274, 85-94.
Li, L.Y., Xiong, X.R., Ibrahim, L.A., Yuan, W., Tao, H.W., and Zhang, L.I. (2015). Differential Receptive Field Properties of Parvalbumin and Somatostatin Inhibitory Neurons in Mouse Auditory Cortex. Cereb Cortex 25, 1782-1791.
Liang, L., Lu, T., and Wang, X. (2002). Neural representations of sinusoidal amplitude and frequency modulations in the primary auditory cortex of awake primates. J Neurophysiol 87, 2237-2261.

Linden, J.F., Liu, R.C., Sahani, M., Schreiner, C.E., and Merzenich, M.M. (2003). Spectrotemporal structure of receptive fields in areas AI and AAF of mouse auditory cortex. J Neurophysiol 90, 2660-2675.
Liu, B.H., Wu, G.K., Arbuckle, R., Tao, H.W., and Zhang, L.I. (2007). Defining cortical frequency tuning with recurrent excitatory circuitry. Nat Neurosci 10, 1594-1600.
Liu, J., Whiteway, M.R., Sheikhattar, A., Butts, D.A., Babadi, B., and Kanold, P.O. (2019). Parallel Processing of Sound Dynamics across Mouse Auditory Cortex via Spatially Patterned Thalamic Inputs and Distinct Areal Intracortical Circuits. Cell Rep 27, 872-885 e877.
Lomber, S.G., and Malhotra, S. (2008). Double dissociation of 'what' and 'where' processing in auditory cortex. Nat Neurosci 11, 609-616.
Lu, T., Liang, L., and Wang, X. (2001). Temporal and rate representations of time-varying signals in the auditory cortex of awake primates. Nat Neurosci 4, 1131-1138.
Meng, X., Winkowski, D.E., Kao, J.P.Y., and Kanold, P.O. (2017). Sublaminar Subdivision of Mouse Auditory Cortex Layer 2/3 Based on Functional Translaminar Connections. The Journal of neuroscience : the official journal of the Society for Neuroscience 37, 10200-10214.
Meredith, M.A., and Lomber, S.G. (2011). Somatosensory and visual crossmodal plasticity in the anterior auditory field of early-deaf cats. Hear Res 280, 38-47.
Metherate, R., Kaur, S., Kawai, H., Lazar, R., Liang, K., and Rose, H.J. (2005). Spectral integration in auditory cortex: mechanisms and modulation. Hear Res 206, 146-158.
Miller, K.D. (2016). Canonical computations of cerebral cortex. Curr Opin Neurobiol 37, 75-84.
Moerel, M., De Martino, F., Ugurbil, K., Yacoub, E., and Formisano, E. (2019). Processing complexity increases in superficial layers of human primary auditory cortex. Sci Rep 9, 5502.
Moore, A.K., and Wehr, M. (2013). Parvalbumin-expressing inhibitory interneurons in auditory cortex are well-tuned for frequency. The Journal of neuroscience : the official journal of the Society for Neuroscience 33, 13713-13723.
Morel, A., and Imig, T.J. (1987). Thalamic projections to fields A, AI, P, and VP in the cat auditory cortex. J Comp Neurol 265, 119-144.
Moshitch, D., Las, L., Ulanovsky, N., Bar-Yosef, O., and Nelken, I. (2006). Responses of neurons in primary auditory cortex (A1) to pure tones in the halothane-anesthetized cat. J Neurophysiol 95, 3756-3769.
Nakata, S., Takemoto, M., and Song, W.J. (2020). Differential cortical and subcortical projection targets of subfields in the core region of mouse auditory cortex. Hear Res 386, 107876.
Natan, R.G., Briguglio, J.J., Mwilambwe-Tshilobo, L., Jones, S.I., Aizenberg, M., Goldberg, E.M., and Geffen, M.N. (2015). Complementary control of sensory adaptation by two types of cortical interneurons. Elife 4.
Natan, R.G., Rao, W., and Geffen, M.N. (2017). Cortical Interneurons Differentially Shape Frequency Tuning following Adaptation. Cell Rep 21, 878-890.
Pachitariu, M., Steinmetz, N., Kadir, S., Carandini, M., and Harris, K. (2016). Fast and accurate spike sorting of high-channel count probes with KiloSort. Adv Neur In 29.
Peng, K., Peng, Y.J., Wang, J., Yang, M.J., Fu, Z.Y., Tang, J., and Chen, Q.C. (2017). Latency modulation of collicular neurons induced by electric stimulation of the auditory cortex in Hipposideros pratti: In vivo intracellular recording. PLoS One 12, e0184097.
Phillips, D.P., Hall, S.E., and Boehnke, S.E. (2002). Central auditory onset responses, and temporal asymmetries in auditory perception. Hear Res 167, 192-205.
Phillips, D.P., Judge, P.W., and Kelly, J.B. (1988). Primary auditory cortex in the ferret (Mustela putorius): neural response properties and topographic organization. Brain Res 443, 281-294.
Pi, H.J., Hangya, B., Kvitsiani, D., Sanders, J.I., Huang, Z.J., and Kepecs, A. (2013). Cortical interneurons that specialize in disinhibitory control. Nature 503, 521-524.
Pollak, G.D., and Bodenhamer, R.D. (1981). Specialized characteristics of single units in inferior colliculus of mustache bat: frequency representation, tuning, and discharge patterns. J Neurophysiol 46, 605-620.
Polley, D.B., Read, H.L., Storace, D.A., and Merzenich, M.M. (2007). Multiparametric auditory receptive field organization across five cortical fields in the albino rat. J Neurophysiol 97, 3621-3638.
Ponulak, F., and Kasinski, A. (2011). Introduction to spiking neural networks: Information processing, learning and applications. Acta Neurobiol Exp (Wars) 71, 409-433.

Qin, L., Chimoto, S., Sakai, M., Wang, J., and Sato, Y. (2007). Comparison between offset and onset responses of primary auditory cortex ON-OFF neurons in awake cats. J Neurophysiol 97, 3421-3431.
Qin, L., Liu, Y., Wang, J., Li, S., and Sato, Y. (2009). Neural and behavioral discrimination of sound duration by cats. The Journal of neuroscience : the official journal of the Society for Neuroscience 29, 15650-15659.
Rauschecker, J.P. (2015). Auditory and visual cortex of primates: a comparison of two sensory systems. Eur J Neurosci 41, 579-585.
Recanzone, G.H. (2000). Response profiles of auditory cortical neurons to tones and noise in behaving macaque monkeys. Hear Res 150, 104-118.
Reinhard, S.M., Abundez-Toledo, M., Espinoza, K., and Razak, K.A. (2019). Effects of developmental noise exposure on inhibitory cell densities and perineuronal nets in A1 and AAF of mice. Hear Res 381, 107781.
Rosen, S. (1992). Temporal information in speech: acoustic, auditory and linguistic aspects. Philos Trans R Soc Lond B Biol Sci 336, 367-373.
Rouiller, E.M., Simm, G.M., Villa, A.E., de Ribaupierre, Y., and de Ribaupierre, F. (1991). Auditory corticocortical interconnections in the cat: evidence for parallel and hierarchical arrangement of the auditory cortical areas. Exp Brain Res 86, 483-505.
Rudy, B., Fishell, G., Lee, S., and Hjerling-Leffler, J. (2011). Three groups of interneurons account for nearly 100% of neocortical GABAergic neurons. Dev Neurobiol 71, 45-61.
Rutkowski, R.G., Miasnikov, A.A., and Weinberger, N.M. (2003). Characterisation of multiple physiological fields within the anatomical core of rat auditory cortex. Hear Res 181, 116-130.
Saha, D., Sun, W., Li, C., Nizampatnam, S., Padovano, W., Chen, Z., Chen, A., Altan, E., Lo, R., Barbour, D.L., and Raman, B. (2017). Engaging and disengaging recurrent inhibition coincides with sensing and unsensing of a sensory stimulus. Nat Commun 8, 15413.
Saldana, E., Aparicio, M.A., Fuentes-Santamaria, V., and Berrebi, A.S. (2009). Connections of the superior paraolivary nucleus of the rat: projections to the inferior colliculus. Neuroscience 163, 372-387.
Schneider, D.M. (2020). Reflections of action in sensory cortex. Curr Opin Neurobiol 64, 53-59.
Scholl, B., Gao, X., and Wehr, M. (2010). Nonoverlapping sets of synapses drive on responses and off responses in auditory cortex. Neuron 65, 412-421.
Schreiner, C.E., and Urbas, J.V. (1988). Representation of amplitude modulation in the auditory cortex of the cat. II. Comparison between cortical fields. Hear Res 32, 49-63.
Serkov, F.N., Kienko, V. M., & Limanskaya, L. I. (1976). Responses of medial geniculate body neurons to auditory cortical stimulation. Neurophysiology 8, 3-9.
Shi, Z., Yan, S., Ding, Y., Zhou, C., Qian, S., Wang, Z., Gong, C., Zhang, M., Zhang, Y., Zhao, Y.*, et al.* (2019). Anterior Auditory Field Is Needed for Sound Categorization in Fear Conditioning Task of Adult Rat. Front Neurosci 13, 1374.
Sollini, J., Chapuis, G.A., Clopath, C., and Chadderton, P. (2018). ON-OFF receptive fields in auditory cortex diverge during development and contribute to directional sweep selectivity. Nat Commun 9, 2084.
Solyga, M., and Barkat, T.R. (2019). Distinct processing of tone offset in two primary auditory cortices. Sci Rep 9, 9581.
Solyga, M., and Barkat, T.R. (2021). Emergence and function of cortical offset responses in sound termination detection. bioRxiv [Preprint].
Stiebler, I., Neulist, R., Fichtel, I., and Ehret, G. (1997). The auditory cortex of the house mouse: left-right differences, tonotopic organization and quantitative analysis of frequency representation. J Comp Physiol A 181, 559-571.
Suga, N. (1964). Single Unit Activity in Cochlear Nucleus and Inferior Colliculus of Echo-Locating Bats. J Physiol 172, 449-474.
Suga, N., Simmons, J.A., and Jen, P.H. (1975). Peripheral specialization for fine analysis of doppler-shifted echoes in the auditory system of the "CF-FM" bat Pteronotus parnellii. J Exp Biol 63, 161-192.
Syka, J., Rybalko, N., Mazelova, J., and Druga, R. (2002). Gap detection threshold in the rat before and after auditory cortex ablation. Hear Res 172, 151-159.
Takahashi, H., Nakao, M., and Kaga, K. (2004). Cortical mapping of auditory-evoked offset responses in rats. Neuroreport 15, 1565-1569.

Takemoto, M., Hasegawa, K., Nishimura, M., and Song, W.J. (2014). The insular auditory field receives input from the lemniscal subdivision of the auditory thalamus in mice. J Comp Neurol 522, 1373-1389.
Takesian, A.E., Bogart, L.J., Lichtman, J.W., and Hensch, T.K. (2018). Inhibitory circuit gating of auditory critical-period plasticity. Nat Neurosci 21, 218-227.
Theunissen, F.E., David, S.V., Singh, N.C., Hsu, A., Vinje, W.E., and Gallant, J.L. (2001). Estimating spatio-temporal receptive fields of auditory and visual neurons from their responses to natural stimuli. Network 12, 289-316.
Threlkeld, S.W., Penley, S.C., Rosen, G.D., and Fitch, R.H. (2008). Detection of silent gaps in white noise following cortical deactivation in rats. Neuroreport 19, 893-898.
Tian, B., Kusmierek, P., and Rauschecker, J.P. (2013). Analogues of simple and complex cells in rhesus monkey auditory cortex. Proc Natl Acad Sci U S A 110, 7892-7897.
Trujillo, M., Measor, K., Carrasco, M.M., and Razak, K.A. (2011). Selectivity for the rate of frequency-modulated sweeps in the mouse auditory cortex. J Neurophysiol 106, 2825-2837.
van der Heijden, K., Rauschecker, J.P., de Gelder, B., and Formisano, E. (2019). Cortical mechanisms of spatial hearing. Nat Rev Neurosci 20, 609-623.
Vasquez-Lopez, S.A., Weissenberger, Y., Lohse, M., Keating, P., King, A.J., and Dahmen, J.C. (2017). Thalamic input to auditory cortex is locally heterogeneous but globally tonotopic. Elife 6.
Wang, X., Lu, T., Bendor, D., and Bartlett, E. (2008). Neural coding of temporal information in auditory thalamus and cortex. Neuroscience 157, 484-494.
Wassle, H. (2004). Parallel processing in the mammalian retina. Nat Rev Neurosci 5, 747-757.
Weible, A.P., Liu, C., Niell, C.M., and Wehr, M. (2014a). Auditory cortex is required for fear potentiation of gap detection. The Journal of neuroscience : the official journal of the Society for Neuroscience 34, 15437-15445.
Weible, A.P., Moore, A.K., Liu, C., DeBlander, L., Wu, H., Kentros, C., and Wehr, M. (2014b). Perceptual gap detection is mediated by gap termination responses in auditory cortex. Curr Biol 24, 1447-1455.
Westheimer, G. (2007). The ON-OFF dichotomy in visual processing: from receptors to perception. Prog Retin Eye Res 26, 636-648.
Williamson, R.S., and Polley, D.B. (2019). Parallel pathways for sound processing and functional connectivity among layer 5 and 6 auditory corticofugal neurons. Elife 8.
Winer, J.A., Miller, L.M., Lee, C.C., and Schreiner, C.E. (2005). Auditory thalamocortical transformation: structure and function. Trends Neurosci 28, 255-263.
Xu, N., Fu, Z.Y., and Chen, Q.C. (2014). The function of offset neurons in auditory information processing. Transl Neurosci 5, 275-285.
Young, E.D., and Brownell, W.E. (1976). Responses to tones and noise of single cells in dorsal cochlear nucleus of unanesthetized cats. J Neurophysiol 39, 282-300.
Yu, Y.Q., Xiong, Y., Chan, Y.S., and He, J. (2004). In vivo intracellular responses of the medial geniculate neurones to acoustic stimuli in anaesthetized guinea pigs. J Physiol 560, 191-205.
Zatorre, R.J., Evans, A.C., and Meyer, E. (1994). Neural mechanisms underlying melodic perception and memory for pitch. The Journal of neuroscience : the official journal of the Society for Neuroscience 14, 1908-1919.
Zeldenrust, F., Wadman, W.J., and Englitz, B. (2018). Neural Coding With Bursts-Current State and Future Perspectives. Front Comput Neurosci 12, 48.
Zhang, G., Tao, C., Zhou, C., Yan, S., Wang, Z., Zhou, Y., and Xiong, Y. (2017). Excitatory effects of the primary auditory cortex on the sound-evoked responses in the ipsilateral anterior auditory field in rat. Neuroscience 361, 157-166.
Zohar, O., Shackleton, T.M., Nelken, I., Palmer, A.R., and Shamir, M. (2011). First spike latency code for interaural phase difference discrimination in the guinea pig inferior colliculus. The Journal of neuroscience : the official journal of the Society for Neuroscience 31, 9192-9204.